NUMERICAL SIMULATION OF DAMAGE AND PROGRESSIVE FAILURES IN COMPOSITE LAMINATES USING THE LAYERWISE PLATE THEORY

By

Yeruva S. Reddy

Dissertation submitted to the Faculty of the
Virginia Polytechnic Institute and State University
in partial fulfillment of the requirements for the degree of
Doctor of Philosophy
in
Engineering Mechanics

APPROVED:

J. N. Reddy, Chairman

D. Frederick

Z. Gurdal

C. E. Knight

D. T. Mook

K. L. Reifsnider

August, 1992
Blacksburg, Virginia

NUMERICAL SIMULATION OF DAMAGE AND PROGRESSIVE FAILURES IN COMPOSITE LAMINATES USING THE LAYERWISE PLATE THEORY

By

Yeruva S. Reddy
J. N. Reddy, Chairman
Engineering Mechanics

(ABSTRACT)

The failure behavior of composite laminates is modeled numerically using the Generalized Layerwise Plate Theory (GLPT) of Reddy and a progressive failure algorithm. The Layerwise Theory of Reddy assumes a piecewise continuous displacement field through the thickness of the laminate and therefore has the ability to capture the interlaminar stress fields near the free edges and cut outs more accurately. The progressive failure algorithm is based on the assumption that the material behaves like a stable progressively fracturing solid. A three-dimensional stiffness reduction scheme is developed and implemented to study progressive failures in composite laminates.

The effect of various parameters such as out-of-plane material properties, boundary conditions, and stiffness reduction methods on the failure stresses and strains of a quasi-isotropic composite laminate with free edges subjected to tensile loading is studied. The ultimate stresses and strains predicted by the Generalized Layerwise Plate Theory (GLPT) and the more widely used First Order Shear Deformation Theory (FSDT) are compared with experimental results. The predictions of the GLPT are found to be in good agreement with the experimental

results both qualitatively and quantitatively, while the predictions of FSDT are found to be different from experimental results both qualitatively and quantitatively. The predictive ability of various phenomenological failure criteria is evaluated with reference to the experimental results available in the literature.

The effect of geometry of the test specimen and the displacement boundary conditions at the grips on the ultimate stresses and strains of a composite laminate under compressive loading is studied. The ultimate stresses and strains are found to be quite sensitive to the geometry of the test specimen and the displacement boundary conditions at the grips. The degree of sensitivity is observed to depend strongly on the lamination sequence. The predictions of the progressive failure algorithm are in agreement with the experimental trends.

Finally, the effect of geometric nonlinearity on the first-ply and ultimate failure loads of a composite laminate subjected to bending load is studied. The geometric nonlinearity is taken in to account in the von *Kármán* sense. It is demonstrated that the nonlinear failure loads are quite different from the linear failure loads, depending on the lamination sequence, boundary conditions, and span-to-depth ratio of the test specimen. Further, it is shown that the First order Shear Deformation Theory (FSDT) and the Generalized Layerwise Plate Theory (GLPT) predict qualitatively different results.

ACKNOWLEDGEMENTS

The present work is carried out under the guidance of Professor J. N. Reddy. I shall be forever indebted to him for his technical and professional guidance during the past three years. Though I could never repay him in full for his time and efforts, I hereby dedicate this dissertation to honor my teacher and mentor Professor J. N. Reddy.

Special thanks are also given to Professors D. Frederick, Z. Gurdal, C. E. Knight, D. T. Mook and K. L. Reifsnider for serving on my Ph.D. committee and for providing technical guidance during the course of this research. I would also like to thank Mr. Somanath Nagendra and Mr. Samuel Kassegne for proof reading the manuscript, and all my friends in the ESM department for their help and advice.

Finally, my deepest appreciation goes to my family, for their support and encouragement during the past three years. I would also like to thank Mrs. Vanessa McCoy for her help in typing this manuscript.

TABLE OF CONTENTS

LIST OF ILLUSTRATIONS

LIST OF TABLES

CHAPTER 1

INTRODUCTION

Composite materials have been successfully used in secondary aircraft structures which are generally designed based on stiffness considerations. These secondary structures constitute only a small portion of the total weight of the aircraft. Dramatic weight savings could be realized if these high strength and light weight materials are used in large and highly strained primary aircraft structures.

One of the major obstacles that prevents application of these materials in primary aircraft structures is the damage induced due to applied or accidental loads and the consequent reduction in stiffness, strength and life of these structures. Therefore, damage resistant and durable composite materials are essential for the design of lighter and easier to maintain aircraft structures.

The composite laminate is the fundamental building block of a composite structure and the strength of a structure must necessarily be related to the strength of the laminate. Hence, understanding the damage development and failure behavior of a composite laminate is a basic requirement for understanding the failure behavior of a structure.

Unlike metals, composite laminates suffer permanent loss of structural integrity under the influence of external loads, giving rise to discontinuities in the continuum in the form of microcracks. This process of permanent loss of integrity is called 'damage'. It is this damage, which is responsible for the simultaneous degradation

of stiffness, strength and life of composite structures. The ability to predict the initiation and evolution of damage is essential for predicting the performance of composite structures. Damage in composite laminates can be classified into three major categories, namely, (1) transverse cracking (2) delamination and (3) fiber breakage. Of the three damage modes the most commonly observed damage modes are transverse cracking and delamination. All these damage modes are not independent, but interact with one another and act concurrently leading to the degradation of mechanical and other properties of composite laminate.

It is possible to predict the first occurrence of failure (first-ply failure) in a composite laminate without much difficulty [1,2]. It is more difficult to predict subsequent failures after the initial damage has occured, since the stress analysis of a composite laminate with thousands of small cracks becomes intractable. In the progressive failure analysis this problem is tackled in an indirect way. The progressive failure analysis is based on the assumption that the damaged material can be replaced with an equivalent material of degraded properties. Thus, the problem of conducting the stress analysis of a laminate with thousands of micro-cracks is conveniently converted into the problem of stress analysis of a composite laminate with layers of dissimilar materials.

Damage initiation and growth in composite laminates is generally governed by a three dimensional state of stress. Hence, in order to predict the failure behavior of composite laminates accurately, a failure analysis technique that could capture both in plane and interlaminar stress components and allows for the interaction of various

damage modes is required.

However, the present day analytical techniques are mostly inadequate to handle the combined effect of various damage modes acting concurrently on composite structures with complex configuration subjected to combined loading conditions. Therefore, one has to resort to numerical techniques such as the finite element method to be able to predict the combined effect of various damage modes.

In the present study a three dimensional finite element procedure is developed for the progressive failure analysis of composite laminates. The Generalized Layerwise Plate Theory (GLPT) of Reddy [3] is used for stress analysis and the material is assumed to behave like a stable progressively fracturing solid [4]. It has been demonstrated in [5] that the GLPT is one such a plate theory which could capture both inplane and interlaminar stresses, and at the same time, is operationally more convenient and computationally more efficient than the conventional 3-D finite element stress analysis.

The literature review in Chapter 2 serves as a background for the present study. Chapter 3 provides the theoretical details of the Generalized Layerwise Plate Theory, Progressive failure analysis, Stiffness reduction methods and Failure criteria. Chapters 4, 5, and 6 contain the details of the application of the present progressive failure algorithm to study the damage and failures in composite laminates subjected to tensile, compressive and bending loads respectively. Finally, a summary of the results and recommendations for future work are presented in Chapter 7.

CHAPTER 2

LITERATURE REVIEW

In the last decade considerable progress has been made in understanding the onset and growth of various damage modes. But, this understanding has been limited to the cases of simple geometry and loading conditions. Besides, much of the research is directed towards understanding the effect of a single damage mode such as matrix cracking or delamination on the stiffness, strength and life of the laminate.

Reifsnider, et al. [6,7] performed both experimental and analytical work to understand the effect of transverse cracking on the stiffness reduction of composite laminates. They developed a one dimensional shear-lag model which as a first step determines the normal (to the cracked surface) stress in the cracked ply. Then, the reduction in the load carrying capacity of the cracked ply is computed and the elastic modulus of the cracked ply is reduced correspondingly. The classical laminate analysis was used to calculate overall stiffness properties of the laminate.

Talreja [8,9] used a continuum approach where the cracks are considered as microstructural entities such as dislocations and voids in metals. He developed a set of four equations for the four inplane stiffness coefficients i.e., E_1, E_2, G_{12}, v_{12} (after transverse cracking) in terms the stiffness coefficients of uncracked lamina and four unknown constants. The unknown constants were determined experimentally.

Hashin [10] used a variational approach to predict the stiffness reduction due to matrix cracking. Admissible stress systems which satisfy equilibrium and all

boundary and interface conditions were constructed and the principle of minimum complimentary energy was employed to find an optimal approximation. The stiffness reduction was computed from the two dimensional stress fields obtained by the above procedure.

Daniel, et al. [11,12] investigated the progressive matrix cracking of cross-ply composite laminates both analytically and experimentally. They developed closed form solutions for the transverse crack density, stress distributions and reduced stiffnesses of damaged plies as well as the entire laminate as a function of applied load and lamina properties.

The effect of delamination on stiffness and strength is not as well understood a subject as the effect of transverse cracking. Most of the effort in the area of delamination is directed towards predicting the initiation and growth of delamination. O'Brien [13,14] analyzed local delaminations and studied their influence on tensile stiffness of composite laminates. He has also studied [15] the effect of delamination on the strength of unnotched quasi-isotropic graphite/epoxy laminates.

Reifsnider, et al. [16] studied the relationship of delamination to other damage modes such as transverse cracking and fiber breakage in quasi-isotropic graphite/epoxy laminates. They found that delamination usually nucleates from the transverse crack and spreads along the length in both directions to join an adjacent crack.

The first attempt to model the failure behavior of composite laminates by progressive failure analysis was due to Petit and Waddoups [17]. They used the

Classical Laminated Plate Theory (CLPT) for stress analysis and an incremental loading procedure for failure analysis. As a first step, the laminae tangent moduli in tension, compression, and inplane shear were obtained experimentally and these properties were stored as data in a pointwise manner. As the incremental loading proceeds, the individual lamina tangent moduli were updated based on the stored data. Ultimate failure of a laminate was assumed to occur when the inplane laminate stiffness matrix [A] becomes singular, or when a diagonal term of [A] becomes negative.

Subsequently, Sandhu and Sendeckyj, et al. [18] followed a similar approach, but they have taken stiffness reduction due to damage into account. The finite element method was used to solve the laminate problem, and the experimental stress-strain curves of lamina were represented as piecewise continuous cubic spline interpolation functions. Lamina failure was determined by using a total strain energy failure criterion and the ply-discount method [19] was used for stiffness reduction.

Chang et al. [20-22] performed progressive failure analysis of notched composite laminates in tension and compression by using the finite element model based on CLPT. They used the nonlinear stress-strain relation advanced by Hahn and Tsai [23] for inplane shear. The resulting nonlinear finite element equations were solved by the modified Newton-Raphson iterative technique. Stiffness reduction was carried out at element level and a failure criterion originally proposed by Yamada and Sun [24] was used.

Tan [25] included the effect of thermal residual stresses and hygroscopic stresses

in his progressive failure model. The CLPT was used for stress analysis, and element stiffness property was taken as average value at the gauss points. Tsai-Wu failure criterion was used for failure prediction.

All the progressive failure analysis models considered so far were based on two dimensional stress analysis and hence could not take into account the delamination type of failure mode. Ochoa and Engblom [26] used a higher order plate theory for stress analysis and computed the transverse shear and normal stresses from the equilibrium equations. Stiffness reduction was carried out at Gauss points and Hashin's failure criterion [27] was used for failure prediction. However, they have failed to predict any delamination type of failure under uniaxial tension.

Lee [28] performed a fully three dimensional failure analysis of biaxially loaded composite laminate with a central hole. The finite element mesh consisted of 8-node brick elements and a special kind of loading condition that has a mirror symmetry with respect to the xy-plane at z=0 and a periodicity of π about z-axis was used. This kind of loading condition made it possible to analyze only a quarter of the entire laminate. Stiffness reduction was carried out at element level taking into account all the three types of damage modes i.e., (1) fiber breakage (2) transverse cracking and (3) delamination. However, during the entire process of progressive failure analysis no delamination was predicted.

Sun [29] performed progressive failure analysis of angle-ply laminates by using an iterative three dimensional finite element approach. The iterative method was basically a modified version of Newton-Raphson method where the tangent stiffness

matrix was taken to be the same as the direct stiffness matrix. The average stress in each element is considered for failure analysis and Hashin's failure criterion was used for failure prediction.

Averill [30] developed and implemented a micromechanics based model for progressive failure analysis of laminated shell structures. The model consists of a finite element code for nonlinear analysis of laminated shells and a micromechanical elasticity solution for predicting the failure and effective composite properties. The finite element code is based on a third order expansion of displacements through the thickness. The model was used to predict failures and to study the effects of constituent properties on the failure behaviour of composite laminates.

In summary, the following observations can be made from the above literature review:

(1) Most of the progressive failure models were predominantly two dimensional in nature.

(2) The failure analysis is carried out by applying an external force rather than displacement.

(3) Not much work has been done to study the influence of geometric nonlinearity and transverse normal stress on the failure behaviour of composite laminates subjected to bending load.

The present study consists of the following new features in order to overcome the above shortcomings:

(1) The Generalized Layer-wise Plate Theory (GLPT) of Reddy which has the ability

to capture both inplane and interlaminar stresses more accurately is used for stress analysis.

(2) A three dimensional stiffness reduction method is developed to reduce the stiffness properties of the damaged material in composite laminates.

(3) External displacement is applied instead of external force in the progressive failure analysis in order to model the simple tension and compression tests more realistically.

(4) The effect of geometric nonlinearity and transverse normal stress on the failure behavior of composite laminates subjected to bending load is investigated.

CHAPTER 3

THEORETICAL BACKGROUND

3.1 Generalized Layerwise Plate Theory (GLPT)

3.1.1 Introduction

The accurate modeling of interlaminar stress fields in composite laminates requires the displacement field to be piecewise continuous along the thickness direction. The displacement field in all the equivalent plate theories such as the CLPT and FSDT is assumed to be continuous through the thickness. The Generalized Layerwise Plate Theory (GLPT) proposed by Reddy and advanced by him and his colleagues assumes piecewise continuous displacement field through the thickness and hence has the ability to capture the interlaminar stress fields near the free edges and cutouts of composite laminates more accurately.

The detailed description of the GLPT and its finite element formulation for linearly elastic problems is available in the literature [31-36]. Barbero and Reddy [37] included geometric nonlinearity (in the von-*Kármán* sense) in GLPT and investigated nonlinear effects in composite laminates. However, they have assumed the transverse normals of the composite laminate to be inextensible. In the present study the above constraint is relaxed and both the direct and tangent stiffness matrices are developed by including the extensibility of transverse normals.

3.1.2 Finite Element Formulation

The basic premise of the Generalized Layerwise Plate Theory (GLPT) is that the

displacement field can be expanded as below:

$$u(x,y,z) = \sum_{m=1}^{N} U_m(x,y)\phi_m(z)$$

$$v(x,y,z) = \sum_{m=1}^{N} V_m(x,y)\phi_m(z) \tag{3.1}$$

$$w(x,y,z) = \sum_{m=1}^{N} W_m(x,y)\phi_m(z)$$

where (u,v,w) are the displacement components along x,y,z directions and N is the total number of nodes along z-direction. The functions $U_m(x,y)$, $V_m(x,y)$, $W_m(x,y)$ represent the inplane displacement field at the m-th interface of the composite laminate. These functions can be expanded in terms of the nodal displacements as below:

$$U_m(x,y) = \sum_{r=1}^{NPE} U_{rm}\psi_r(x,y)$$

$$V_m(x,y) = \sum_{r=1}^{NPE} V_{rm}\psi_r(x,y) \tag{3.2}$$

$$W_m(x,y) = \sum_{r=1}^{NPE} W_{rm}\psi_r(x,y)$$

where NPE is the number of nodes in the xy-plane, U_{rm}, V_{rm}, W_{rm} are the nodal displacement components at the r-th node of the m-th interface, and $\psi_r(x,y)$ are the 2-D Lagrangian interpolation functions in the xy-plane.

The shape functions $\phi_m(z)$ are the 1-D Lagrangian interpolation functions along the z-direction. These are piecewise continuous along the thickness (z) direction. For example, if $\phi_m(z)$ represents a linear Lagrangian interpolation function, then $\phi_1(z)$ is defined only between the thickness nodes 1 and 2, and $\phi_2(z)$ is defined only between

the thickness nodes 1 and 3. Typical variation of 1-D linear Lagrange interpolation functions along the thickness direction is shown in Figure 3.1.

The strain-displacement relationship for the above displacement field can be obtained as below:

$$\begin{aligned}
\epsilon_1 &= \frac{\partial u}{\partial x} + \frac{1}{2}\left(\frac{\partial w}{\partial x}\right)^2 \\
&= \frac{\partial U_m}{\partial x}\phi_m + \underline{\frac{1}{2}\left[\frac{\partial W_m}{\partial x}\frac{\partial W_n}{\partial x}\phi_m\phi_n\right]} \\
\epsilon_2 &= \frac{\partial u}{\partial y} + \frac{1}{2}\left(\frac{\partial w}{\partial y}\right)^2 \\
&= \frac{\partial V_m}{\partial y}\phi_m + \underline{\frac{1}{2}\left[\frac{\partial W_m}{\partial y}\frac{\partial W_n}{\partial y}\phi_m\phi_n\right]} \\
\epsilon_3 &= \frac{\partial w}{\partial z} = W_m\frac{d\phi_m}{dz} \\
\epsilon_4 &= \frac{1}{2}\left(\frac{\partial v}{\partial z} + \frac{\partial w}{\partial y}\right) \\
&= \frac{1}{2}\left(V_m\frac{d\phi_m}{dz} + \frac{\partial W_m}{\partial y}\phi_m\right) \qquad (3.3) \\
\epsilon_5 &= \frac{1}{2}\left(\frac{\partial u}{\partial z} + \frac{\partial w}{\partial x}\right) \\
&= \frac{1}{2}\left(U_m\frac{d\phi}{dz} + \frac{\partial W_m}{\partial x}\phi_m\right) \\
\epsilon_6 &= \frac{1}{2}\left(\frac{\partial u}{\partial y} + \frac{\partial v}{\partial x} + \frac{\partial w}{\partial x}\frac{\partial w}{\partial y}\right) \\
&= \frac{1}{2}\left(\frac{\partial U_m}{\partial y}\phi_m + \frac{\partial V_m}{\partial x}\phi_m + \underline{\frac{\partial W_m}{\partial x}\frac{\partial W_n}{\partial y}\phi_m\phi_n}\right)
\end{aligned}$$

where ϵ_1, ϵ_2, ϵ_3 are the normal strains along the x, y, z directions and ϵ_4, ϵ_5, ϵ_6 are the shear strains in the yz, xz, xy planes respectively. The underlined terms of (3.3)

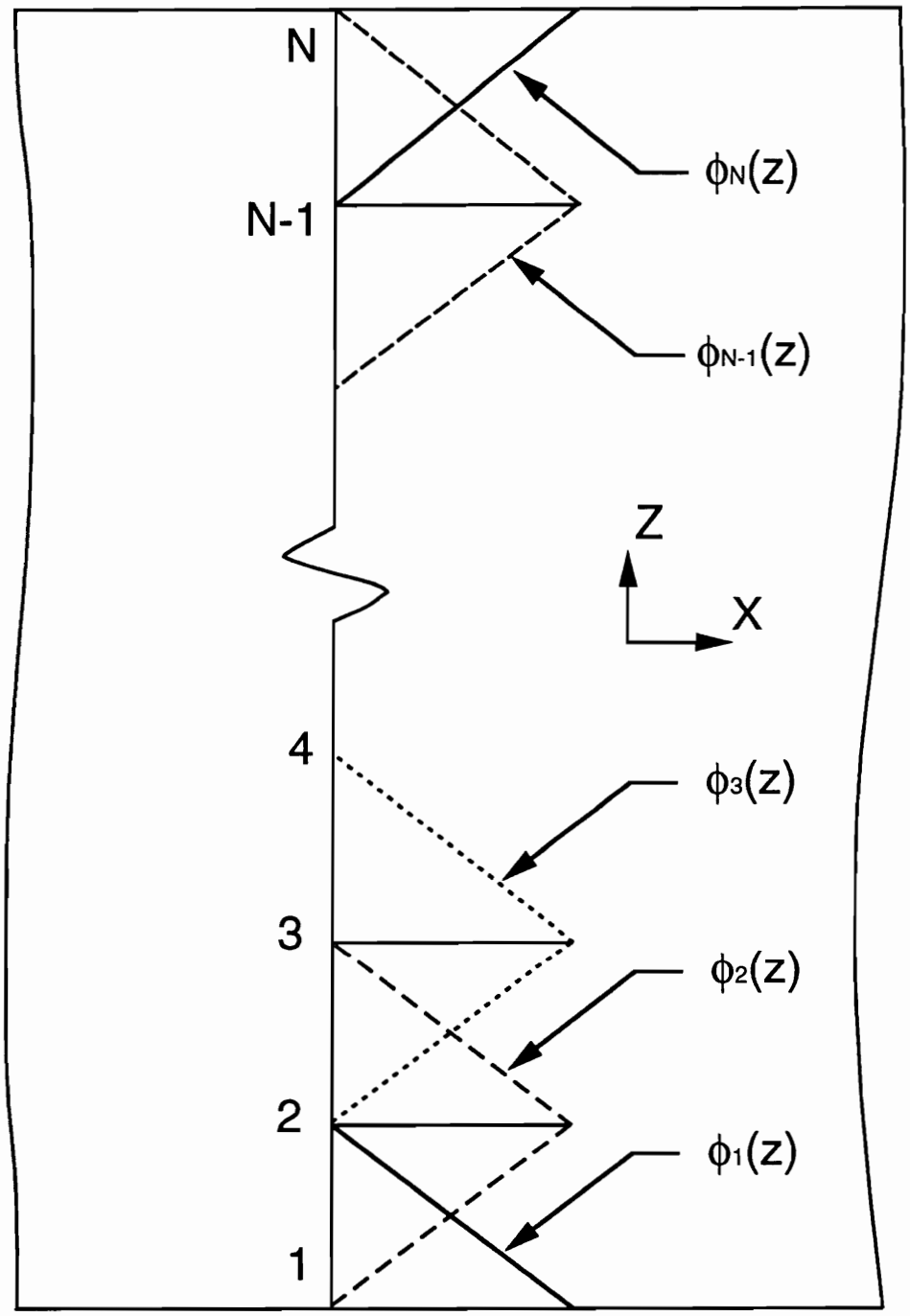

Figure 3.1 Typical variation of 1-D linear Lagrange type of interpolation fuctions along z-direction

are due to the inclusion of geometric nonlinearity in the von-*Kármán* sense. The stress-strain relationships are given as below:

$$\begin{aligned}\sigma_i =& Q_{ij}\phi_k\epsilon^1_{jk} + Q_{ij}\frac{d\phi_k}{dz}\epsilon^2_{jk} \\ &+ Q_{ij}\phi_k\phi_\ell\epsilon^3_{jk\ell}\end{aligned} \tag{3.4}$$

where σ_1, σ_2, σ_3 are the normal stresses along x, y, z directions and σ_4, σ_5, σ_6 are shear stresses in the yz, xz, xy planes respectively. Q_{ij} is the transformed stiffness matrix of the composite lamina in the global (x,y,z) coordinates.

The strain components ϵ^1_{jk}, ϵ^2_{jk}, ϵ^3_{jk} in the above equation (3.4) are defined as below:

$$\begin{gathered}\epsilon^1_{1k} = \frac{\partial U_k}{\partial x} \;,\; \epsilon^1_{2k} = \frac{\partial V_k}{\partial y} \;,\; \epsilon^1_{3k} = 0 \\ \epsilon^1_{4k} = \frac{\partial W_k}{\partial y} \;,\; \epsilon^1_{5k} = \frac{\partial W_k}{\partial x} \;,\; \epsilon^1_{6k} = \frac{\partial U_k}{\partial y} + \frac{\partial V_k}{\partial x} \\ \epsilon^2_{3k} = W_k \;,\; \epsilon^2_{4k} = V_k \;,\; \epsilon^2_{5k} = U_k \\ \epsilon^3_{1k\ell} = \frac{\partial W_k}{\partial x}\frac{\partial W_\ell}{\partial x} \;,\; \epsilon^3_{2k\ell} = \frac{\partial W_k}{\partial y}\frac{\partial W_\ell}{\partial y} \;,\; \epsilon_{6k\ell} = \frac{\partial W_k}{\partial x}\frac{\partial W_\ell}{\partial y}\end{gathered} \tag{3.5}$$

All other strain components are zero.

The laminate constitutive equations for GLPT are given as below:

$$\begin{aligned}N_{im} &= \int_{-\frac{h}{2}}^{+\frac{h}{2}} \sigma_i\phi_m dz \\ &= A_{ijkm}\epsilon^1_{jk} + B_{ijkm}\epsilon^2_{jk} \\ &+ E_{ijk\ell m}\epsilon^3_{jk\ell}\end{aligned} \tag{3.6a}$$

$$\begin{aligned}Q_{im} &= \int_{-\frac{h}{2}}^{+\frac{h}{2}} \sigma_i\frac{d\phi_m}{dz} dz \\ &= C_{ijkm}\epsilon^1_{jk} + D_{ijkm}\epsilon^2_{jk} \\ &+ F_{ijk\ell m}\epsilon^3_{jk\ell}\end{aligned} \tag{3.6b}$$

$$N_{imn} = \int_{-\frac{h}{2}}^{+\frac{h}{2}} \sigma_i \phi_m \phi_n dz$$
$$= E_{ijkmn}\epsilon^1_{jk} + G_{ijkmn}\epsilon^2_{jk}$$
$$+ H_{ijk\ell mn}\epsilon^3_{jk\ell} \tag{3.6c}$$

where A_{ijkm}, B_{ijkm}, C_{ijkm}, D_{ijkm}, E_{ijklm}, F_{ijklm}, G_{ijkmn}, H_{ijklmn} are defined as below:

$$A_{ijkm} = \int_{-\frac{h}{2}}^{+\frac{h}{2}} Q_{ij}\phi_k\phi_m dz \tag{3.7a}$$

$$B_{ijkm} = \int_{-\frac{h}{2}}^{+\frac{h}{2}} Q_{ij}\frac{d\phi_k}{dz}\phi_m dz \tag{3.7b}$$

$$C_{ijkm} = \int_{-\frac{h}{2}}^{+\frac{h}{2}} Q_{ij}\phi_k\frac{d\phi_m}{dz} dz \tag{3.7c}$$

$$D_{ijkm} = \int_{-\frac{h}{2}}^{+\frac{h}{2}} Q_{ij}\frac{d\phi_k}{dz}\frac{d\phi_m}{dz} dz \tag{3.7d}$$

$$E_{ijk\ell m} = \int_{-\frac{h}{2}}^{+\frac{h}{2}} Q_{ij}\phi_k\phi_\ell\phi_m dz \tag{3.7e}$$

$$F_{ijk\ell m} = \int_{-\frac{h}{2}}^{+\frac{h}{2}} Q_{ij}\phi_k\phi_\ell\frac{d\phi_m}{dz} dz \tag{3.7f}$$

$$G_{ijkmn} = \int_{-\frac{h}{2}}^{+\frac{h}{2}} Q_{ij}\frac{d\phi_k}{dz}\phi_m\phi_n dz \tag{3.7g}$$

$$H_{ijk\ell mn} = \int_{-\frac{h}{2}}^{+\frac{h}{2}} Q_{ij}\phi_k\phi_\ell\phi_m\phi_n dz \tag{3.7h}$$

By applying the principle of virtual work, the equilibrium equations of GLPT are derived as below:

$$\frac{\partial N_{1m}}{\partial x} + \frac{\partial N_{6m}}{\partial y} - Q_{5m} = 0 \tag{3.8a}$$

$$\frac{\partial N_{6m}}{\partial x} + \frac{\partial N_{2m}}{\partial y} - Q_{4m} = 0 \tag{3.8b}$$

$$\frac{\partial N_{5m}}{\partial x}+\frac{\partial N_{4m}}{\partial y}-Q_{3m}$$
$$+\frac{\partial}{\partial x}\left(N_{1mn}\frac{\partial W_n}{\partial x}+N_{6mn}\frac{\partial W_n}{\partial y}\right)$$
$$+\frac{\partial}{\partial y}\left(N_{2mn}\frac{\partial W_n}{\partial y}+N_{6mn}\frac{\partial W_n}{\partial x}\right)$$
$$+q(x,y,z_k)\delta_{mk}=0 \tag{3.8c}$$

where $q(x,y,z_k)$ is the transverse distributed load on the xy-plane defined by z_k. δ_{mk} is the Kronecker delta and k is the number of interface corresponding to the z_k co-ordinate. Finally, we have $(3 \times m)$ equations of equilibrium at m number of interfaces.

By multiplying the equilibrium equations (3.8) with the inplane shape function $\psi_s(x,y)$ and then integrating by parts the finite element equilibrium equations are obtained as below:

$$\begin{bmatrix} [K^{11}_{smrk}] & [K^{12}_{smrk}] & [K^{13}_{smrk}] \\ [K^{21}_{smrk}] & [K^{22}_{smrk}] & [K^{23}_{smrk}] \\ [K^{31}_{smrk}] & [K^{32}_{2mrk}] & [K^{33}_{smrk}] \end{bmatrix} \begin{Bmatrix} \{U_{rk}\} \\ \{V_{rk}\} \\ \{W_{rk}\} \end{Bmatrix} = \begin{Bmatrix} \{F^1_{sm}\} \\ \{F^2_{sm}\} \\ \{F^3_{sm}\} \end{Bmatrix} \tag{3.9}$$

The expressions for $[K^{\alpha\beta}_{smrk}](\alpha,\beta = 1,3)$ is given in Appendix A and the expressions for $\{F^{\alpha}_{sm}\}(\alpha = 1,3)$ are given in Appendix B.

3.1.3 Tangent Stiffness Matrix

The finite element stiffness matrix derived in the last section is called the direct stiffness matrix and can be used for nonlinear analysis of composite laminates by the direct stiffness method. However, the direct stiffness matrix is not symmetric

and therefore, requires all the elements of the stiffness matrix to be stored in the computer memory. Moreover, the convergence of the displacement field in the direct stiffness method is much slower than the Newton-Raphson method. Hence, in the present study the tangent stiffness matrix is derived and the nonlinear equations of equilibrium are solved by using the Newton-Raphson iteration method.

The tangent stiffness matrix is derived as below:

$$\begin{aligned}[T] &= \frac{\partial}{\partial\{\Delta\}}\{F\} \\ &= \frac{\partial}{\partial\{\Delta\}}\{[K]\{\Delta\}\} \\ &= [K] + \{\Delta\}\frac{\partial[K]}{\partial\{\Delta\}} \\ &= [K] + [R] \end{aligned} \tag{3.10}$$

where $[K]$, $[T]$ are the direct and tangent stiffness matrices and $[F]$, $[\Delta]$ are the total force and displacement vectors respectively. The matrix $[R]$ consists of the additional stiffness terms to be added to the direct stiffness matrix $[K]$ to obtain the tangent stiffness matrix $[R]$. The expression for $[T]$ is given in Appendix C.

3.2 Progressive Failure Algorithm

The progressive failure algorithm is based on the assumption that the material behaves like a stable progressively fracturing solid. This ideal material has the following properties (see [4]).

(1) loses stiffness due to stable progressive fracture or damage during loading,

(2) unloads in a linear elastic manner, and losses stiffness depending on the extent of progressive fracture or damage prior to unloading, and

(3) has the property that the material may always be returned to a state of zero stress and strain by linear-elastic unloading.

For a material possessing the above properties, the direct stiffness matrix and the tangent stiffness matrix become one and the same. Therefore, the nonlinear iteration due to damage can be performed by the direct stiffness method. The algorithm for progressive failure analysis based on the direct stiffness method is given below:

(1) Find the displacement field throughout the laminate for a small externally applied displacement, based on the current stiffness properties.

(2) Compute the stresses at each Gauss point in lamina coordinates for the above displacement field and stiffness properties.

(3) Check whether any of the Gauss points have failed by applying the chosen failure criterion.

(4) Reduce the stiffness properties of the failed Gauss points in accordance with the stiffness reduction method.

(5) Compute the failure load by integrating the stresses through the thickness and print the results.

(6) Go to Step 1 and repeat the iteration until no further damage takes place at the same externally applied displacement.

(7) If no damage takes place (i.e. no more Gauss points fail) then increase the externally applied displacement and repeat the Steps 1 to 6.

(8) Repeat the above procedure until the failure load reaches a peak value and then falls down rapidly.

(9) Print the peak failure load and strain as the ultimate failure load and strain of the laminate.

3.3 Stiffness Reductions Methods

Progressive failure analysis is based on the assumption that the damaged material could be substituted with an equivalent material of degraded properties. However, it is not an easy task to determine the degraded properties of the damaged material with certainty. In the presented study the degraded properties are assumed to be a constant multiple of the original properties of the undamaged material. The constant which is to be determined experimentally, is called Stiffness Reduction Coefficient (SRC). When the value of SRC is known for a given lamination sequence, it is assumed that the same value of SRC holds good for any other lamination sequence as long as the same material system is maintained.

In the present study two different types of stiffness reduction methods are used to study the influence of stiffness reduction methods on the failure loads and strains. These are classified as (1) Independent and (2) Interactive methods. In the independent method it is assumed that each stress would contribute only towards the degradation of the corresponding stiffness property. For example, σ_1 would contribute only towards the degradation of E_1 and the values of G_{12}, G_{13} would remain unaffected. In the interactive method coupling is assumed between the normal and shear stiffness properties. Thus, the degradation of E_1 would also result in the degradation of G_{12}, G_{13}. The details of the two methods are given below:

3.3.1 Stiffness Reduction Method-I (Independent)

(1) Compute the stress-to-strength ratio for all the six components of stress at a given Gauss point and find the maximum of the six values.

(2) If the maximum value is due to σ_1, then substitute the following degraded stiffness properties:

$$E_{1D} = (SRC)(E_1) \; ; \; v_{12D} = (SRC)(v_{12}) \; ; \; v_{13D} = (SRC)(v_{13})$$

(3) If the maximum value is due to σ_2, then substitute the following degraded stiffness properties:

$$E_{2D} = (SRC)(E_2) \; ; \; v_{21D} = (SRC)(v_{21}) \; ; \; v_{23D} = (SRC)(v_{23})$$

(4) If the maximum value is due to σ_3, then substitute the following degraded stiffness properties:

$$E_{3D} = (SRC)(E_3) \; ; \; \nu_{31D} = (SRC)(v_{31}) \; ; \; v_{32D} = (SRC)(\nu_{32})$$

(5) If the maximum value is due to σ_4, then substitute the following degraded stiffness properties

$$G_23D = (SRC)(G_{23})$$

(6) If the maximum value is due to σ_5, then substitute the following degraded stiffness properties:

$$G_{13D} = (SRC)(G_{13})$$

(7) If the maximum value is due to σ_6, then substitute the following degraded stiffness properties:

$$G_{12D} = (SRC)(G_{12})$$

(8) Appropriate logic is included in the computer code such that restrictions on elastic constants are maintained.

3.3.2 Stiffness Reduction Method-II (Interactive)

(1) Compute the contribution of each stress component towards the failure index of the Tsai-Wu failure criterion and identify the stress component which contributes the maximum.

(2) If the maximum is due to σ_1, then the failure mode is fiber breakage.

If the maximum value is due to σ_2 or σ_6, then the failure mode is transverse cracking.

If the maximum value is due to σ_3 or σ_4 or σ_5, then the failure mode is delamination.

(3) If the failure mode is fiber breakage, then substitute the following degraded stiffness properties:

$$E_{1D} = (SRC)(E_1) \; ; \; G_{13D} = (SRC)(G_{13}) \; ; \; G_{12D} = (SRC)(G_{12})$$

$$v_{13D} = (SRC)(v_{13}) \; ; \; v_{12D} = (SRC)(v_{12})$$

(4) If the failure mode is transverse cracking, then substitute the following degraded stiffness properties:

$$E_{2D} = (SRC)(E_2) \; ; \; G_{23D} = (SRC)(G_{23}) \; ; \; G_{12D} = (SRC)(G_{12})$$

$$v_{1D} = (SRC)(v_{21}) \; ; \; v_{23D} = (SRC)(v_{23})$$

(5) If the failure mode is delamination then substitute the following degraded stiffness

properties:

$$E_{3D} = (SRC)(E_3) \; ; \; G_{23D} = (SRC)(G_{23}) \; ; \; G_{13D} = (SRC)G_{13})$$

$$v_{31D} = (SRC)(v_{31}) \; ; \; v_{32D} = (SRC)(v_{32})$$

(6) Appropriate logic is included in the computer code such that restrictions on elastic constants are maintained.

3.4 Review of Failure Criteria

Failure criteria for composite laminates can be classified into two groups, independent failure criteria and polynomial failure criteria, which are discussed below:

(a) Independent Failure Criteria

The maximum stress and maximum strain failure criteria belong to this category. In the maximum stress criterion, failure of a given material is assumed to occur if any of the following conditions are satisfied:

$$\begin{aligned} \sigma_1 \geq X_T \; , \; \sigma_4 \geq R \\ \sigma_2 \geq Y_T \; , \; \sigma_5 \geq S \\ \sigma_3 \geq Z_T \; , \; \sigma_6 \geq T \end{aligned} \tag{3.11}$$

where σ_1, σ_2, σ_3 are the normal stresses and σ_4, σ_5, σ_6 are shear stresses in the lamina coordinates. X_T, Y_T, Z_T are the lamina normal strengths in the 1, 2, 3 directions and R, S, T the shear strengths in the 23, 13, 12 planes respectively. When σ_1, σ_2, σ_3 are of compressive nature then they should be compared with X_C, Y_C, Z_C, which are the normal strengths in compression along the 1, 2, 3 directions respectively.

In the maximum strain criterion, failure of the material is assumed to occur if any of the following conditions are satisfied:

$$\epsilon_1 \geq X_{\epsilon T},\ \epsilon_4 \geq R_\epsilon$$

$$\epsilon_2 \geq Y_{\epsilon T},\ \epsilon_5 \geq S_\epsilon \tag{3.12}$$

$$\epsilon_3 \geq Z_{\epsilon T},\ \epsilon_6 \geq T_\epsilon$$

where ϵ_1, ϵ_2, ϵ_3 are the normal strains and σ_4, σ_5, σ_6 are shear strains in the lamina coordinates. $X_{\epsilon T}$, $Y_{\epsilon T}$, $Z_{\epsilon T}$ are the lamina normal strain strengths in the 1, 2, 3 directions and R_ϵ, S_ϵ, T_ϵ the shear strain strengths in the 23, 13, 12 planes respectively. When ϵ_1, ϵ_2, ϵ_3 are of compressive nature then they should be compared with $X_{\epsilon C}$, $Y_{\epsilon C}$, $Z_{\epsilon C}$, which are the normal strain strengths in compression along the 1, 2, 3 directions respectively.

(b) Polynomial Failure Criterion

The most general polynomial failure criterion for composite materials is the tensor polynomial failure criterion proposed by Tsai [38]. All other polynomial failure criteria are degenerate cases of this criterion. In index notation the tensor polynomial failure criterion is expressed as

$$F_i\sigma_i + F_{ij}\sigma_i\sigma_j + F_{ijk}\sigma_i\sigma_j\sigma_k + \ldots \geq 1 \tag{3.13}$$

Particular cases of above criterion are discussed below:

(i) Tsai-Wu Criterion

Tsai-Wu criterion is a particular case of the tensor polynomial failure criteion, where the first two terms of (3.13) are considered. Therefore, the Tsai-Wu criterion

is given by

$$F_i\sigma_i + F_{ij}\sigma_i\sigma_j \geq 1 \tag{3.14}$$

where

$$F_1 = (1/X_T - 1/X_C),\ F_2 = (1/Y_T - 1/Y_C),\ F_3 = (1/Z_T - 1/Z_C),$$

$$F_{11} = (1/X_T X_C),\ F_{22} = (1/Y_T Y_C),\ F_{33} = (1/Z_T Z_C),$$

$$F_{44} = (1/R)^2,\ F_{55} = (1/S)^2,\ F_{66} = (1/T)^2,$$

$$F_{12} = (-1/2)(X_T X_C Y_T Y_C)^{-1/2}, \tag{3.15}$$

$$F_{13} = (-1/2)(X_T X_C Z_T Z_C)^{-1/2},$$

$$F_{23} = (-1/2)(Y_T Y_C Z_T Z_C)^{-1/2}.$$

The coefficients F_1, F_2, F_3 correspond to the linear stress terms and F_{11}, F_{22}, F_{33}, F_{44}, F_{55}, F_{66} correspond to the quadratic stress terms. F_{12}, F_{13}, F_{23} are the coefficients which take into account the interaction effect of various normal stress components.

(ii) Hoffman Failure Criterion

Hoffman criterion is a special case of the tensor polynomial failure criterion for the following choice of parameters.

$$F_{12} = (-1/2)(1/X_T X_C + 1/Y_T Y_C - 1/Z_T Z_C),$$

$$F_{13} = (-1/2)(1/X_T X_C - 1/Y_T Y_C + 1/Z_T Z_C), \tag{3.16}$$

$$F_{23} = (-1/2)(-1/X_T X_C + 1/Y_T Y_C + 1/Z_T Z_C).$$

All other parameters are same as those in the Tsai-Wu failure criterion.

(ii) Tsai-Hill Failure Criterion

Tsai-Hill criterion can be obtained as a particular case of the Hoffman failure criterion by substituting the compressive strengths equal to the tensile strengths in the parameters F_i and F_{ij}. As a result, F_i become equal to zero and the linear stress terms in the Tsai-Hill failure criterion do not appear. Appropriate values of X_T or X_C, Y_T or Y_C, Z_T or Z_C should be chosen depending on the sign of σ_1, σ_2 and σ_3.

CHAPTER 4

STUDY OF DAMAGE AND FAILURES IN TENSION

4.1 An Example Problem

The progressive failure analysis of an 8-ply quasi-isotropic composite laminate under axial extension is chosen as an example problem for tensile loading. The geometry and other details of the problem are shown in Figure 4.1. The laminates are made of AS4/3501-6 graphite/epoxy pre-preg. The inplane material properties of the pre-peg are shown in Table 4.1. The lamination sequences considered in the example problem are shown in Table 4.2. The loading angle is changed by cutting the tensile test specimens from the same laminate at different angles with respect to the 0-degree ply.

Experiments conducted by Sun, et al. [39] revealed that although the inplane-stiffness is the same for all the laminates, the tensile strength is strongly dependent on the loading angle. Further, it was observed that the Classical Laminated Plate Theory (CLPT) coupled with the ply-discount method and Tsai-Hill failure criterion predicts almost the same failure load for all the laminates (A to D) and the predicted loads are very much higher than the experimental failure loads.

In order to predict the failure loads more accurately, Sun, et al. [39] performed a quasi-three dimensional stress analysis on a single cross-section of the laminate, and proposed a new failure criterion based on the average interlaminar shear stress and surface-ply failure. Symmetry has been assumed about both xy and xz-planes and

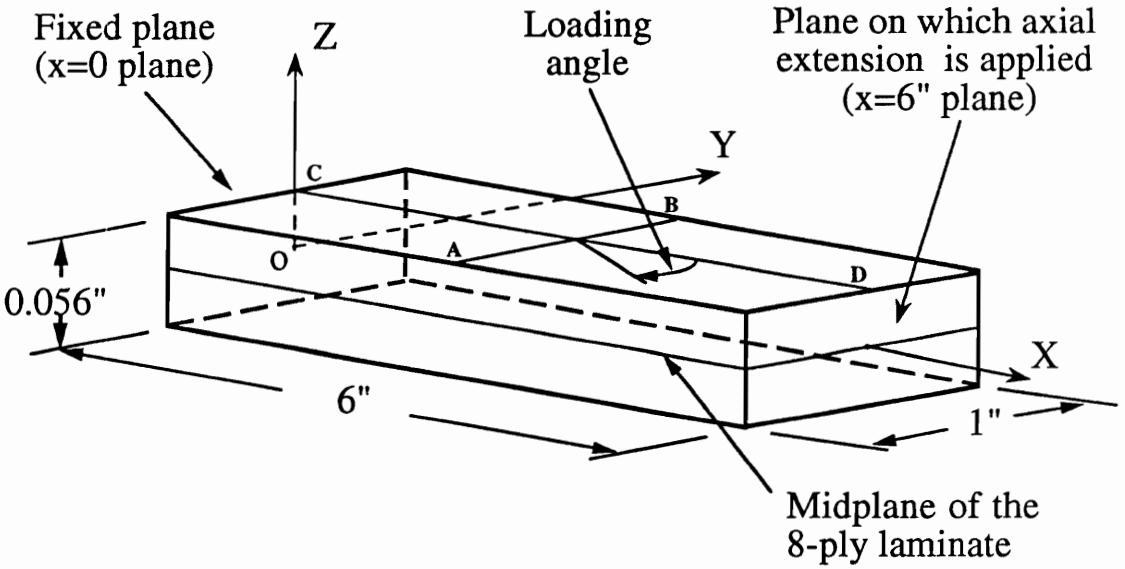

Figure 4.1 Geometry and other details of the example problem for tensile loading

Table 4.1 Inplane material properties of AS4/3501-6 graphite/epoxy pre-peg

Properties	Values		Properties	Values	
E_1	20.16×10^6	psi	X_T	320.00×10^3	psi
$E_2 = E_3$	1.43×10^6	psi	X_C	292.00×10^3	psi
$G_{12} = G_{13}$	0.76×10^6	psi	$Y_T = Z_T$	8.20×10^3	psi
$\nu_{12} = \nu_{13}$	0.3000		$Y_C = Z_C$	30.00×10^3	psi
Ply thickness	0.0052	in.	S = T	16.00×10^3	psi

Table 4.2 Laminate designation, Loading angle and Stacking sequence of various laminates considered for progressive failure analysis in tension

Laminate designation	Loading angle	Stacking sequence*
A	0.0	$(0.0/ 90.0/45.0/-45.0)_S$
B	7.5	$(7.5/ 97.5/52.5/-37.5)_S$
C	15.0	$(15.0/105.0/60.0/-30.0)_S$
D	22.5	$(22.5/112.5/67.5/-22.5)_S$

(*s=Symmetric laminate)

the stress analysis was performed only on one quarter cross-section of the plate.

In the present work, no symmetry is assumed about the xz-plane (since it does not exist) and stress analysis is performed on one half of the total laminate. Since the stress analysis is carried out on the total volume of the test specimen, interaction of the failure modes throughout the laminate is taken into account. The stresses are computed at the reduced integration Gauss points of the finite element mesh.

4.2 Results and Discussion

4.2.1 Introduction

(i) Out-of-Plane Material Properties

Three-dimensional stress analysis requires the knowledge of both in-plane and out-of-plane material properties (stiffness and strengths) of the ply. The in-plane (12-plane) material properties of various plies are readily available in the literature. However, due to the small thickness (0.0052") of the ply, its out-of-plane (23-plane) stiffness and strength properties (ν_{23}, G_{23}, R) are not easily measurable. The usual practice is to assume these properties to be the same as those in the 12-plane [see 39].

In the present study the upper and lower bounds on ν_{23} and G_{23} are obtained by applying the condition of transverse isotropy and thermodynamic constraints [40]. The upper and lower bounds on ν_{23} are found to be 0.987 and 0.113, and the corresponding lower and upper bounds on G_{23} are found to be 0.36 msi and 0.64 msi respectively. The lower bound for the shear strength in the 23-plane (R) is chosen to be the shear strength of the matrix material and the upper bound is chosen to be the shear strength in the 12-plane [41]. A parametric study is conducted to

investigate the effect of these material properties on failure loads and strains. The values of ν_{23}, G_{23}, and R for the parametric study are chosen such that these values are well within the lower and upper bounds.

(ii) Displacement Boundary Conditions

Failure analysis of composite laminates subjected to inplane load is usually performed by applying a uniform external force because of the insufficient understanding of the nature of displacement boundary conditions at the grips in a simple tension or compression test. However, the assumption of uniform force is not appropriate in case of composite laminates made of layers of different orientations and the assumption becomes increasingly invalid as the process of damage development continues due to unloading of the damaged plies.

In the present study a uniform u-displacement is applied and parametric study is conducted to understand the influence of various v-displacement boundary conditions on the ultimate failure loads and strains of composite laminate. Failure analysis is performed on a composite laminate subjected to four different kinds of boundary conditions on v-displacement. The four different boundary conditions are defined below:

BC1: x=0 plane: v is fixed at the center of the plane

x=6" plane: v is totally free (i.e rigid body rotation is allowed about the fixed end)

BC2: x=0 plane: v is fixed at the center of the plane

x=6" plane: v is fixed at the center of the plane

BC3: x=0 plane: v is fixed along the top and the bottom edges of the plane

x=6" plane: v is fixed along the top and the bottom edges of the plane

BC4: x=0 plane: v is fixed throughout the plane

x=6" plane: v is fixed throughout the plane.

The x=0 plane corresponds to the fixed grip and the x=6" plane corresponds to the grip where axial extension is applied. The actual length of the tensile test specimen is 9" and end tabs of 1.5" long are used at each end. Therefore, the above boundary conditions specified on a single cross-section actually represent the constraint posed by the total grip including the end tabs.

(iii) Finite Element Mesh

Conventionally the convergence study on the finite element mesh is conducted by applying a given load and refining the mesh until convergence is obtained on the displacement. In the present case a known displacement is applied and the u-displacement of a given point (point A of Figure 4.1) on the free-edge of the laminate is considered for the purpose of convergence study. The geometry and loading of the example problem are symmetric about z=0 plane. Therefore, only one half of the laminate (upper half) is considered for finite element analysis. Refined mesh is used near the free edges and grips as shown in Figure 4.2.

Linear Lagrange type of interpolation functions are used for both in-plane and thickness directions. Therefore, each element corresponds to an 8-node brick element in the conventional 3-D finite element analysis. The convergence study is conducted first with respect to the number of elements along the y-axis for a fixed number of

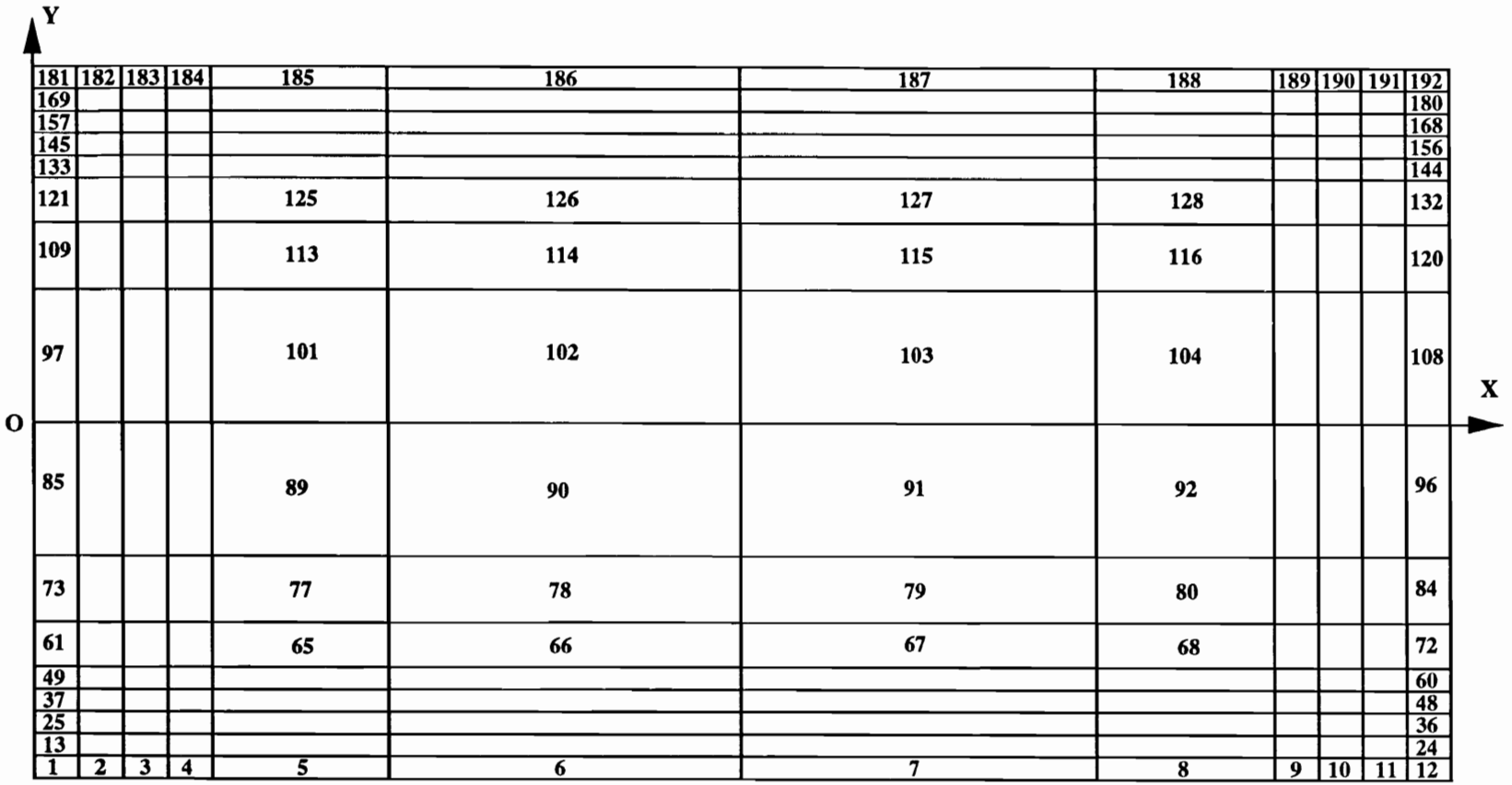

Figure 4.2 Details of the finite element mesh in the XY-Plane for tensile loading

elements (4) along the x and z-axes. Then, convergence study is conducted with respect to the number of elements along the x-axis, the number of elements along the y are chosen to be 16 and those along the z axis are fixed to be 4. Finally, convergence study is conducted with respect to the number of elements along the z-axis for a fixed number of elements along the x and y axes (12 and 16 elements respectively).

The convergence of u-displacement at point A for various laminates with respect to the number of elements along the y,x, and z-axes are shown in Figures 4.3, 4.4, 4.5, respectively. The final mesh contains 12,16,8 elements along x,y,z axes respectively. A typical variation of the u and v-displacements along the lines AB and CD (see Figure 1) for various laminates is shown in Figures 4.6 and 4.7 respectively. A sharp gradient is observed in the displacement field near the free edges and at the grips.

4.2.2 Influence of Out-of-Plane Stiffness Properties

Parametric study is conducted on out-of-plane stiffness properties (v_{23} and G_{23}) for a given boundary condition (BC1) and out-of-plane strength property (R=6000 psi). Stiffness reduction method-I (independent) is used for progressive failure analysis. The value of stiffness reduction coefficient (SRC) is chosen to be very small (10^{-6}) and a maximum displacement of 0.1" is applied in 12 steps.

The results of the parametric study are presented in Tables 4.3 and 4.4. Table 4.3 shows the variation of first-ply failure loads and strains with respect to v_{23} and G_{23}. The first-ply failure loads and strains are observed to decrease as the value of v_{23} is increased. Table 4.4 contains the ultimate failure loads and strains for various values of v_{23} and G_{23}. These values do not follow a particular trend but are less sensitive

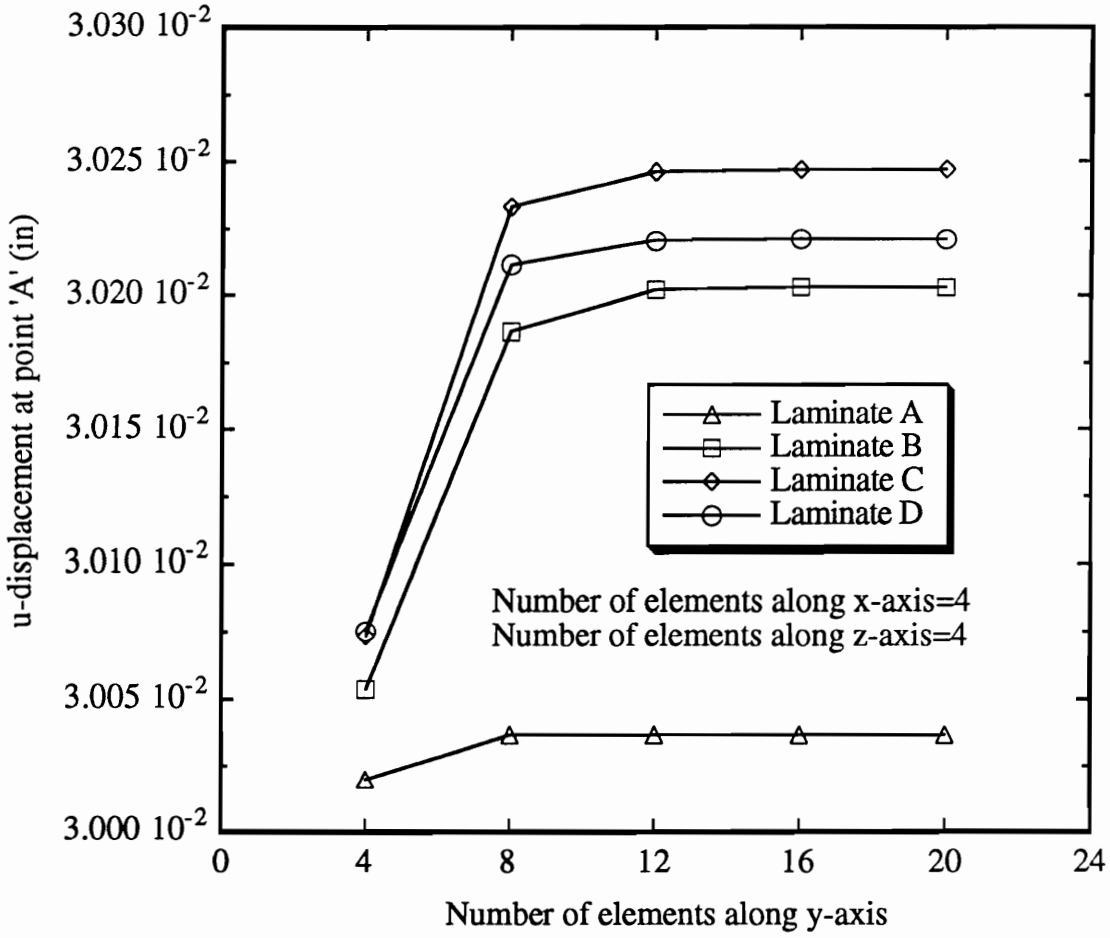

Figure 4.3 Convergence of u-displacement at point 'A' (see Figure 4.1) for Laminates A,B,C and D as a function of number of elements along y-axis

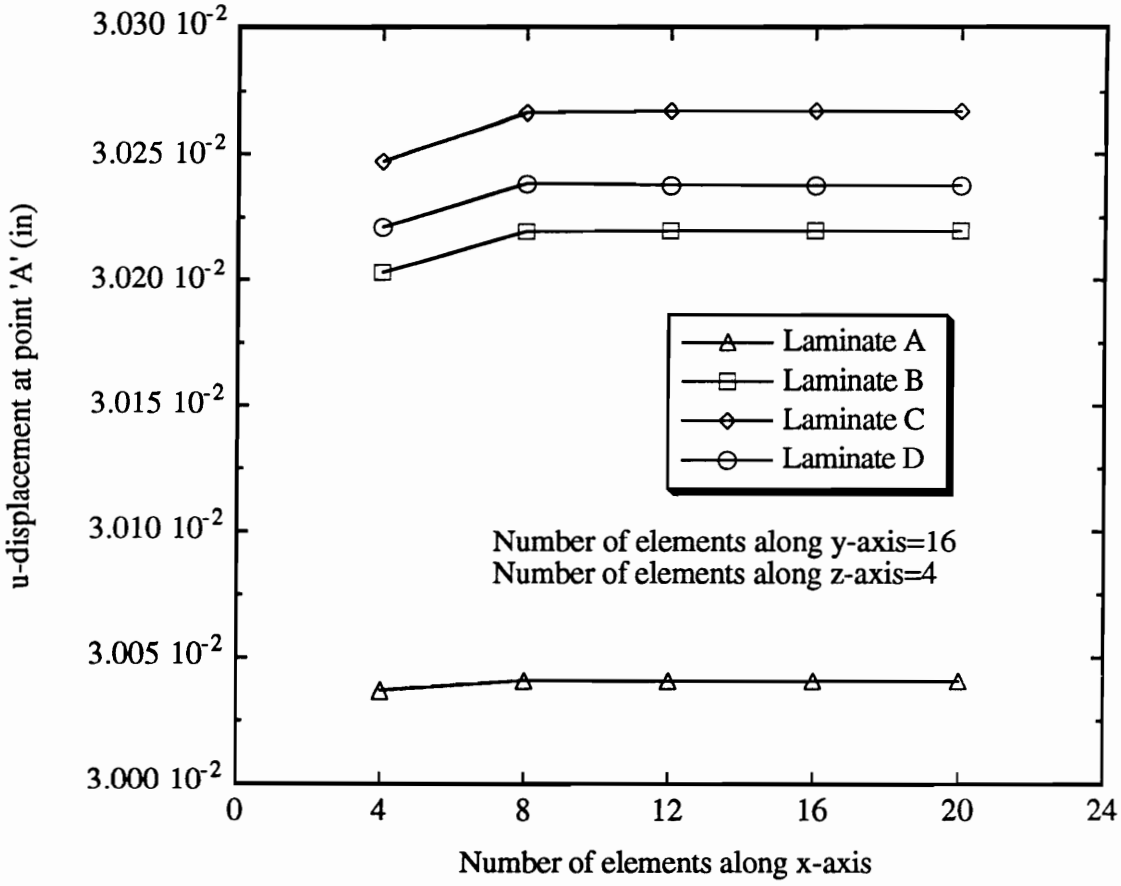

Figure 4.4 Convergence of u-displacement at point 'A' (see Figure 4.1) for Laminates A,B,C and D as a function of number of elements along x-axis

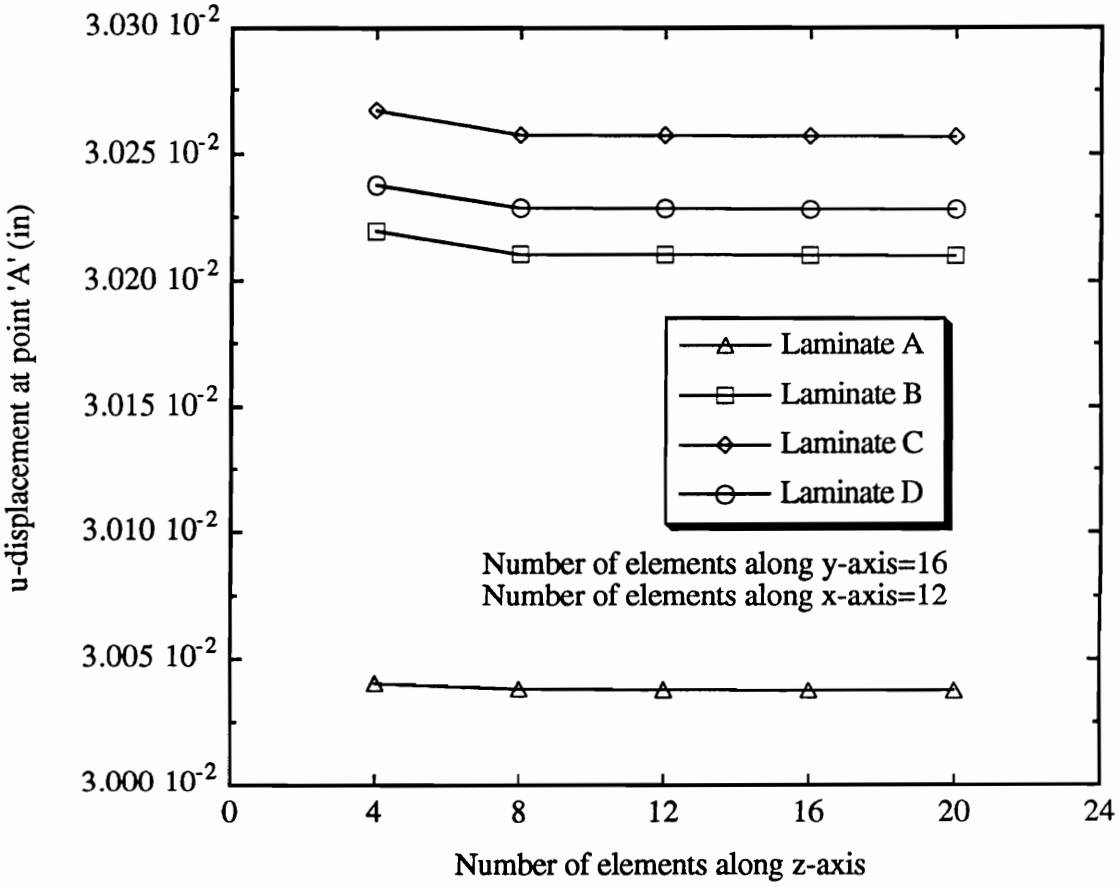

Figure 4.5 Convergence of u-displacement at point 'A' (see Figure 4.1) for Laminates A,B,C and D as a function of number of elements along z-axis

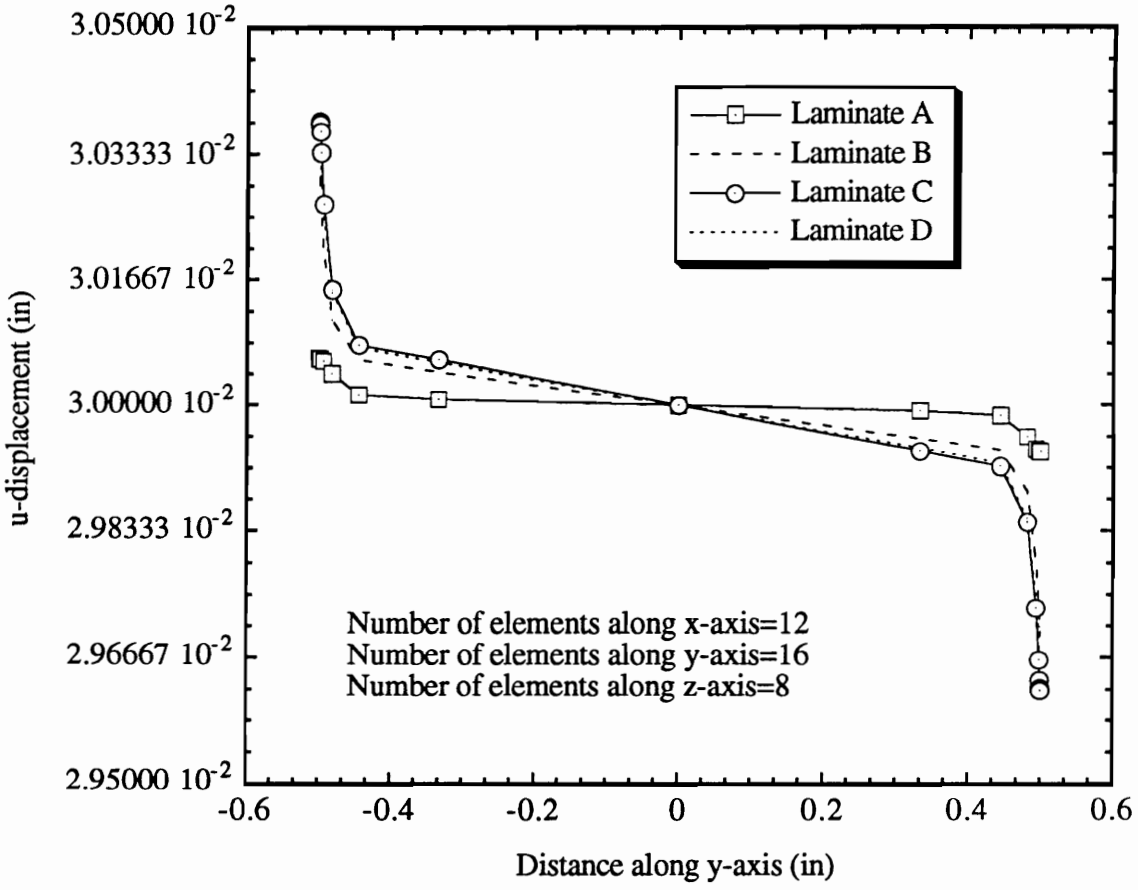

Figure 4.6 Typical variation of u-displacement along line 'AB' (see Figure 4.1) for Laminates A, B, C and D subjected to BC2

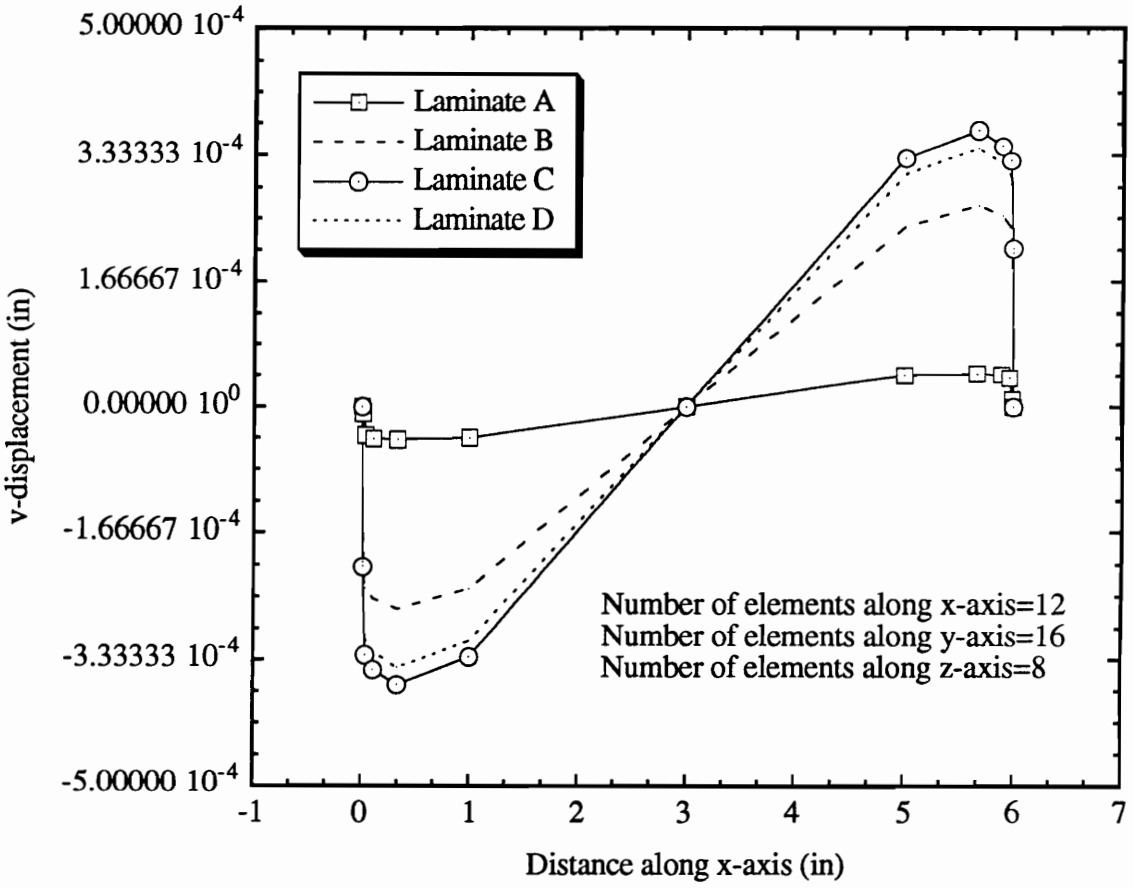

Figure 4.7 Typical variation of v-displacement along line 'CD' (see Figure 4.1) for Laminates A, B, C and D subjected to BC2

Table 4.3 Variation of first ply failure loads and strains with respect to ν_{23} and G_{23}

Properties	Laminate A Load, lbs (Strain, %)	Laminate B Load, lbs (Strain, %)	Laminate C Load, lbs (Strain, %)	Laminate D Load, lbs (Strain, %)
ν_{23}=0.2 (G_{23}=0.60 msi)	1148 (0.355)	838 (0.260)	688 (0.214)	632 (0.197)
ν_{23}=0.5 (G_{23}=0.48 msi)	1016 (0.314)	734 (0.228)	570 (0.178)	518 (0.162)
ν_{23}=0.8 (G_{23}=0.40 msi)	744 (0.230)	543 (0.169)	416 (0.130)	383 (0.120)

Table 4.4 Variation of ultimate failure loads and strains with respect to ν_{23} and G_{23}

Properties	Laminate A Load, lbs (Strain, %)	Laminate B Load, lbs (Strain, %)	Laminate C Load, lbs (Strain, %)	Laminate D Load, lbs (Strain, %)
ν_{23}=0.2 (G_{23}=0.60 msi)	3673 (1.238)	2563 (0.867)	2308 (0.780)	2238 (0.783)
ν_{23}=0.5 (G_{23}=0.48 msi)	3694 (1.244)	2556 (0.862)	2308 (0.781)	2240 (0.784)
ν_{23}=0.8 (G_{23}=0.40 msi)	3660 (1.316)	2479 (0.822)	2306 (0.783)	2229 (0.784)
Experimental (From Ref. 39)	3718 (1.187)	2838 (0.972)	2495 (0.843)	2358 (N/A)

to the out-of-plane stiffness properties. This implies that the common practice of assuming the out-of-plane stiffness properties same as the inplane properties would not introduce any error in the predicted values of ultimate failure loads and strains for inplane loading.

It is observed that the ultimate failure loads and strains decrease sharply from Laminate A to D (i.e. as the loading angle is increased) for all values of ν_{23}. This indicates that the out-of-plane stiffness properties do not affect variation of failure loads and strains for different lamination sequences in a qualitative sense. It is encouraging to note that the predicted failure loads and strains (see Table 4.4) are in good agreement with the experimental results [39] for all values of ν_{23}.

4.2.3 Influence of Out-of-Plane Strength Property

Parametric study is conducted on out-of-plane strength property R for the following stiffness properties: $v_{23} = 0.5$ and $G_{23} = 0.48$ msi. All other conditions are maintained the same as in the previous case. Tables 4.5 and 4.6 contain the results of the parametric study. Table 4.5 contains first-ply failure loads and strains for various values of R. The first-ply failure loads and strains are observed to be insensitive to the value of R. This is not surprising since the first-ply failure mode, i.e. transverse cracking, is not sensitive to the out-of-plane shear strength property R of the ply.

The variation of ultimate failure loads and strains with respect to R is presented in Table 4.6. It is clear that the ultimate failure loads and strains are quite sensitive to the value of R. This indicates that the common practice of assuming the out-of-plane

Table 4.5 Variation of first ply failure loads and strains with respect to R

Properties	Laminate A Load, lbs (Strain, %)	Laminate B Load, lbs (Strain, %)	Laminate C Load, lbs (Strain, %)	Laminate D Load, lbs (Strain, %)
R=6000 psi	1016 (0.314)	734 (0.228)	570 (0.178)	518 (0.162)
R=11000 psi	1024 (0.317)	743 (0.231)	574 (0.179)	518 (0.162)
R=16000 psi	1025 (0.317)	746 (0.231)	575 (0.179)	519 (0.162)

Table 4.6 Variation of ultimate failure loads and strains with respect to R

Properties	Laminate A Load, lbs (Strain, %)	Laminate B Load, lbs (Strain, %)	Laminate C Load, lbs (Strain, %)	Laminate D Load, lbs (Strain, %)
R=6000 psi	3694 (1.244)	2556 (0.861)	2308 (0.780)	2240 (0.784)
R=11000 psi	3895 (1.291)	2812 (0.932)	2399 (0.786)	2328 (0.786)
R=16000 psi	4083 (1.371)	2889 (0.951)	2467 (0.799)	2373 (0.788)
Experimental (From Ref. 39)	3718 (1.187)	2838 (0.952)	2495 (0.843)	2358 (N/A)

shear strength property same as the inplane shear strength may introduce considerable error in the predicted values of ultimate failure loads and strains. However, this error is dependent on the lamination sequence and it is not proportional to the error in R. For example Laminate A is more sensitive to the value of R than other laminates, and a 260% increase in R would contribute towards 10% increase in the ultimate failure load and strain of that laminate.

Even in this case, it is observed that the ultimate failure loads and strains decrease sharply from Laminates A to D for all values of R. This indicates that the out-of-plane shear strength property does not affect the failure loads and strains in a qualitative sense. The predicted failure loads and strains are in good agreement with the experimental results only when R is less than 11000 psi.

4.2.4 Influence of Displacement Boundary Conditions

A parametric study is conducted by applying different displacement boundary conditions at the grips. The out-of-plane strength property R is chosen to be 6000 psi. All other conditions are maintained to be the same as in the previous case. Tables 4.7 and 4.8 contain the results of the parametric study. Table 4.7 contains the variation of first-ply failure loads and strains with respect to various boundary conditions. The first-ply failure loads and strains are observed to be quite sensitive to the way boundary conditions on v-displacement are applied. A sharp drop is observed in the failure loads and strains when the constraint on v-displacement is shifted from the center (BC2) to the edges (BC3).

Table 4.8 contains the variation of ultimate failure loads and strains with respect

Table 4.7 Variation of first ply failure loads and strains with respect to various boundary conditions

Boundary Condition	Laminate A Load, lbs (Strain, %)	Laminate B Load, lbs (Strain, %)	Laminate C Load, lbs (Strain, %)	Laminate D Load, lbs (Strain, %)
BC1	1016 (0.314)	734 (0.228)	570 (0.178)	518 (0.162)
BC2	1017 (0.315)	736 (0.229)	573 (0.179)	521 (0.163)
BC3	569 (0.176)	448 (0.139)	359 (0.112)	332 (0.104)
BC4	528 (0.164)	512 (0.159)	483 (0.151)	492 (0.154)

Table 4.8 Variation of ultimate failure loads and strains with respect to various boundary conditions

Boundary Condition	Laminate A Load, lbs (Strain, %)	Laminate B Load, lbs (Strain, %)	Laminate C Load, lbs (Strain, %)	Laminate D Load, lbs (Strain, %)
BC1	3694 (1.244)	2556 (0.862)	2308 (0.781)	2240 (0.784)
BC2	3694 (1.243)	2583 (0.871)	2309 (0.781)	2240 (0.784)
BC3	3691 (1.243)	2448 (0.809)	2279 (0.772)	2258 (0.787)
BC4	3548 (1.193)	3206 (1.089)	3288 (1.205)	3250 (1.184)
Experimental (From Ref. 39)	3718 (1.187)	2838 (0.972)	2495 (0.843)	2358 (N/A)

to various boundary conditions. In this case no drastic change is observed in failure loads and strains when the boundary condition is changed from BC2 to BC3. This implies that the conclusions made in the case of first-ply failure loads and strains can not be routinely applied to ultimate failure loads and strains. In this case, the ultimate failure loads and strains decrease sharply from Laminates A to D only for BC1, B C2 and BC3. For BC4 the failure loads and strains are almost same for Laminates B, C and D. This indicates that the nature of boundary condition would affect the variation of failure loads and strains for different lamination sequences both qualitatively and quantitatively.

4.2.5 Influence of the Stiffness Reduction Method and Stiffness Reduction Coefficient

A parametric study is conducted to study the influence of stiffness reduction methods and stiffness reduction coefficients. The boundary condition is chosen to be BC2 and all other parameters are maintained same as previous case. The results of the parametric study are presented in Tables 4.9 and 4.10. Table 4.9 shows the variation of ultimate failure loads and strains with respect to stiffness reduction method-I and method-II. The ultimate failure loads and strains are observed to be quite sensitive to the way stiffness properties are reduced in order to account for damage. For a given value of Stiffness Reduction Coefficent (SRC), the interactive stiffness reduction method predicts lower values of failure loads and strains than those of independent method.

Table 4.10 contains the variation of ultimate failure loads and strains with respect

Table 4.9 Variation of ultimate failure loads and strains with respect to stiffness reduction methods

Stiffness Reduction Method	Laminate A Load, lbs (Strain, %)	Laminate B Load, lbs (Strain, %)	Laminate C Load, lbs (Strain, %)	Laminate D Load, lbs (Strain, %)
Independent	3694 (1.244)	2583 (0.871)	2309 (0.781)	2240 (0.784)
Interactive	2930 (1.391)	2121 (0.676)	2017 (0.657)	1921 (0.642)

Table 4.10 Variation of ultimate failure loads and strains with respect to Stiffness Reduction Coefficient (SRC)

Stiffness Reduction Coefficient	Laminate A Load, lbs (Strain, %)	Laminate B Load, lbs (Strain, %)	Laminate C Load, lbs (Strain, %)	Laminate D Load, lbs (Strain, %)
SRC=10^{-6}	2930 (1.391)	2121 (0.676)	2017 (0.657)	1921 (0.642)
SRC=10^{-2}	3380 (1.299)	2361 (0.796)	2156 (0.778)	2062 (0.770)
SRC=10^{-1}	3782 (1.366)	2692 (0.962)	2394 (0.869)	2399 (0.874)
Experimental (From Ref. 39)	3718 (1.187)	2838 (0.972)	2495 (0.843)	2358 (N/A)

to various Stiffness Reduction Coefficients (SRC). The interactive stiffness reduction method is used to account for the damage. The values of ultimate failure loads and strains are observed to increase as the value of SRC is increased. The results are in good agreement with experimental results when SRC=0.1. This implies that it is possible to arrive at experimental results in more than one way by adjusting two parameters with mutually opposing tendencies suitably.

In this case, the independent stiffness reduction method coupled with a Stiffnesss Reduction Coefficient (SRC) of 10^{-6} and the interactive stiffness reduction method coupled with a Stiffness Reduction Coefficient (SRC) of 10^{-1} would predict almost the same ultimate failure loads and strains.

4.2.6 Evaluation of Various Phenomenological Failure Criteria

The predictions of the following phenomenological failure criteria are compared with the experimental results: (1) Maximum stress, (2) Maximum strain, (3) Tsai-Hill. (4) Hoffman, and (5) Tsai-Wu. The first two are called independent failure criteria since they do not account for the interaction of various stress components in the failure prediction. All the other criteria are called polynomial or quadratic failure criteria and they take the interaction of various stress components into account.

Figures 4.8 and 4.9 show the comparison of the predictions of various failure criteria with the experimental results. The results are obtained for the following out-of-plane material properties: $v_{23} = 0.5$, $G_{23} = 0.48$ msi, $R = 6000$ msi. BC2 boundary condition and independent stiffness reduction method are used. The stiffness reduction coefficient is chosen to be 10^{-6} for all cases. Figure 4.8 shows

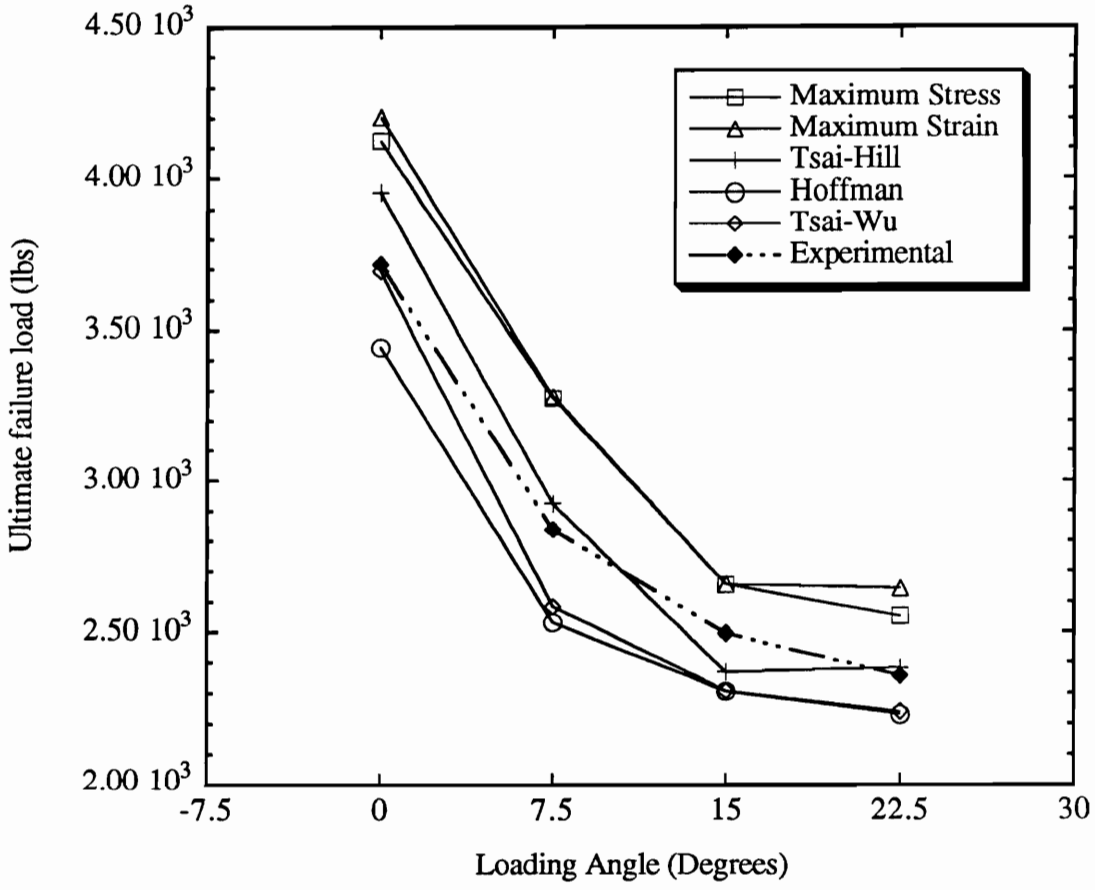

Figure 4.8 Comparison of Ultimate failure loads predicted by various failure criteria with experimental results

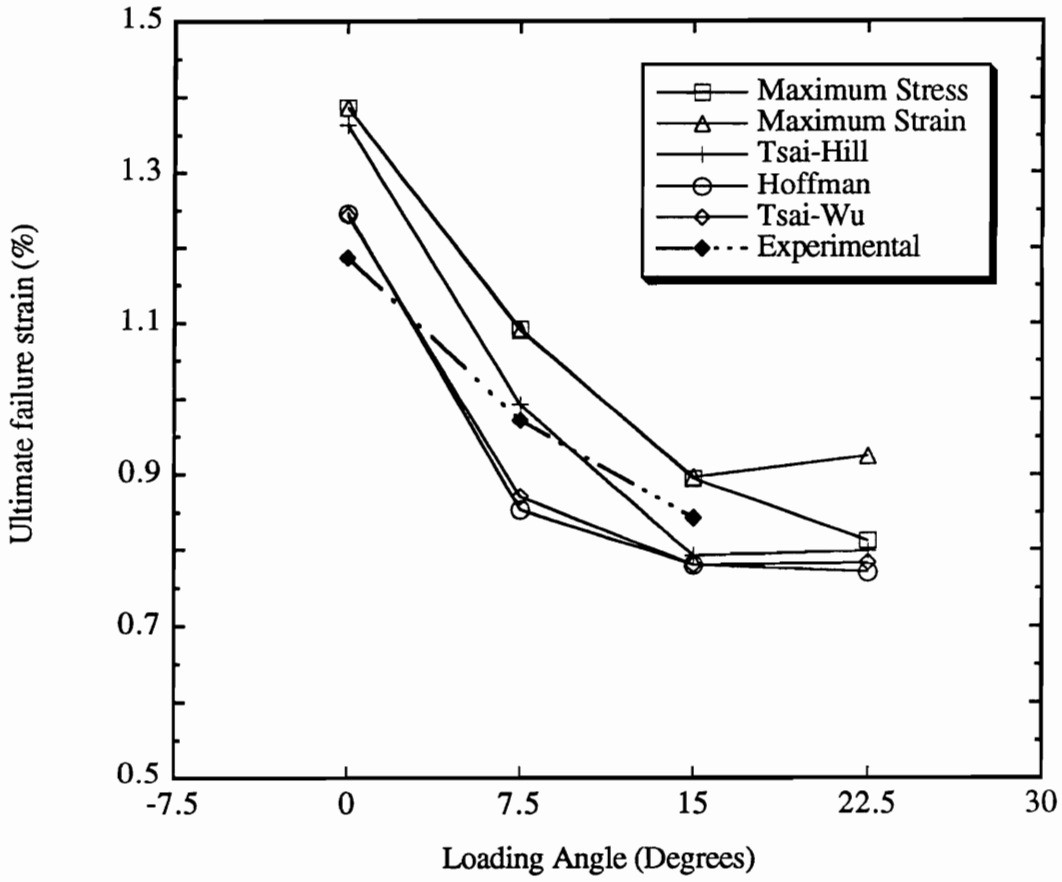

Figure 4.9 Comparison of Ultimate failure strains predicted by various failure criteria with experimental results

that the Maximum stress and Maximum strain failure criteria over-predict the failure loads while the Hoffman and Tsai-Wu failure criteria under-predict the failure loads for all laminates.

The Tsai-Hill failure criteria over-predicts the failure loads A,B,D and under-predicts the failure load for laminate C. Thus it does not follow the experimental trends consistently. The inability of the Tsai-Hill criterion to capture the experimental trends indicates that the polynomial failure criterion must be complete. i.e., it must have both linear and quadratic terms. The Hoffman and Tsai-Wu failure criteria have both linear and quadratic terms in the polynomial that describes the failure surface in the stress space.

Figure 4.9 shows that failure strains also follow the same trends except that in this case both Hoffman and Tsai-Wu failure criteria over predict the failure strain of laminate A. This leads to the observation that in general, the failure loads are in better agreement with experimental results than the failure strains.

4.2.7 Comparison of the Predictions of GLPT and FSDT

As explained previously the Generalized Layerwise Plate Theory (GLPT) has the ability to capture the interlaminar stress components more accurately near the free edges and cut outs. It is proposed to demonstrate the importance of these stresses in the failure prediction of composite laminates by obtaining the same results using an equivalent single layer plate theory. The equivalent single layer plate theories assume a C1 continuous displacement field along the thickness direction of the plate and hence do not have the ability to capture the interlaminar stress fields. In the present

study the First order Shear Deformation Theory (FSDT) is chosen as a representative equivalent single layer plate theory.

Figures 4.10 and 4.11 show the comparison of the predictions of the Generalized Layerwise Plate Theory (GLPT) and the First order Shear Deformation Theory (FSDT) with the experimental results. The Tsai-Wu failure criterion is used in both the cases. All other parameters are chosen to be the same as in the previous case. It is interesting to note the qualitatively different trends predicted by FSDT and GLPT. The results suggest that ignoring the interlaminar stress fields in the failure analysis of composite laminates could lead to erroneous conclusions regarding their strength.

Figure 4.12 shows the load versus displacement curves as predicted by GLPT. The failure load reaches a peak value and drops down rapidly after the peak. In the present study the peak value is taken as the ultimate failure load. It can be noted that laminate A is linearly elastic until failure. This behavior is in agreement with the experimental results [42].

The progression of damage as predicted by FSDT and GLPT for laminate A is shown in Tables 4.11 and 4.12, respectively. It is observed that in the case of FSDT all the elements in a given ply fail simultaneously (see Table 4.11), because, FSDT predicts a state of uniform stress throughout the ply including the free edges and grips. Whereas, GLPT predicts more severe state of stress at the free edges and grips, and hence, predicts initiation of damage at the free edges and grips (see Table 4.12), amd then a gradual progression of damage from the free edges to the interior of the laminate.

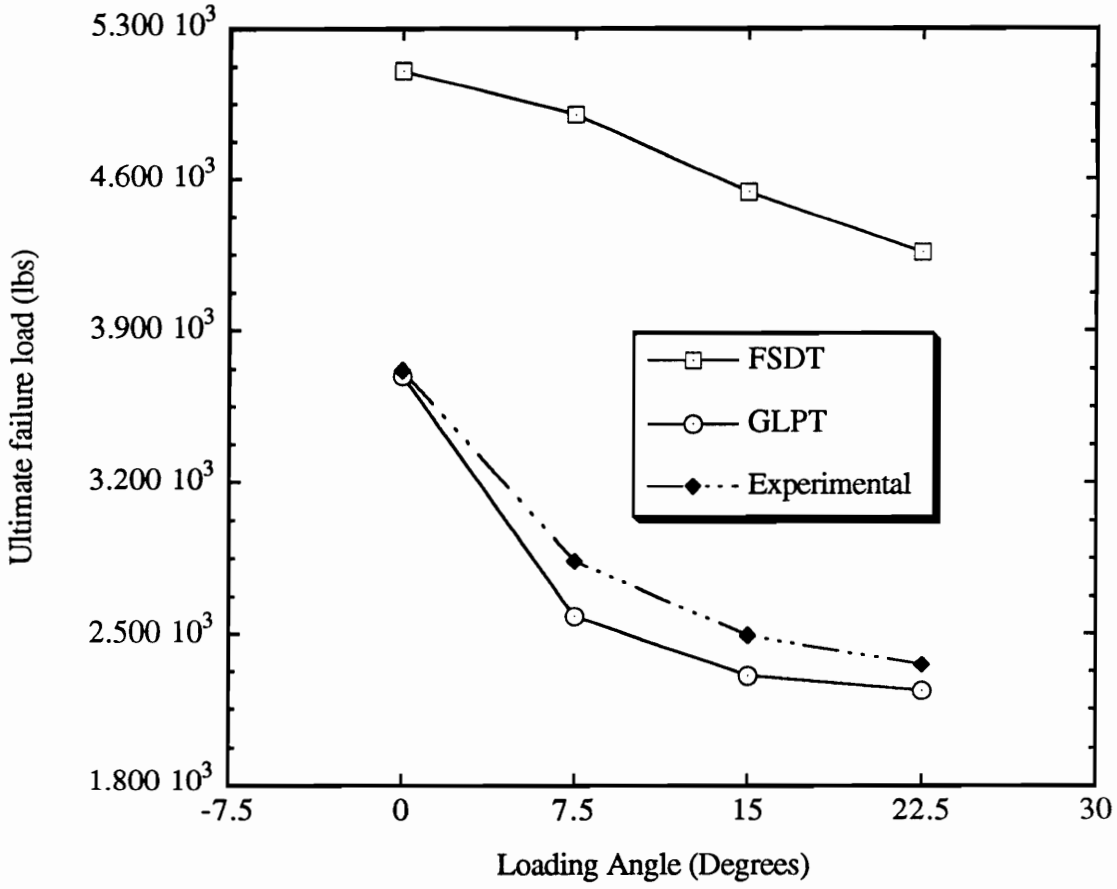

Figure 4.10 Comparison of Ultimate failure loads predicted by FSDT and GLPT with experimental results

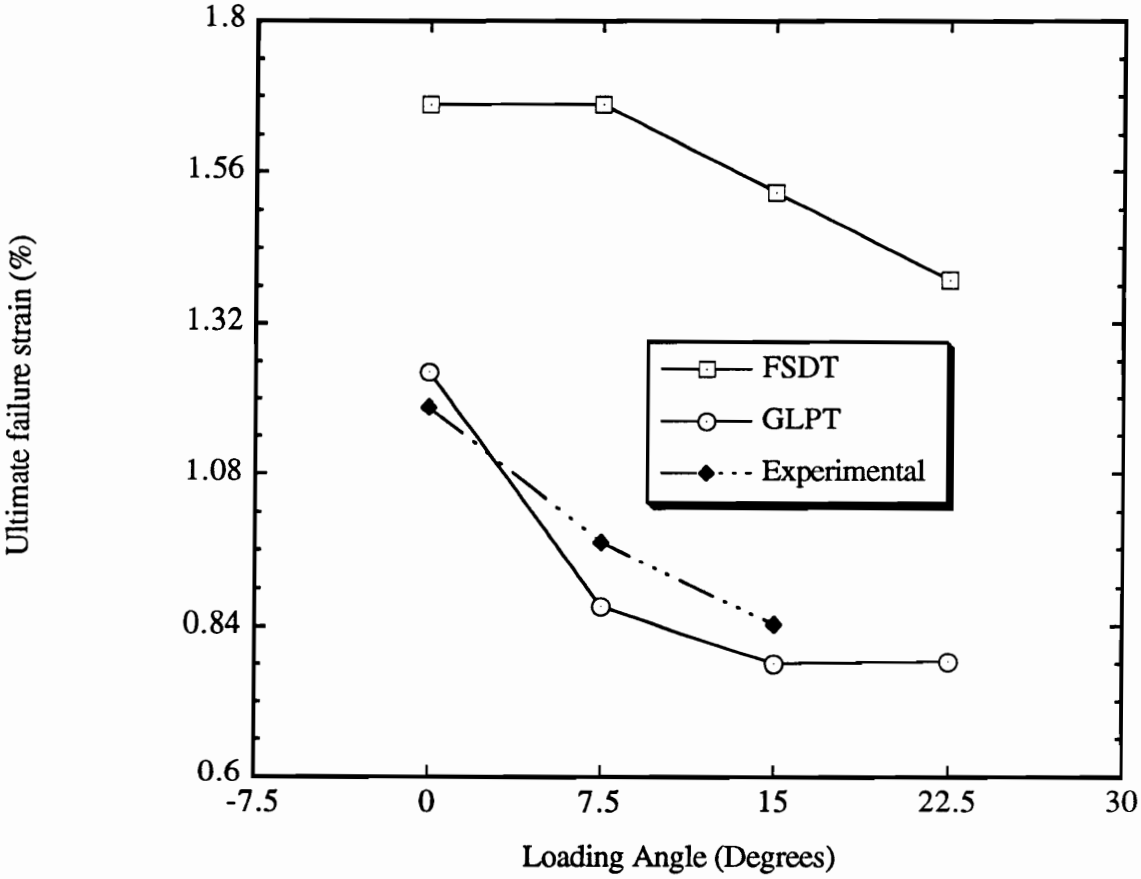

Figure 4.11 Comparison of Ultimate failure strains predicted by FSDT and GLPT with experimental results

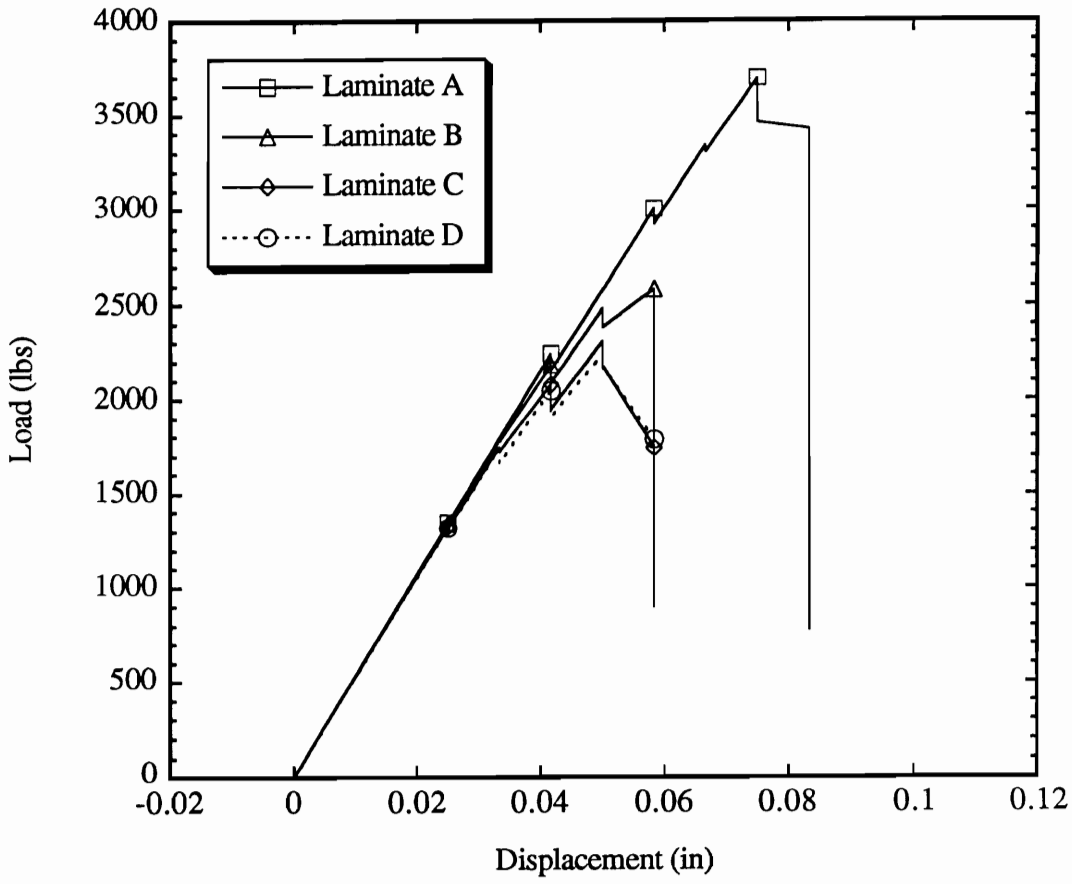

Figure 4.12 Load versus displacement curves for various laminates as predicted by GLPT

Table 4.11 Progression of damage for laminate A as predicted by FSDT

Displacement (in)	Load (lbs)	FPL	FTL	FMD	FEL
0.00833	452	0	0	0	0
0.01667	904	0	0	0	0
0.02500	1356	0	0	0	0
0.03333	1808	0	0	0	0
0.04167	2260 (b)	2	1	2	All
			2	2	All
	2172 (a)	0	0	0	0
0.05000	2607	0	0	0	0
0.05833	3041 (b)	3	1	2	All
			2	2	All
		4	1	2	All
			2	2	All
	2978 (a)	0	0	0	0
0.06667	3404	0	0	0	0
0.07500	3829	0	0	0	0
0.08333	4254	0	0	0	0
0.09167	4680	0	0	0	0
0.10000	5105 (b)	1	1	1	All
			2	1	All
		3	1	6	All
			2	6	All
		4	1	6	All
			2	6	All
	1191 (a)	0	0	0	0

FPL = Failed Ply Number
FTL = Failed Thickness Location Number
FMD = Failed Mode Number
FEL = Failed Element Number
(b) = Before Stiffness Reduction
(a) = After Stiffness Reduction
(See the end of Table 4.12 for more explanation about FPL, FTL, FMD and FEL)

Table 4.12 Progression of damage for laminate A as predicted by GLPT

Displacement (in)	Load (lbs)	FPL	FTL	FMD	FEL
0.00833	448	0	0	0	0
0.01667	896	0	0	0	0
0.02500	1344 (b)	2	1	2	1-25
			2	2	1-25
	1344 (a)	2	1	2	26-32,36
			2	2	26,37
0.03333	1794 (b)	2	1	2	33-35,37-44,48,49,61,72,73, 84,85,96
			2	2	27-36,38,49,61,72,73,84,85,96
		3	1	2	37,49
			2	2	72,73,84,85,96
				4	60
		4	1	2	60,61,72,73,84,85,96
			2	2	72,73,84,85,96
	1793 (a)	2	1	2	45-47,50,51,60,62,83,86,95
			2	2	39,45-47,50,60
		3	1	2	1,12,13,25,61,72,73,84,85,96
			2	2	60,61
		4	2	2	60,61
0.04167	2241 (b)	2	1	2	52-59,63-71,74-82,87-94
			2	2	40-44,48,51-59,62-71,74-83, 86-95
				4	2
		3	1	2	2,3,9-11,14,22-24,26,27,33-36, 38,48,60
				4	39-47,51-59
			2	2	49
				4	2,4-10,14,16-22,34,48,59,72, 84,85,96
		4	1	2	48,49
				4	72,73,84,85,96
			2	2	12,24,36,48,49

(Continued·····)

Table 4.12 Progression of damage for laminate A as predicted by GLPT (Continued)

Displacement (in)	Load (lbs)	FPL	FTL	FMD	FEL
0.04167	2152 (a)	2	2	3	3-12,24
		3	1	2	15,45,46,64-71
				3	12
				4	4-10,16-22,27-35,50
			2	2	1,13,25,33,34,37,39-46
				4	3,11,15,23-36,47,71,73
				6	48
		4	1	2	36
				6	12,24,60
0.05000	2579 (b)	2	2	4	14,23
		3	1	2	4-8,16-21,28-32,39-44,47,59
				4	3,11,15,23,38
			2	2	9,23,26,27,35,47,63-71
				4	1,2,13,33,38,70
				5	60,62
				6	59,84
		4	1	2	4-8,12,24
				4	2,3,9-11,15-23,28,32-35,60
				6	29-31,36,37,48,61,72,84,85,96
			2	2	1-11,16-23,28-35
				6	60
	2577 (a)	2	2	3	36
				4	3,10,11,15,26,35
		3	1	2	62,82,95
				4	12,24,26,36
			2	2	4,8,10,11,16,20-22,28-32,38,83
				4	25,58
				5	36,48
				6	60,85,96
		4	1	2	3,9,16-20,33
				4	4,8,12,24,27,34,47
				6	48,72
0.05833	3005 (b)	2	2	3	23
				4	4-9,16-22,27,34
		3	1	2	50,51,74-81,86-94

(Continued·····)

Table 4.12 Progression of damage for laminate A as predicted by GLPT (Continued)

Displacement (in)	Load (lbs)	FPL	FTL	FMD	FEL
0.05833	3005 (b)	3	1	4	37,49,64-69
				5	12,24
				6	52-57
			2	2	3-7,15-19,48,62,70,74-82,87-95
				4	37,46
				5	12,24
				6	61,72,73
		4	1	2	2,10,15,21,27,28,32,34,47, 75-82,87-94
				4	5-7,14,26,36,46
				5	12,84
				6	39-45,59,63
			2	2	14,26,39-46,75-82,87-94
				6	12,24,36,59,63,84
	2923 (a)	1	2	1	13
		2	2	4	28-32,38,39
		3	1	2	58
				4	63,70
				6	1,13
			2	2	2,14,86
				4	83
				6	58
		4	1	2	11,14,22,23,26,35,46
				4	29,30,31,45
				5	72,96
				6	71
			2	2	38
				6	96
0.06667	3339 (b)	1	1	1	49
			2	1	1,3,15,25,27,37,39,49-51
		2	1	3	1
			2	4	1,13,33,40,47
		3	1	2	52
				3	11
				4	2,14,62
				6	25,96

(Continued·····)

Table 4.12 Progression of damage for laminate A as predicted by GLPT (Continued)

Displacement (in)	Load (lbs)	FPL	FTL	FMD	FEL
0.06667	3339 (b)	3	2	2	58
				4	39,82
				6	36,52-57
		4	1	2	29,31,45,74,86,95
				4	1,13,25,39-44
				5	60,83,85
				6	38,51-58,64-69
			2	2	74,86
				6	51-58,61,64-69,73,85
	3305 (a)	1	1	1	1,3,13,15,25,27,37,39,50,51, 61-63
			2	1	61-63
				3	2,14,38
				5	26
		2	1	4	1,13
			2	3	35
				4	41,46
		3	1	4	1,13,25,61
				6	37,49,85
			2	2	59
				5	47
				6	12,24,50,51,64-69
		4	1	2	39-44
				5	71,73
				6	83
			2	6	71
0.07500	3694 (b)	1	1	1	65-70,73-75,83,84
				6	64
			2	1	32,44,56,65-70,73-75,83-85,96
				6	64
		2	1	3	13
				4	25,37
				6	49
			2	4	42-45,50,59
				6	1,13,25,37,49,61
		3	1	3	1,23

(Continued·····)

Table 4.12 Progression of damage for laminate A as predicted by GLPT (Continued)

Displacement (in)	Load (lbs)	FPL	FTL	FMD	FEL
0.07500	3694 (b)	3	1	4	86,95
				6	50,51,61-63,73,75,76
			2	4	40,95
				5	23,35,59
				6	1,13,25,49,62,63,71
		4	1	2	25,30,71
				3	11
				4	38
				5	48,61
				6	49,50,62
			2	2	25
				6	49,50,62
	3461 (a)	1	1	1	53-56,58,72,85-87,95,96
				2	71
				5	1,13,25
				6	49
			2	1	8,20,31,33,43,45,53-55,57,58, 72,87,95
				2	71
				4	49,61
				5	1,13,25,86
				6	37
		2	1	5	49
				6	1,13,25,37,61,73
			2	4	12,24,36,48,51
				5	25,37,49,61
				6	63,73,84,85,96
		3	1	3	13,25
				4	76
				5	11,37,49,61
				6	74,83,84,87
			2	2	51
				3	1,13,25
				4	61,76
				5	11,73,84,85,96
				6	37,74,75,83
		4	1	1	73

(Continued·····)

Table 4.12 Progression of damage for laminate A as predicted by GLPT (Continued)

Displacement (in)	Load (lbs)	FPL	FTL	FMD	FEL
0.07500	3461 (a)	4	1	2	38,63,83
				3	13
				4	48,61
				5	11,86,95
				6	25,47,74,75
			2	2	63
				3	1
				4	11
				6	37,74,75
0.08333	3424 (b)	1	1	1	9-12,21-24,33-36,44-46,48,81
				2	57,59,60,61
				3	1
				4	37
				6	47,62,63,70-73,84,86,95,96
			2	1	7,9-12,19,22-24,30,34-36,42, 46,48,59,82,94
				2	60
				3	21
				4	1,13,37,72-74,84,85,96
				6	25,47,61-63,70,71,83,86,95
		2	1	3	12,24
				4	9,11,21,23,35,76,82,83,86, 94,95
				5	1,13,61,73
				6	47,62,63,70-72,74,84,85,96
			2	3	22
				4	25,37,49,60,62,71,76,82,83, 86,94,95
				5	1,13,73,84,85,96
				6	70,72
		3	1	2	56,57
				4	48,73-75,83-85,94,96
				5	1,13
				6	10,11,22,23,34,35,46,58,69-72, 80-82,86,88,95
			2	1	73,84,96
				2	50

(Continued·····)

Table 4.12 Progression of damage for laminate A as predicted by GLPT (Continued)

Displacement (in)	Load (lbs)	FPL	FTL	FMD	FEL
0.08333	3424 (b)			3	72,85
				4	45,49,63,64,75,94
				5	61,71,74,83
				6	2,3,10,11,14,15,22,26,27,34, 38,39,46,47,70,81,82-88,95
		4	1	1	61,75,83-85,96
				3	72
				5	25,49,50,59,74
				6	2,3,11,14,15,23,26,27,35, 46,70,82,86,87,94,95
			2	1	75
				2	13,71,83,95
				3	72,85
				4	3,73,84,96
				6	1,38,70,82,86,87,94
	778 (a)	1	1	1	47,57,59,60,71
				2	72,84
				5	37
				6	10-12,22-24,35,36,48,58,82
			2	1	21,71,81
				2	47,70
				4	46,60
				5	57-59
				6	10-12,22-24,34-36,48,72,82,84
		2	1	4	10,12,22,24,34-36,45,47,49, 57-59,70,71,81,84,96
				5	46,72,83
				6	9,11,23,35,48,60,69,82
			2	3	34,50
				4	57,58,70,81,84,96
				5	72,83
				6	10-12,22-24,35,36,46-48, 59,60,69,71,82
		3	1	1	11,23,35,58,59,71
				3	10,22,34,46,50,84
				4	81
				5	36,45,47,48,62,70,72,83

(Continued·····)

Table 4.12 Progression of damage for laminate A as predicted by GLPT (Continued)

Displacement (in)	Load (lbs)	FPL	FTL	FMD	FEL
0.08333	778 (a)			6	12,24,38,60,64
			2	1	11,12,47,59,60,61,72
				3	2,14,24,36,37,48,58,84
				5	1,10,22,25,26,34,38,46, 49,50,62
				6	4,9,16,21,23,28,35,40,45
		4	1	1	3,48,71,72
				2	51,59,62
				3	15,23-25,27,35,36,60,84
				4	49,50,58
				5	2,14,26,37,38,82
				6	1,4,10,13,22,34,76,81
			2	2	59,62
				3	2,3,12-15,24-26,36,37, 48-51,58,84
				4	1,10,22,60,72
				5	38
				6	11,23,27,34,35,39,47,76,81,83

FPL = Failed Ply Number
= 1, 2, 3, 4 correspond to 0, 90, +45, -45 degree plies, respectively

FTL = Failed Thickness Location Number
= 1, 2 correspond to top and bottom of the ply, respectively

FMD = Failed Mode Number
= 1, 2, 3, 4, 5, 6 correspond to σ_1, σ_2, σ_3, σ_4, σ_5, σ_6, respectively

FEL = Failed Element Number, (See Figure 4.2 for element numbering scheme)
Note that the progression of damage as predicted by GLPT is anti-symmetric about x-axis, therefore, only half the number of failed elements (1 to 96) are shown in Table 4.12

(b) = Before Stiffness Reduction

(a) = After Stiffness Reduction

The reduction of stiffness properties does not cause any further damage in the case of FSDT, due to its inability to capture the interaction of various damage modes. However, predicts substantial amount of damage after the stiffness reduction at a given displacement increment. The progression of damage is very slow and gradual in the case of GLPT, whereas FSDT predicts the failure of a total ply in more than one failure mode simultaneously. Similar trends are observed for laminates B to D.

The interaction of various damage modes and gradual progression of damage from the free edges to the interior of the laminate finally reduces the net load bearing cross section of the laminate. The area of load bearing cross section that remains intact before ultimate failure, determines the strength of the laminate. GLPT predicts a sharp reduction in the load bearing area as the loading angle is increased from 0 to 22.5 degrees (i.e. for laminates A to D), on the other hand, FSDT was not able to capture this reduction in the cross sectional area before ultimate failure. Hence, GLPT predicts a sharp reduction in the ultimate failure loads and strains of laminates A to D, and FSDT over-predicts the ultimate failure loads and strains as shown in Figures 4.10 and 4.11.

CHAPTER 5

STUDY OF DAMAGE AND FAILURES IN COMPRESSION

5.1 An Example Problem

Experiments conducted by Clark, et al. [43] revealed that the compressive strength of composite laminates is very sensitive to the specimen size and boundary conditions and the degree of sensitivity depends strongly on the lamination sequence. They have considered three different lamination sequences, namely, (1) uni-directional (2) quasi-isotropic and (3) angle-ply, and conducted experiments on test specimens of different lengths and widths. Most of the laminates considered were of 16-ply thick and some of them are of 8-ply thick. Two differrent test methods were used. The Illinois Institute of Technology Research Institute (IITRI) "wedge grip" compression fixture was used for short (0.5") specimens, and a "face supported" compression fixture was used for long (6.0") specimens. The compressive strength of the angle-ply laminate is found to be most sensitive to the specimen size and test method used.

The above problem was chosen as an example problem to study damage and failures in compression and to verify whether the present progressive failure algorithm could predict the experimental trends. The geometry and other details of the problem are shown in Figure 5.1. The laminates are made of T300/5208 graphite/epoxy pre-peg. The material properties of the pre-peg are shown in Table 5.1. The lamination sequences and the lengths and widths of test specimens considered for the progressive failure analysis are shown in Table 5.2.

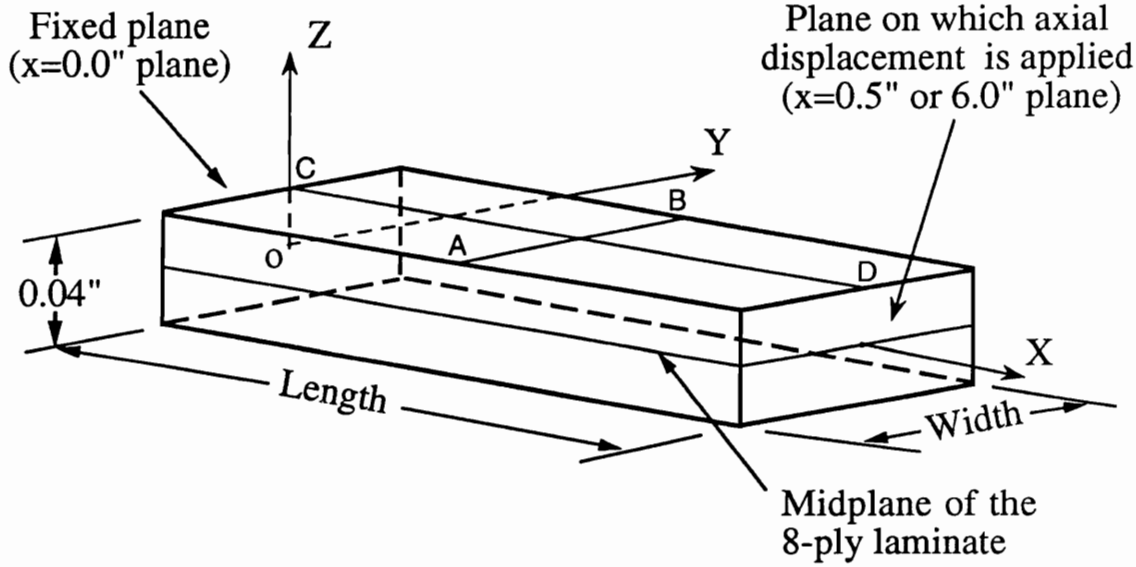

Figure 5.1 Geometry and other details of the example problem for compressive loading

Table 5.1 Material properties of T300/5208 graphite epoxy pre-peg

Properties	Values	Properties	Values
E_1	19.2×10^6 psi	X_T	219.5×10^3 psi
E_2	1.56×10^6 psi	X_C	246.0×10^3 psi
E_3	1.56×10^6 psi	$Y_T = Z_T$	6.35×10^3 psi
$G_{12}=G_{13}$	0.82×10^6 psi	$Y_C = Z_C$	23.85×10^3 psi
G_{23}	0.49×10^6 psi	R	9.80×10^3 psi
$\nu_{12}=\nu_{13}$	0.24	S=T	12.6×10^3 psi
ν_{23}	0.49	Ply thickness	0.005 in.

Table 5.2 Laminate designation, Length, Width and Stacking sequence for various laminates considered for progressive failure analysis in compression

Laminate designation	Length (in)	Width (in)	Stacking sequence*
A	0.5, 6.0	0.5, 1.0, 2.0	$(0.0/0.0/0.0/0.0)_S$
B	0.5, 6.0	0.5, 1.0, 2.0	$(0.0/+45/-45/+90)_S$
C	0.5, 6.0	0.5, 1.0, 2.0	$(+45/-45/-45/+45)_S$

(*s=Symmetric laminate)

Keeping in view the computational cost associated with the three dimensional stress analysis of composite laminates, only 8-ply thick laminates were considered for progressive failure analysis. It is assumed that the 8-ply thick laminates would exhibit the same experemental trends as those of 16-ply thick laminates in a qualitative sense.

5.2 Results and Discussion

5.2.1 Introduction

A schematic representation of a typical test specimen and end grips used in the compression testing of composite laminates is shown in Figure 5.2. The x=0.0" plane corresponds to the fixed grip and the x=0.5" or 6.0" plane corresponds to the grip where axial compressive displacement is applied. In case of 0.5" long finite element model, the actual length of the test specimen is 8.5" and end tabs of 4.0" long are used at each end. For the 6.0" long finite element model, the actual length of the test specimen is 11.0" and end tabs of 2.5" are used at each end. Therefore, the boundary conditions specified on a single cross-section, actually represent the constraint posed by the total grip on the cross section in an average or approximate sense.

The geometry and loading of the example problem are symmetric about z=0 plane. Therefore, only one half of the laminate (upper half) is considered for finite element analysis. The convergence study is conducted on the largest finite element model (i.e. 6" long and 2" wide) and the same mesh is used for all other models. Refined mesh is used near the free edges and grips as shown in Figure 5.3.

Linear Lagrange type of interpolation functions are used for both inplane and thickness directions. Therefore, each element corresponds to an 8-node brick element

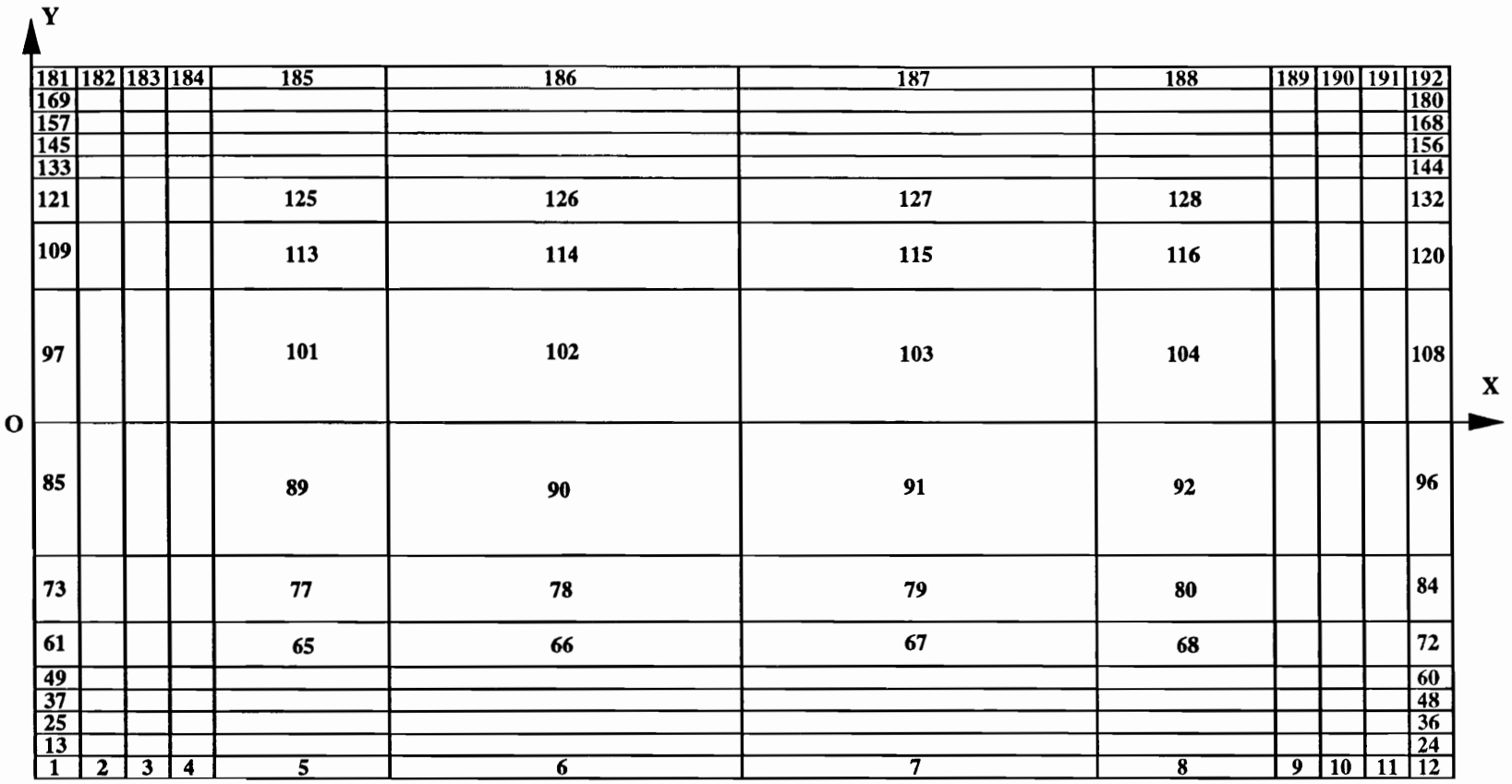

Figure 5.2 Details of the finite element mesh in the XY-Plane for compressive loading

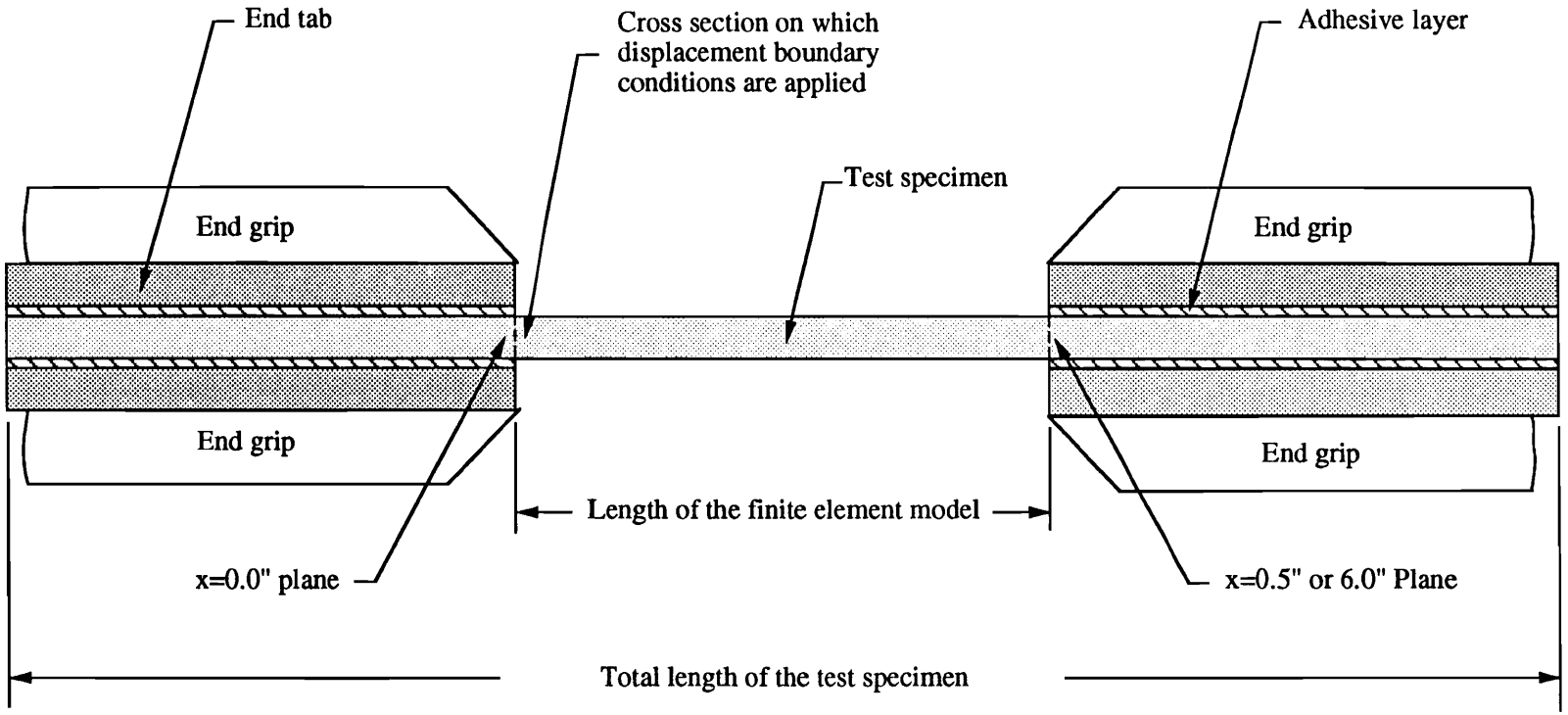

Figure 5.3 A schematic representation of the test specimen and end grips

in the conventional 3-D finite element analysis. The convergence study is conducted first with respect to the number of elements along the x-axis for a fixed number of elements (4 elements) along the y and z-axes. Then, a convergence study is conducted with respect to the number of elements along the y-axis for a fixed number of elements along the x and z-axes (12 and 4 respectively). Finally, convergence study is conducted with respect to the number of elements along the z-axis for a fixed number of elements along the x and y-axes (12 and 16 respectively).

The convergence of u-displacement at point A for various laminates with respect to the number of elements along x, y and z-axes are shown in Figures 5.4, 5.5 and 5.6 respectively. The final mesh contains 12, 16 and 8 elements along the x, y and z-axes respectively. A typical variation of the u and v-displacements along the lines AB and CD (see Figure 5.1) for various laminates is shown in Figures 5.7 and 5.8 respectively. A sharp gradient is observed in the displacement field near the free edges and at the grips. Because of this, refined mesh is used at the free edges and grips.

Ultimate stresses and strains for three different lamination sequences designated as (1) laminate A (uni-directional) (2) laminate B (quasi-isotropic) and (3) laminate C (angle-ply) are computed by using a three dimensional progressive failure algorithm and an incremental strain method. Two different lengths (0.5" and 6.0") and three different widths (0.5", 1.0", 2.0") of the test specimens are considered. A uniform u-displacement and four different types of v-displacements are used to simulate the grips.

In order to determine the optimum strain increment size a parametric study is

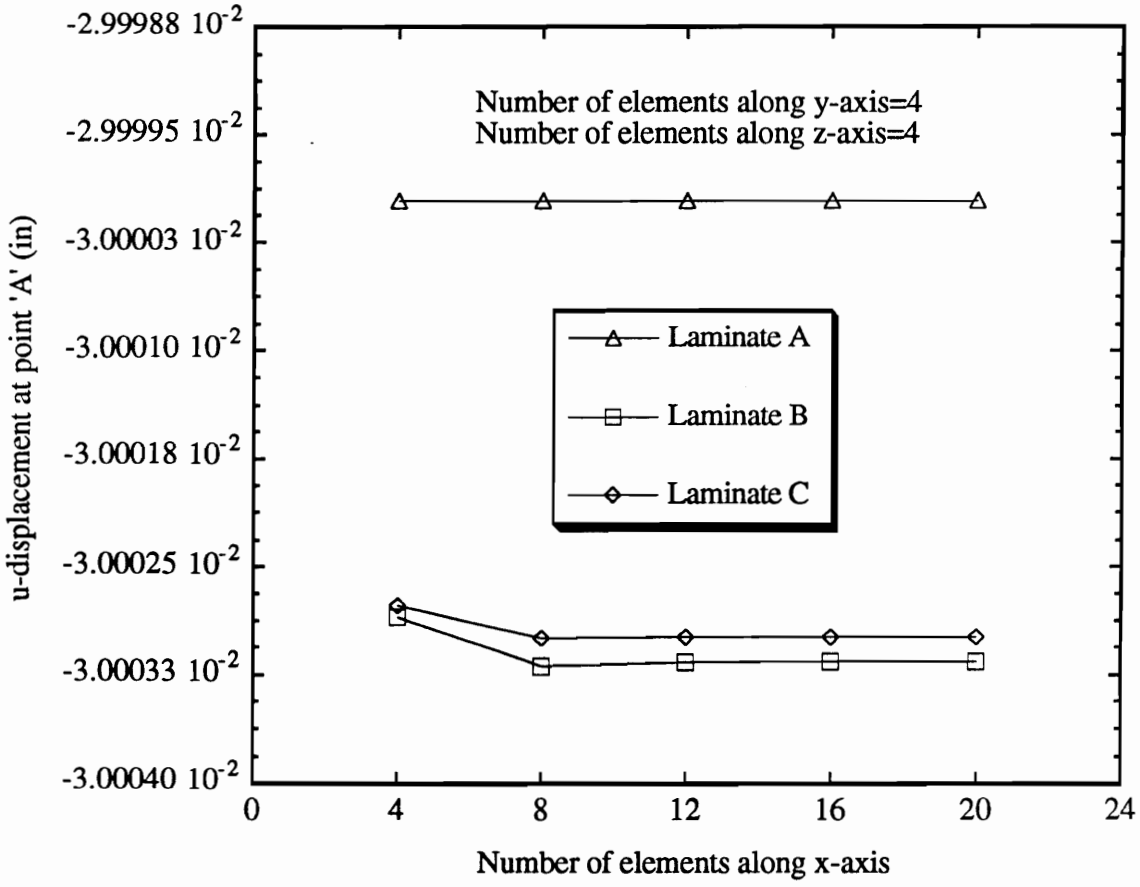

Figure 5.4 Convergence of u-displacement at point 'A' (see Figure 5.1) for laminates A,B and C of length 6" and width 2" as a function of number of elements along x-axis

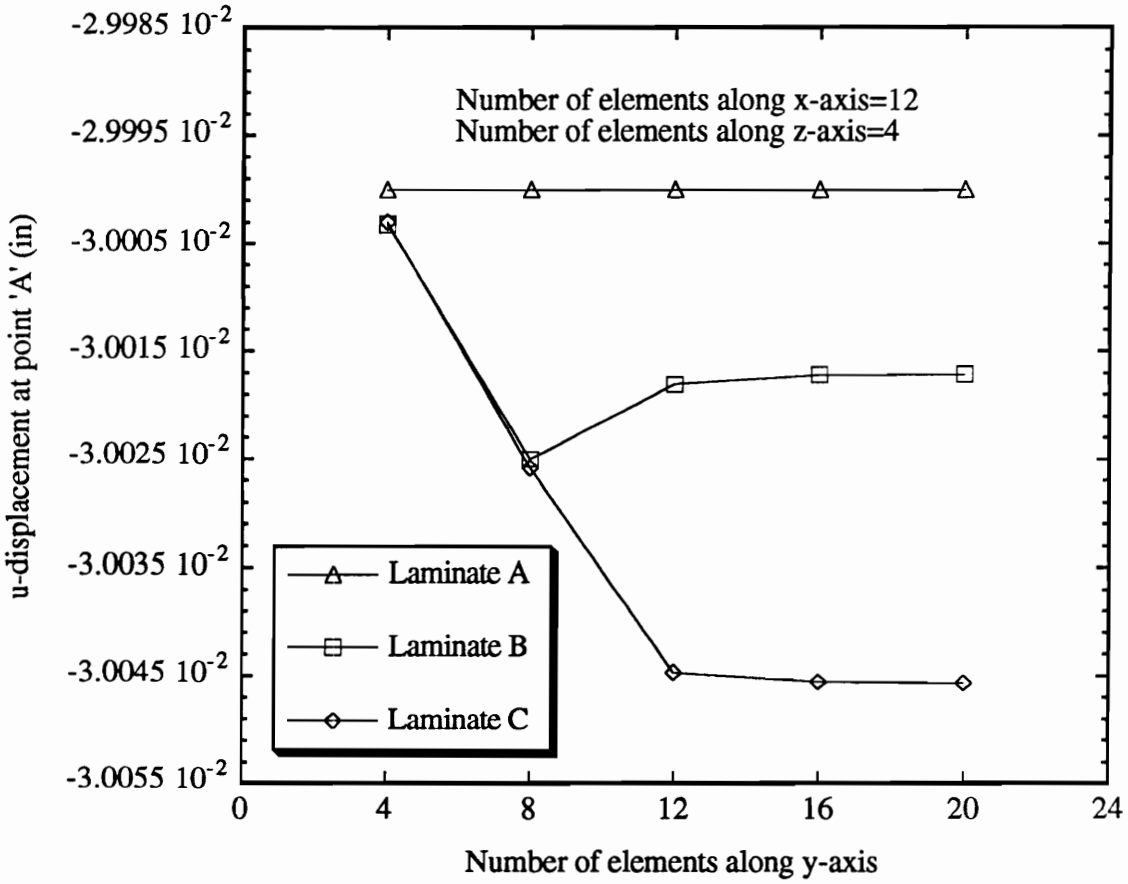

Figure 5.5 Convergence of u-displacement at point 'A' (see Figure 5.1) for laminates A,B and C of length 6" and width 2" as a function of number of elements along y-axis

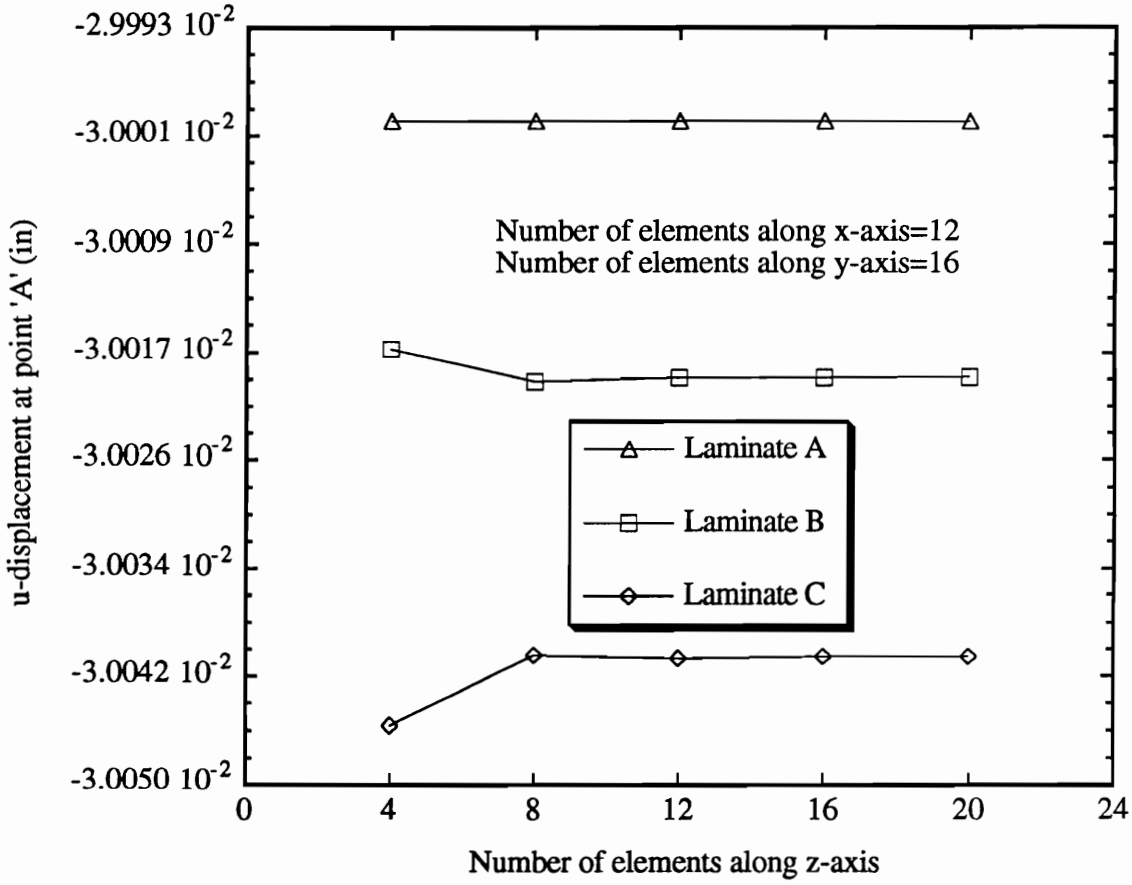

Figure 5.6 Convergence of u-displacement at point 'A' (see Figure 5.1) for laminates A,B and C of length 6" and width 2" as a function of number of elements along z-axis

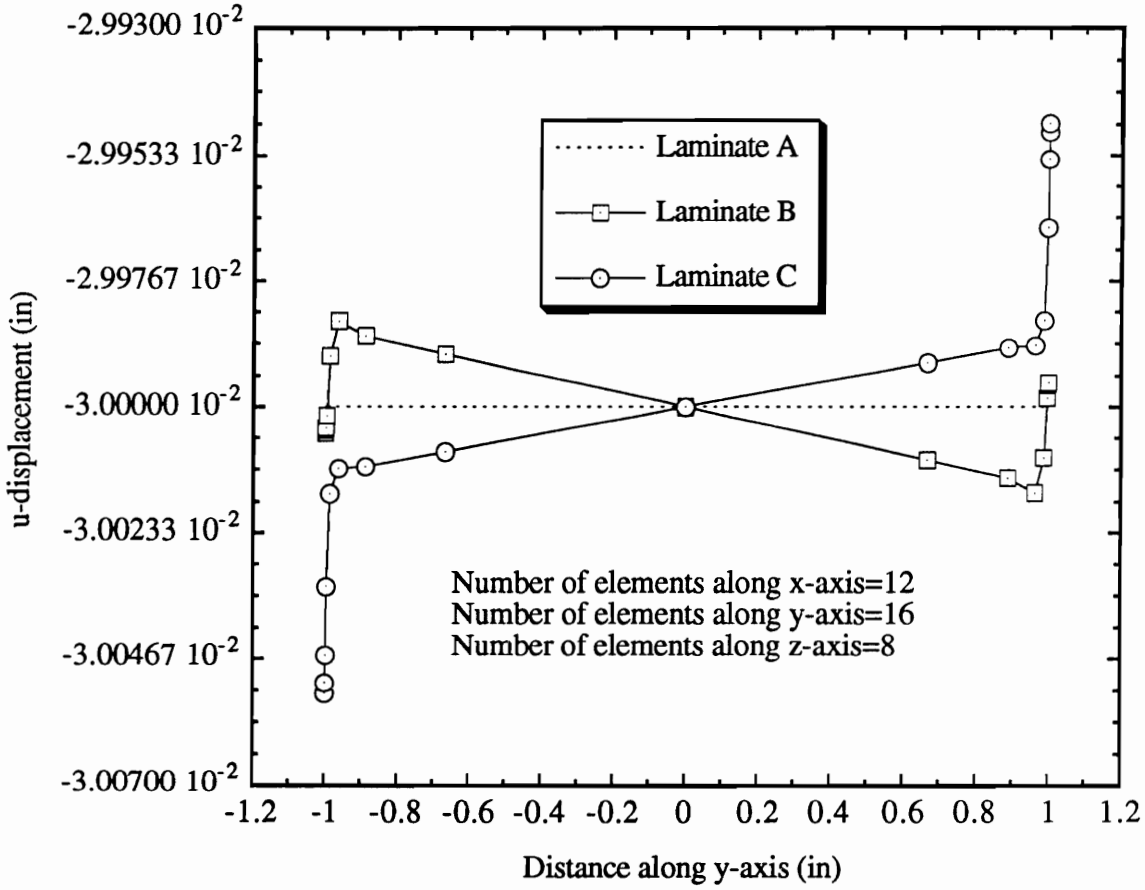

Figure 5.7 Typical variation of u-displacement along line 'AB' (see Figure 5.1) for laminates A, B and C of length 6" and width 2" subjected to BC2

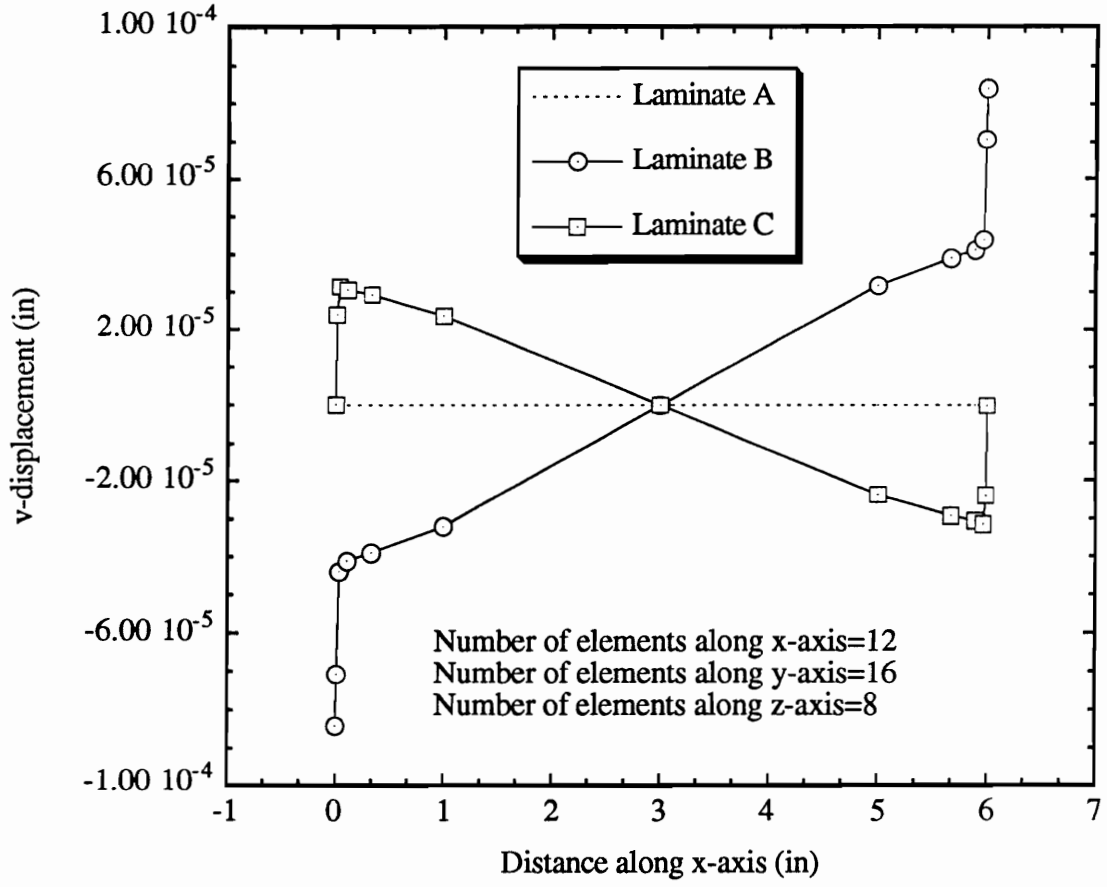

Figure 5.8 Typical variation of v-displacement along line 'CD' (see Figure 5.1) for laminates A, B and C of length 6" and width 2" subjected to BC2

conducted on the strain increment size. The results of the parametric study are presented in Figures 5.9 and 5.10. Figure 5.9 shows the influence of the strain increment size on the ultimate stress and Figure 5.10 shows its influence on the ultimate strain. The results show that there is no single strain increment size which would give both the ultimate stresses and ultimate strains accurately. Therefore, an average strain increment size of 0.1% is used in the present study.

A parametric study was conducted on the stiffness reduction method and Stiffness Reduction Coefficient (SRC). The results of the parametric study on stiffness reduction method are shown in Tables 5.3-5.6. Barring one exception in case of quasi-isotropic specimen of length 0.5", in all other cases the difference is observed to be very small. Therefore, only one stiffness reduction method (i.e. the independent stiffness reduction method) is used for computing the ultimate stresses and strains through out the present study.

The results of the parametric study on the Stiffness Reduction Coefficient are shown in Tables 5.7 and 5.8. Two values of the Stiffness Reduction Coefficients, 10^{-3} and 10^{-9} are chosen for the parametric study. The results show that the ultimate stresses and strains for the lamination sequences and material system considered in the example problem are not much sensitive to the value of the Stiffness Reduction Coefficient (SRC). Therefore, a fixed value of SRC equal to 10^{-6} is used through out the present study.

The principal objective of the present work is to study the influence of the geometry of the test specimen and the displacement boundary conditions at the grips,

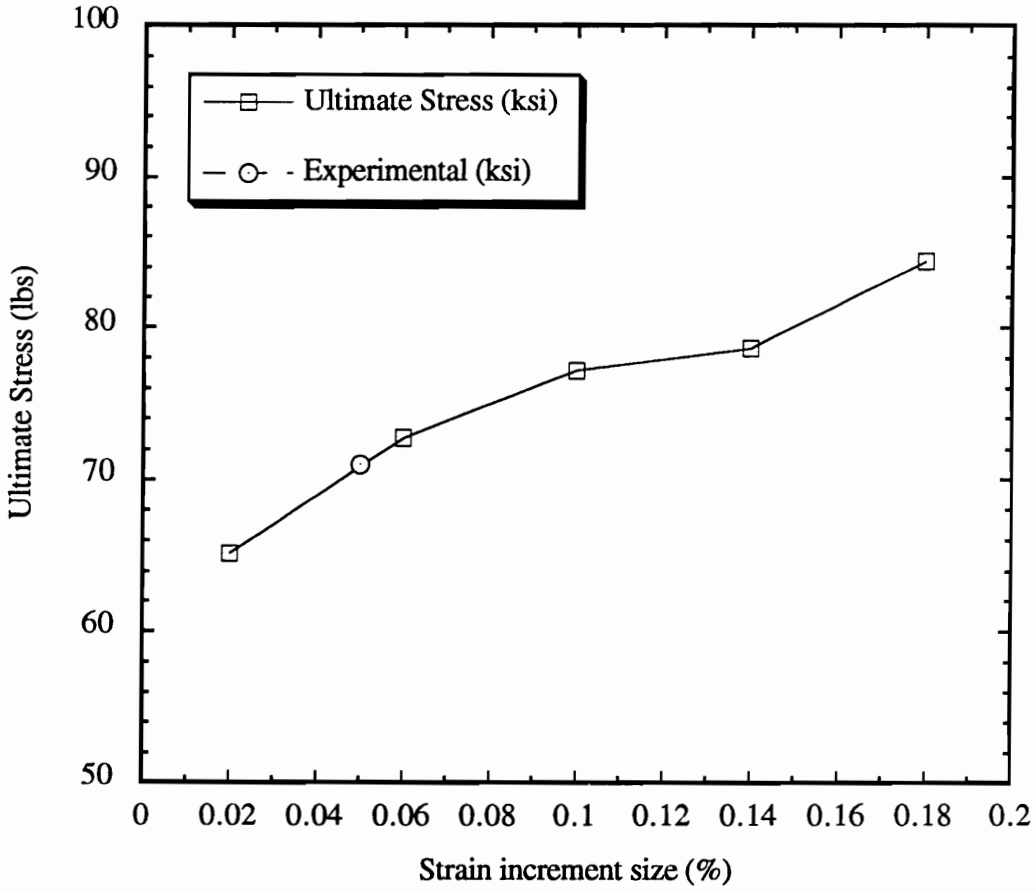

Figure 5.9 Ultimate stress versus strain increment size for laminate B of length 0.5" and width 1"

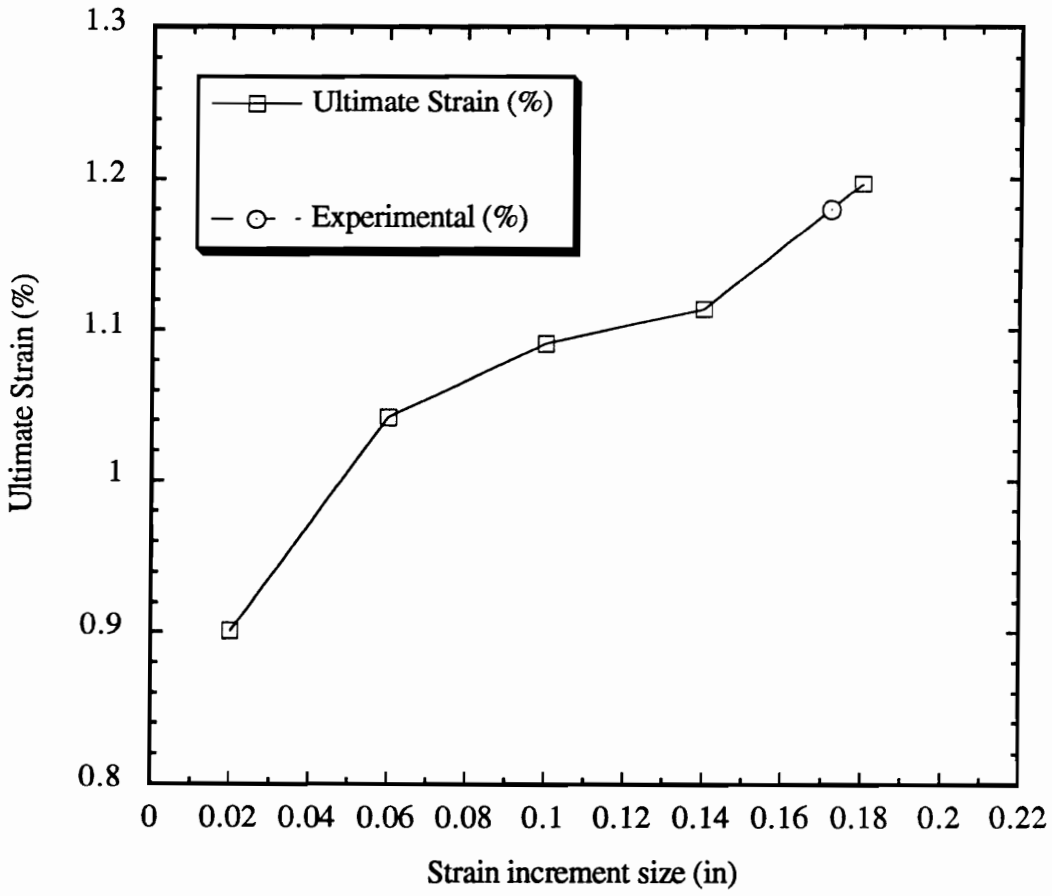

Figure 5.10 Ultimate strain versus strain increment size for laminate B of length 0.5" and width 1.0"

Table 5.3 Variation of ultimate stresses and strains with respect to stiffness reduction methods for various laminates of length 0.5" subjected to BC1

Laminate Designation	Stiffness Reduction Method	Width = 1"		Width = 2"	
		Ultimate Stress (ksi)	Ultimate Strain (%)	Ultimate Stress (ksi)	Ultimate Strain (%)
A	Independent	249.60	1.3000	249.60	1.3000
	Interactive	249.60	1.3000	249.60	1.3000
B	Independent	80.509	1.0841	80.423	1.0844
	Interactive	70.086	0.9367	70.540	0.9369
C	Independent	28.306	0.9933	28.338	0.9934
	Interactive	28.284	0.9936	28.326	0.9932

Table 5.4 Variation of ultimate stresses and strains with respect to stiffness reduction methods for various laminates of length 0.5" subjected to BC4

Laminate Designation	Stiffness Reduction Method	Width = 1"		Width = 2"	
		Ultimate Stress (ksi)	Ultimate Strain (%)	Ultimate Stress (ksi)	Ultimate Strain (%)
A	Independent	247.71	1.3091	294.35	1.7127
	Interactive	259.33	1.5086	276.73	1.6094
B	Independent	91.370	1.4601	100.02	1.2952
	Interactive	87.496	1.2396	92.467	1.2702
C	Independent	50.922	1.2835	73.895	1.5784
	Interactive	50.967	1.2011	67.984	1.3520

Table 5.5 Variation of ultimate stresses and strains with respect to stiffness reduction methods for various laminates of length 6.0" subjected to BC1

Laminate Designation	Stiffness Reduction Method	Width = 1"		Width = 2"	
		Ultimate Stress (ksi)	Ultimate Strain (%)	Ultimate Stress (ksi)	Ultimate Strain (%)
A	Independent	249.60	1.3000	249.60	1.3000
	Interactive	249.60	1.3000	249.60	1.3000
B	Independent	83.835	1.1980	88.693	1.1994
	Interactive	83.431	1.1898	88.260	1.1923
C	Independent	28.408	0.9997	28.439	0.9997
	Interactive	28.408	0.9997	28.439	0.9997

Table 5.6 Variation of ultimate stresses and strains with respect to stiffness reduction methods for various laminates of length 6.0" subjected to BC4

Laminate Designation	Stiffness Reduction Method	Width = 1"		Width = 2"	
		Ultimate Stress (ksi)	Ultimate Strain (%)	Ultimate Stress (ksi)	Ultimate Strain (%)
A	Independent	249.58	1.3012	248.90	1.3041
	Interactive	249.37	1.3009	248.32	1.3048
B	Independent	84.586	1.2087	89.097	1.2146
	Interactive	85.491	1.2048	88.355	1.2052
C	Independent	29.816	1.0554	31.328	1.1142
	Interactive	29.697	1.0507	30.807	1.0995

Table 5.7 Variation of ultimate stresses and strains with respect to stiffness reduction coefficients (SRC) for various laminates of length 0.5" subjected to BC4

Laminate Designation	Stiffness Reduction Coefficient (SRC)	Width = 1"		Width = 2"	
		Ultimate Stress (ksi)	Ultimate Strain (%)	Ultimate Stress (ksi)	Ultimate Strain (%)
A	10^{-3}	249.05	1.3015	277.01	1.6093
	10^{-9}	259.33	1.5086	276.73	1.6094
B	10^{-3}	88.185	1.2330	92.820	1.2687
	10^{-9}	87.496	1.2396	92.469	1.2702
C	10^{-3}	51.017	1.2006	71.801	1.4508
	10^{-9}	50.967	1.2011	67.984	1.3520

Table 5.8 Variation of ultimate stresses and strains with respect to stiffness reduction coefficients (SRC) for various laminates of length 6.0" subjected to BC4

Laminate Designation	Stiffness Reduction Coefficient (SRC)	Width = 1"		Width = 2"	
		Ultimate Stress (ksi)	Ultimate Strain (%)	Ultimate Stress (ksi)	Ultimate Strain (%)
A	10^{-3}	249.37	1.3009	248.45	1.3046
	10^{-9}	249.37	1.3009	248.32	1.3048
B	10^{-3}	85.277	1.2026	88.462	1.2063
	10^{-9}	85.491	1.2048	88.355	1.2052
C	10^{-3}	29.688	1.0508	30.812	1.0996
	10^{-9}	29.687	1.0507	30.807	1.0995

on the ultimate stresses and strains of a composite laminates of different stacking sequences under compression loading. Therefore, a parametric study is conducted on the geometry of the test specimen and the displacement boundary conditions at the grips, for three different lamination sequences. The results of the parametric study pertaining to each lamination sequence are presented below:

5.2.2 Unidirectional Laminate (Laminate A)

The results of the parametric study on the geometry of the test specimen and the displacement boundary conditions at the grips for laminate A (uni-directional) are shown in Tables 5.9 and 5.10. The results show that the ultimate stresses and strains predicted by BC1 and BC2 are exactly same. This implies that constraining of the rigid body rotation of the test specimen has no influence on the ultimate stresses and strains. These boundary conditions also predict the same values of ultimate stresses and strains for all the geometries of the test specimen, which is not in agreement with the experimental results. Therefore, it can be concluded that these boundary conditions do not exactly represent the actual constraint posed by the grips in case of uni-directional laminates.

The ultimate stresses and strains predicted by BC3 and BC4 are sensitive to the geometry of the test specimen. However, it is not possible to ascertain as to which is a better approximation than the other to simulate the actual constraint posed by the grip, since experimental results were available only for 16-ply laminates. The large scatter in the experimental results for the 16-ply laminates [43] indicates that, even if experimental results were available for the 8-ply laminates, it is not desirable to

Table 5.9 Variation of ultimate stresses and strains with respect to various boundary conditions and widths for laminate A of length 0.5"

Boundary condition	Width = 0.5"		Width = 1.0"		Width = 2.0"	
	Ultimate Stress (ksi)	Ultimate Strain (%)	Ultimate Stress (ksi)	Ultimate Strain (%)	Ultimate Stress (ksi)	Ultimate Strain (%)
BC1	249.60	1.3000	249.60	1.3000	249.60	1.3000
BC2	249.60	1.3000	249.60	1.3000	249.60	1.3000
BC3	216.58	1.2256	224.53	1.2088	249.60	1.3000
BC4	247.20	1.3024	247.71	1.3019	294.40	1.7130
Expt. (16-ply)	205(10)*	1.3(0.12)	220(13)	1.5(0.17)	230(19)	1.7(0.31)

* Values within the parenthesis indicate standard deviation

Table 5.10 Variation of ultimate stresses and strains with respect to various boundary conditions and widths for laminate A of length 6.0"

Boundary condition	Width = 0.5"		Width = 1.0"		Width = 2.0"	
	Ultimate Stress (ksi)	Ultimate Strain (%)	Ultimate Stress (ksi)	Ultimate Strain (%)	Ultimate Stress (ksi)	Ultimate Strain (%)
BC1	249.60	1.3000	249.60	1.3000	249.60	1.3000
BC2	249.60	1.3000	249.60	1.3000	249.60	1.3000
BC3	229.67	1.1967	229.83	1.1999	191.31	1.0029
BC4	249.55	1.2999	249.58	1.3012	248.90	1.3041
Expt. (16-ply)	N/A	N/A	190(8)*	1.2(0.1)	171(5)	1.1(0.22)

* Values within the parenthesis indicate standard deviation

look for a quantitative agreement between the experimental results and numerical predictions. Hence, in the present study the numerical predictions are compared with the experimental results, only to check whether there is an agreement between the two, in a qualitative sense.

5.2.3 Quasi-Isotropic Laminate (Laminate B)

The results of the parametric study on the geometry of the test specimen and the displacement boundary conditions at the grips for laminate B (quasi-isotropic) are shown in Tables 5.11 and 5.12. In this case, the boundary conditions BC1 and BC2 predict different values for different lengths of the specimen. But, they predict the same ultimate stresses and strains for different widths, when the length of the test specimen is fixed. This implies that BC1 and BC2 are not able to capture the size effect fully and hence do not represent the correct boundary conditions posed by the grip even on a quasi-isotropic laminate.

The ultimate stresses and strains predicted by BC3 and BC4 are more sensitive to the width of the test specimen when the specimen length is 0.5". When the specimen length is increased from 0.5" to 6.0" they predict less sensitivity to the width effect. This is in agreement width the experimental trends observed in case of 16-ply thick quasi-isotropic laminates. Comparison of the numerical results with the experimental results (see Table 11) shows that the results predicted by BC3 are in better agreement with the ultimate stresses, while the predictions of BC4 are in better agreement with the ultimate strains. This suggests that the actual constraint posed by the grips may be somewhere in between the constraint posed by BC3 and BC4.

Table 5.11 Variation of ultimate stresses and strains with respect to various boundary conditions and widths for laminate B of length 0.5"

Boundary condition	Width = 0.5"		Width = 1.0"		Width = 2.0"	
	Ultimate Stress (ksi)	Ultimate Strain (%)	Ultimate Stress (ksi)	Ultimate Strain (%)	Ultimate Stress (ksi)	Ultimate Strain (%)
BC1	77.133	1.0910	80.509	1.0841	80.423	1.0844
BC2	77.025	1.0921	80.134	1.0850	80.425	1.0845
BC3	74.237	1.1120	79.933	1.0850	78.307	1.0907
BC4	86.929	1.2509	91.370	1.4601	100.02	1.2952
Expt. (8-ply)	70(11)*	1.2(0.26)	71(4)	1.3(0.18)	71(6)	1.3(0.15)

* Values within the parenthesis indicate standard deviation

Table 5.12 Variation of ultimate stresses and strains with respect to various boundary conditions and widths for laminate B of length 6.0"

Boundary condition	Width = 0.5"		Width = 1.0"		Width = 2.0"	
	Ultimate Stress (ksi)	Ultimate Strain (%)	Ultimate Stress (ksi)	Ultimate Strain (%)	Ultimate Stress (ksi)	Ultimate Strain (%)
BC1	84.428	1.1972	83.835	1.1980	88.693	1.1994
BC2	84.538	1.1988	83.900	1.1990	88.693	1.1994
BC3	83.561	1.1855	82.369	1.1765	82.236	1.1178
BC4	84.927	1.2045	84.586	1.2087	89.097	1.2146
Expt. (16-ply)	74(5)*	1.3(0.11)	75(4)	1.3(0.17)	74(4)	1.3(0.05)

* Values within the parenthesis indicate standard deviation

5.2.4 Angle-Ply Laminate (Laminate C)

The results of the parametric study on the geometry of the test specimen and the displacement boundary conditions at the grips for laminate C (angle-ply) are shown in Tables 5.13 and 5.14. In this case the boundary conditions BC1 and BC2 are not able to capture both length and width effects on the ultimate stresses and strains. This demonstrates the inability of BC1 and BC2 to simulate the actual constraint posed by the grips for all the three lamination sequences.

For the 0.5" long specimen, the predictions of BC3 and BC4 differ from each other by almost by 100%. This implies that the angle-ply laminates of short length are extremely sensitive to the boundary conditions. Also, for these short specimens of length 0.5", BC4 predicts about 50% sensitivity to the width effect, while BC3 is not able to capture this kind of width effect quantitatively. When the length of the test specimen is increased from 0.5" to 6.0", BC4 predicts less sensitivity to the width effect. The numerical trends predicted by BC4 are in good agreement with the experimental trends observed in case of 16-ply thick angle-ply laminates.

However, the observed agreement between the trends predicted by BC4 and the experimental trends is not adequate to conclude that BC4 represents the actual constraint posed by the grips. A close look at the construction of the test specimen (see Figure 5.3) reveals that the constraining of v-displacement throughout the cross section (which is assumed in case of BC4) is inappropriate. Also, the application of a uniform u-displacement throughout the cross section, is also only a first order approximation to the reality.

Table 5.13 Variation of ultimate stresses and strains with respect to various boundary conditions and widths for laminate C of length 0.5"

Boundary condition	Width = 0.5"		Width = 1.0"		Width = 2.0"	
	Ultimate Stress (ksi)	Ultimate Strain (%)	Ultimate Stress (ksi)	Ultimate Strain (%)	Ultimate Stress (ksi)	Ultimate Strain (%)
BC1	28.242	0.9945	28.306	0.9933	28.338	0.9934
BC2	28.243	0.9947	28.308	0.9936	28.339	0.9937
BC3	27.832	1.0760	28.788	0.9354	33.121	0.8009
BC4	40.406	1.3455	50.922	1.2835	73.894	1.5784
Expt. (16-ply)	28(1)*	3.3(0.23)	32(1)	3.8(0.34)	48(4)	4.9(0.09)

* Values within the parenthesis indicate standard deviation

Table 5.14 Variation of ultimate stresses and strains with respect to various boundary conditions and widths for laminate C of length 6.0"

Boundary condition	Width = 0.5"		Width = 1.0"		Width = 2.0"	
	Ultimate Stress (ksi)	Ultimate Strain (%)	Ultimate Stress (ksi)	Ultimate Strain (%)	Ultimate Stress (ksi)	Ultimate Strain (%)
BC1	28.347	0.9997	28.408	0.9997	28.439	0.9997
BC2	28.347	0.9997	28.408	0.9997	28.439	0.9997
BC3	28.335	0.9994	28.199	0.9941	27.892	0.9885
BC4	29.060	1.0264	29.816	1.0554	31.328	1.1142
Expt. (16-ply)	N/A	N/A	29(1)*	2.2(0.23)	30(1)	2.3(0.25)

* Values within the parenthesis indicate standard deviation

The actual load/displacement transfer takes place due to the frictional contact between the end tabs and the grips. The presence of the adhesive layer between the end tabs and the test specimen makes the load/displacement transfer mechanism more complicated. It may be possible to simulate the constraint posed by the end grips more accurately by including the end tabs and the adhesive layer in the mathematical model. But, this increases the computational cost enormously and the resulting accuracy may not be proportional to the computational cost. In view of this, it may be concluded that simple gripping methods that are amenable to analysis are desirable in order to model the compression testing of composite laminates accurately.

CHAPTER 6

STUDY OF DAMAGE AND FAILURES IN BENDING

6.1 An Example Problem

Turvey [44], and Reddy, et al. [2] demonstrated that the first-ply failure loads of composite laminates subjected to bending loads are extremely senstive to the effect of geometric nonlinearity. Turvey used a dynamic relaxation (DR) technique for laminate analysis. In the DR technique static equilibrium of a vibrating system is achieved by applying near critical damping and specifying a maximum tolerable error on the velocities of the vibrating system. Thus, the DR technique ensures static equilibrium only in an approximate sense. Reddy, et al. used the finite element method for the laminate analysis. The finite element model was based on the First order Shear Deformation Theory (FSDT) and the geometric nonlinearity was taken in to account in the von *Kármán* sense.

Linear and nonlinear first-ply failure loads were computed for composite laminates under uniformly distributed transverse load with simply supported and clamped boundary conditions. The difference between linear and nonlinear first-ply failure loads was shown to be very sensitive to the laminate thickness and boundary conditions. The difference was found to be large for thin laminates and simply supported boundary conditions and much less for thick and clamped boundary conditions. However, the study was limited to only first-ply failures and FSDT.

In the present study the effect of geometric nonlinearity (in the von *Kármán*

sense), is studied both on the first-ply and progressive failure loads, and the predictions of FSDT and GLPT are compared. The three-point bending test is chosen as an example problem. The geometry and other details of the example problem are shown in Figure 6.1. Due to symmetry about the x and y-axes, only one quarter of the test specimen is considered for finite element modeling. The lamination sequences, support span and widths of the test specimens considered for the first-ply and progressive failure analysis are shown in Table 6.1. The depth (d) of the test specimen is 0.04". The span (S) of 0.64" corresponds to an S/d ratio of 16 and that of 1.28" corresponds to an S/d ratio of 32. The material properties (T300/5208) are given in Table 5.1.

Two different boundary conditions are considered for the first-ply and progressive failure analysis. In the first case the laminate is assumed to slide freely on the supports in the x-direction, and in the second case the u- displacement is restrained at the support. These boundary conditions are designated as BC1 and BC2 respectively. In the case of FSDT both the u and w-displacements are restrained at the midplane of the laminate, while in the case of GLPT they are restrained at the bottom surface of the laminate. However, along the axes of symmetry the displacements are restrained throughout the thickness.

6.2 Results and Discussion

6.2.1 Introduction

First-ply and progressive failure loads are computed for different lamination sequences, boundary conditions, and span-to-depth ratios of the test specimen. Both

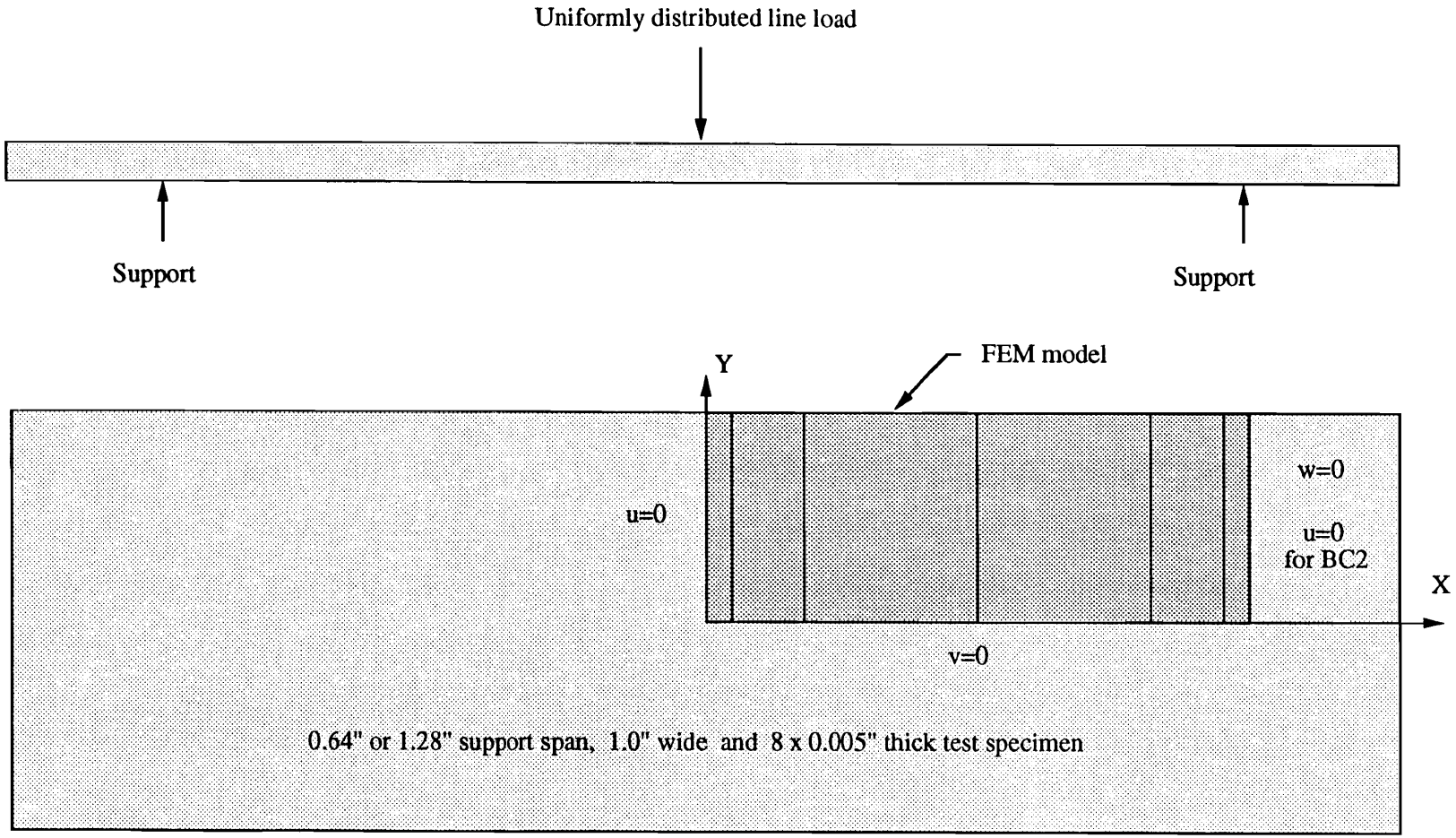

Figure 6.1 Geometry and other details of the example problem in bending

Table 6.1 Laminate designation, Support span, Width and Stacking sequence for various laminates considered for progressive failure analysis in bending

Laminate designation	Support span (in)	Width (in)	Stacking sequence*
A	0.64, 1.28	1.0	$(0.0/0.0/0.0/0.0)_S$
B	0.64, 1.28	1.0	$(90.0/90.0/90.0/90.0)_S$
C	0.64, 1.28	1.0	$(0.0/0.0/90.0/90.0)_S$

(*s=Symmetric laminate)

linear and nonlinear failure loads are computed by using the Tsai-Wu failure criterion and the finite element method. The finite element model is developed based on both the First Order Shear Deformation Theory (FSDT) and the Generalized Layerwise Plate Theory (GLPT). The Newton-Raphson iteration procedure is used to solve the nonlinear algebraic equations of the finite element model.

Reduced integration is used to evaluate all the transverse stiffness terms and full integration is used to evaluate all other stiffness terms in the case of FSDT. However, this type of selective reduced integration is not desirable in the case of GLPT, because it gives rise to spurious energy modes and abnormal out-of-plane deflections. Therefore, full integration is used throughout in the case of GLPT.

(i) Computation of Stresses

The stresses are computed at the reduced integration Gauss points. However, in the case of transverse loading the maximum normal stress occurs always at the top and bottom surfaces of the laminate. Therefore, the Gauss point stresses are extrapolated to the corner nodes of the finite element before applying the failure criterion, and the stiffness properties are reduced at the corner nodes. These nodal stiffness properties are again interpolated to obtain the stiffness properties at the Gauss points to compute the direct and tangent stiffness matrices. Linear Lagrange interpolation functions are used to interpolate the stiffness properties. It is not desirable to use quadratic interpolation or extrapolation functons, because when the stiffness property at the center nodes is made equal to zero, there is a possibility of the stiffness properties getting negative in betwen the nodes.

When the stresses are extrapolated form the Gauss points to the nodes, there is a possibility that maximum stress may occur at a node which has already failed. In order to avoid this possibility the stresses are not extrapolated to the nodes which have already failed. Also, the First Order Shear Deformation Theory predicts transverse shear stresses even on the free (top and bottom) surfaces, which is not correct in reality. These stresses could have an influence on the failure loads when a polynomial failure criterion such as the Tsai-Wu criterion is used to predict the failures. Therefore, the transverse shear stresses are enforced to be zero at the top and bottom surfaces.

(ii) Finite Element Mesh

The finite element mesh used in the progressive failure analysis is shown in Figure 6.1. A refined mesh is used near the support and at the middle of the test specimen, where the uniformly distrbuted line load is applied. The number of elements along the x-axis are chosen to be 6, after conducting a convergence study for a fixed number of elements along the y and z-axes (1 and 4 respectively). The results of the convergence study are shown in Tables 6.2 and 6.3. Table 6.2 contains both linear and nonlinear first-ply failure loads as predicted by FSDT for various number of elements along the x-axis. It can be observed that the mesh refinement has no effect on the failure loads predicted by FSDT.

However, in the case of GLPT, a sharp reduction in the failure loads is observed, when the number of elements are increased from 4 to 6 (see Table 6.3). This is due to the change in the mode and location of failure. In the case of 4 elements the failure

Table 6.2 Results of the convergence study on the first-ply failure load of various laminates with respect to the number of elements along x-axis (NEX) by using FSDT

Laminate Designation	Finite Element Model	First-Ply Failure Load (lbs) NEX=2	NEX=4	NEX=6	NEX=10
A	Linear	147.1	146.9	146.9	146.9
	Nonlinear	155.8	152.7	152.8	155.0
B	Linear	5.244	5.245	5.246	5.246
	Nonlinear	5.299	5.245	5.246	5.246
C	Linear	113.7	113.7	113.7	113.7
	Nonlinear	116.8	115.7	115.7	115.6

Table 6.3 Results of the convergence study on the first-ply failure load of various laminates with respect to the number of elements along x-axis (NEX) by using GLPT

Laminate Designation	Finite Element Model	First-Ply Failure Load (lbs) NEX=2	NEX=4	NEX=6	NEX=10
A	Linear	169.9	151.6	72.03	73.00
	Nonlinear	174.5	151.6	74.68	75.92
B	Linear	6.801	5.391	5.292	5.273
	Nonlinear	6.909	5.391	5.292	5.273
C	Linear	127.1	118.4	74.61	73.74
	Nonlinear	143.6	124.0	77.42	73.74

is due to the flexural stress and took place at the midspan of the test specimen, whereas in the case of 6 elements the failure is due to σ_3 and occured near the support. When the number of elements are increased from 6 to 10 no change is observed in the failure loads. Therefore, the number of elements along the x-axis are chosen to be 6.

6.2.2 First-Ply Failure Analysis

The first-ply failure analysis is based on the assumption that a given ply would fail when the failure index at any point within the ply reaches a value of unity. The failure index is defined as $F_i\sigma_i + F_{ij}\sigma_{ij}$, where F_i and F_{ij} are as defined in (3.5). The computation of the first-ply failure load for the nonlinear formulation requires an iterative procedure. The steps used in the iterative procedure are listed below:

Step 1 Find the displacement field for a small initial load

Step 2 Find the stresses for the above displacement field

Step 3 Transform the stresses into the material coordinates

Step 4 Find the maximum failure index

Step 5 Check whether the laminate has failed or not

Step 6 If not, increase or decrease the initial load appropriately

Step 7 Repeat the Steps 1 to 6 until the laminate fails

The maximum failure index is deterimined by carrying out a sequential search at certain chosen points within the laminte. The sequence of the search is as follows:

(1) Consider the first element of the finite element mesh

(2) Consider the first Gauss point within the element

(3) Consider the first ply (from the bottom) of the laminate

(4) Consider the bottom of the current ply

(5) Find the failure index at that location

(6) Check whether the failure index is greater than the previous value

(7) If the answer is YES, store the element number, Gauss point number, ply number, the location within the ply (i.e. top or bottom), the failure index and goto the next location

(8) If the answer is NO, then do not store the failure data, but goto the next location and repeat Steps 5 to 8

(9) Continue the search until all the elements in the finite element mesh are searched for the maximum failure index.

The laminate failure is checked by comparing the absolute value of (maximum failure index - 1) with a predetermined value of maximum tolerable error ' e '. In the present study the value of ' e ' is chosen to be 0.01. For the linear failure analysis the initial load is chosen to be unity and for the nonlinear failure analysis the initial load is chosen to be the linear failure load. At the end of each iteration, the initial load for the next iteration is computed as below:

Initial load for the next iteration = (Initial load of current iteration) (λ)

where λ is a multiplication factor to be computed as below:

For the independent failure criteria λ is given as

$$\lambda = 1/(Maximum\ failure\ index)$$

For the polynomial failure criteria λ is obtained by solving the following quadratic

equation:

$$\lambda^2(F_{ij}\sigma_i\sigma_j) + \lambda(F_i\sigma_i) - 1 = 0$$

The real and smaller value of λ obtained from the above equation is used to compute the initial load for the next iteration. The results of the first-ply failure analysis are discussed below:

Figure 6.2 shows the results of first-ply failure analysis for an S/d ratio of 16 and BC1. The linear and nonlinear loads are found to be almost same in this case. This is due to the small S/d ratio. The failure loads predicted by the GLPT are much smaller than those of FSDT in the case of lamintes A and C. Because, the loads are not corresponding to the same failure mode and locations. In the case of FSDT the failure took place at the center of the span and is due to σ_1 for laminate A and due to σ_2 for laminate C. Whereas, in the case of GLPT the failure took place at the support of the span and is due to σ_3 for both laminates. However, for laminate B, both FSDT and GLPT predict the failure at the midspan due to σ_2. This is due to the fact that the transverse strength (Y) of the composite is much smaller than the longitudinal strength (X).

Figure 6.3 shows the results of first-ply failure analysis for an S/d ratio of 16 and BC2. The results show that for a given S/d ratio, when the specimen is not allowed to slide on the support (BC2), FSDT predicts an increased effect of geometric nonlinearity for laminate A. GLPT predicts the same linear and nonlinear failure loads, because the failure took place at the support. The effect of geometric nonlinearity is not appreciable in case of laminate B, because it failed at a very small

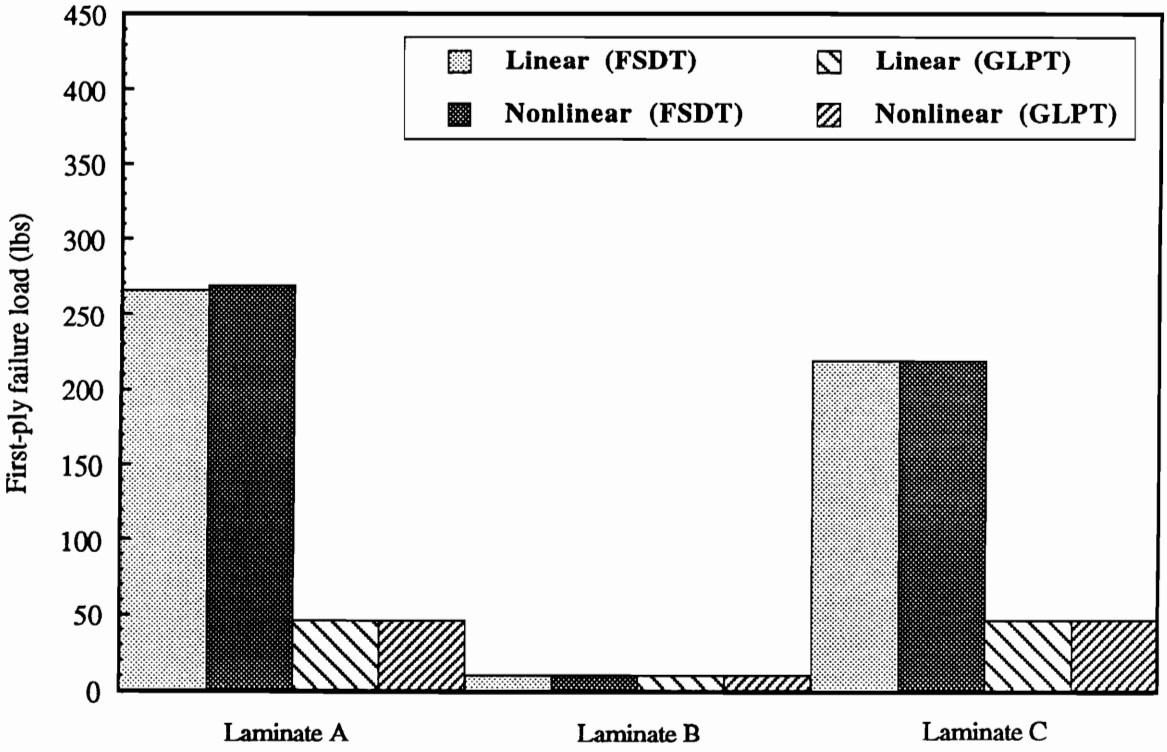

Figure 6.2 Comparison of linear and nonlinear first-ply failure loads as predicted by FSDT and GLPT for different laminates (S/d =16, BC1)

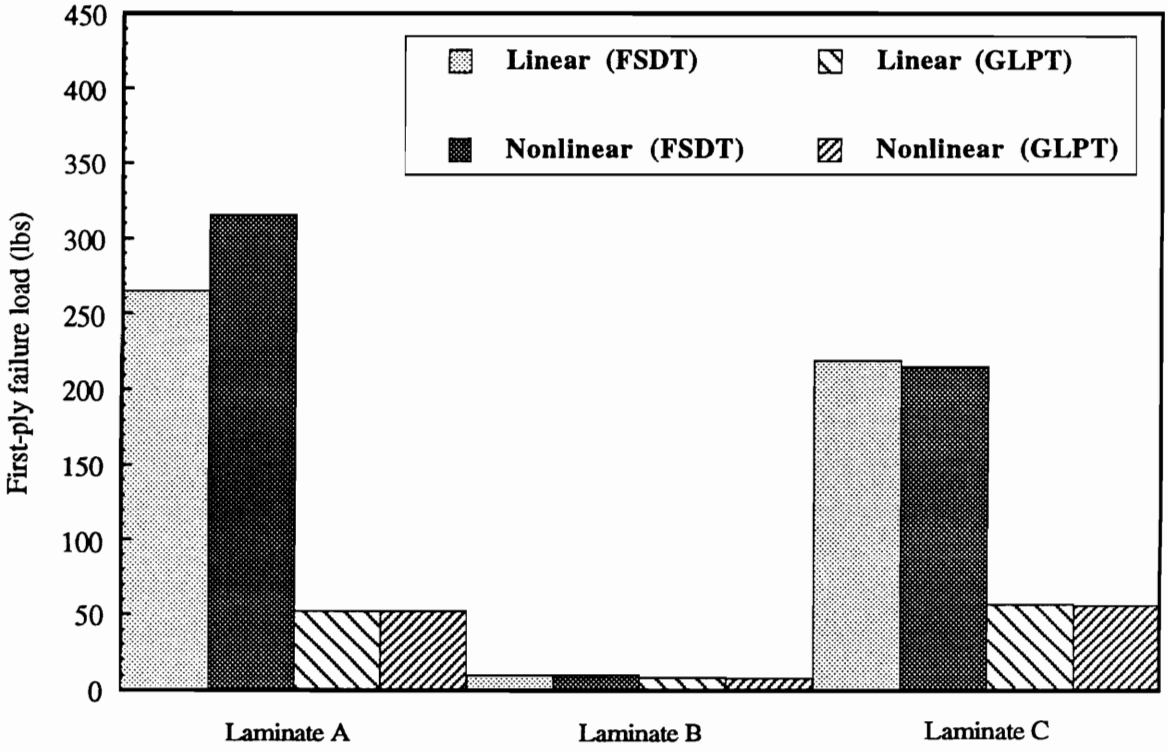

Figure 6.3 Comparison of linear and nonlinear first-ply failure loads as predicted by FSDT and GLPT for different laminates (S/d =16, BC2)

center displacement (0.16 times laminate thickness) whereas laminate A failed at a center displacement of 0.4 times the laminate thickness. For laminate C, the nonlinear failure load predicted by FSDT is observed to be slightly smaller than the linear failure load. This is due to the fact that the failure takes place interior to the laminate, in between the midplane and bottom surface, at a relatively small displacement (0.25 times the laminate thickness).

Figure 6.4 shows the results of first-ply failure analysis for an S/d ratio of 32 and BC1. The results show that for the same boundary condition (BC1), when the S/d ratio is increased, there is a sharp drop in the failure loads for all those laminates which fail at the midspan. Whereas, for those laminates which fail at the support, an increase is observed in the failure loads. Thus, both FSDT and GLPT predict a decrease in failure load for laminate B, while for laminates A and C, FSDT predicts a decrease and GLPT predicts an increase in the failure load.

Figure 6.5 shows the results of first-ply failure analysis for an S/d ratio of 32 and BC2. The results indicate that for the same S/d ratio, when the boundary condition is changed from BC1 to BC2, there is a 100% increase in the nonlinear failure load for laminate A, whereas the linear failure load remains the same. This is due to the fact that the linear failure load is not sensitive to the stretching effect of the laminate, which happens in case of BC2. In the case of laminate B, GLPT predicts the linear failure load more than the nonlinear failure load, because the linear failue is predicted at the support and the nonlinear failure is predicted at the midspan. For laminate C the effect of geometric nonlinerity is not to the same degree as in the case of laminate

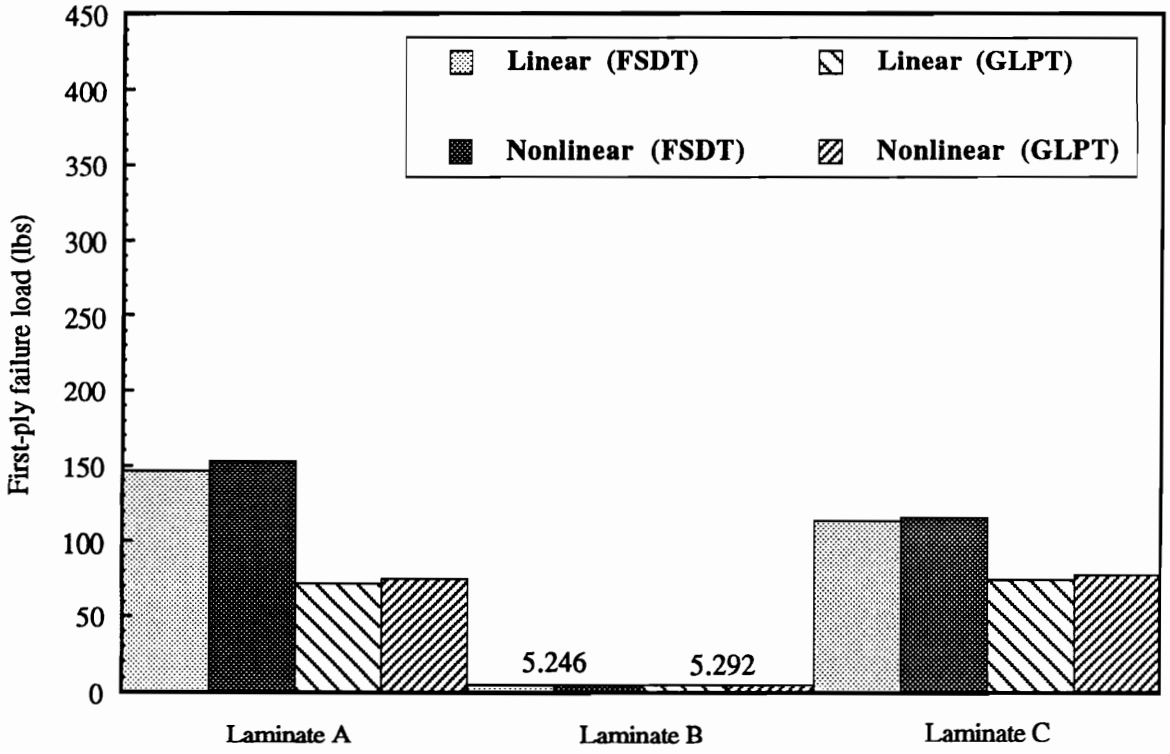

Figure 6.4 Comparison of linear and nonlinear first-ply failure loads as predicted by FSDT and GLPT for different laminates (S/d =32, BC1)

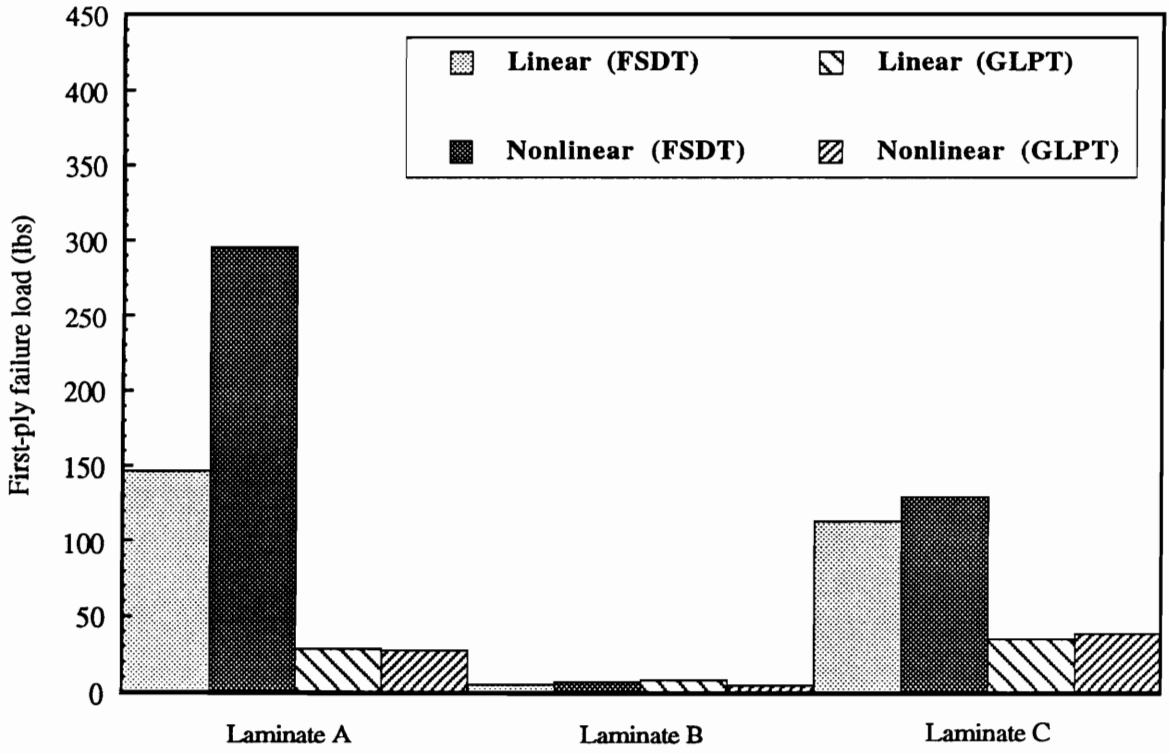

Figure 6.5 Comparison of linear and nonlinear first-ply failure loads as predicted by FSDT and GLPT for different laminates (S/d =32, BC2)

A. This is attributed to the fact that Laminate C is more compliant than laminate A, and hence less sensitive to the stretching effect.

6.2.3 Progressive Failure Analysis

The same progressive failure algorithm used in the case of inplane loads is used for bending loads. However, in the case of bending, a uniformly distributed line load is applied instead of displacement. In the case of nonlinear progressive failure analysis, the stiffness reduction is carried out only after the displacement has converged. The progressive failure loads in the nonlinear failure analysis are found to be very sensitive to the load increment size. A large load step would make the specimen excessively stiff due to the effect of geometric nonlinearity and a small step size would make the specimen too compliant due to the effect of damage. In the present study a load increment size of approximately 5% of the first-ply failure load is used. The interactive stiffness reduction method and a Stiffness Reduction Coefficient (SRC) of 10^{-6} are used. The results of the progressive failure analysis are discussed below:

Figure 6.6 shows the results of progressive failure analysis for an S/d ratio of 16 and BC1. The results show that there is large difference between the first-ply and progressive failure loads as predicted by GLPT. Whereas, in the case of FSDT the difference is considerably less. This is because of the fact that in the case of FSDT both first-ply failure and the progression of damage take place at the midspan, while GLPT predicts first-ply failure at the support and progression of failure both at the support and at the midspan. It is also interesting to note that the linear failure loads predicted by GLPT are less than the nonlinear failure loads. This is due to the fact

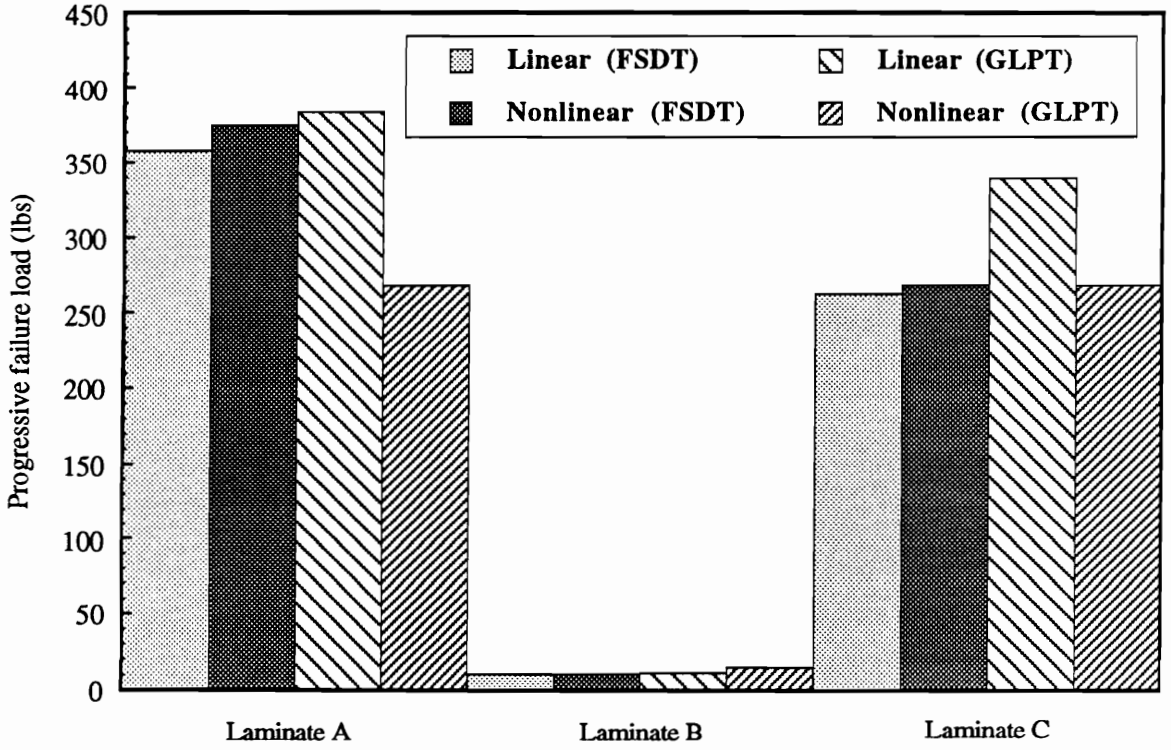

Figure 6.6 Comparison of linear and nonlinear progressive failure loads as predicted by FSDT and GLPT for different laminates (S/d =16, BC1)

that the nonlinear failure analysis predicts more damage at the support than the linear failure analysis. However, this is not true in the case of laminate B, because for this laminate progression of damage takes place only at the midspan. Also, it is interesting to note that the linear failure loads predicted by GLPT are larger than those of FSDT. This is attributed to the fact that full integration is used in the case of GLPT and selective reduced integration is used in the case of FSDT.

Figure 6.7 shows the results of progressive failure analysis for an S/d ratio of 16 and BC2. The same trends as discussed in the case of BC1 hold good even in this case with a few exceptions. For example, in this case the linear failure load predicted by GLPT is more than the nonlinear failure load for laminate B. Because, in this case the nonlinear failure analysis predicts damage both at the midspan and at the support even for laminate B. Also, considerable increase in the progressive failure load is observed in the case of laminate A, while for laminate C the increase is neglible. This again confirms the previous observation that laminate A is more sensitive to the stretching effect than laminate C.

Figure 6.8 shows the results of progressive failure analysis for an S/d ratio of 32 and BC1. The figure shows that, when the S/d ratio is increased from 16 to 32, a sharp reduction is observed in the failure loads and the difference between the linear and nonlinear failure loads predicted by GLPT decreases. This is due to the increased effect of flextural stresses at the midspan and decreased effect of damage at the supports. Due to this phenomenon the nonlinear failure load predicted by GLPT for laminate C, even exceeds the linear failure load.

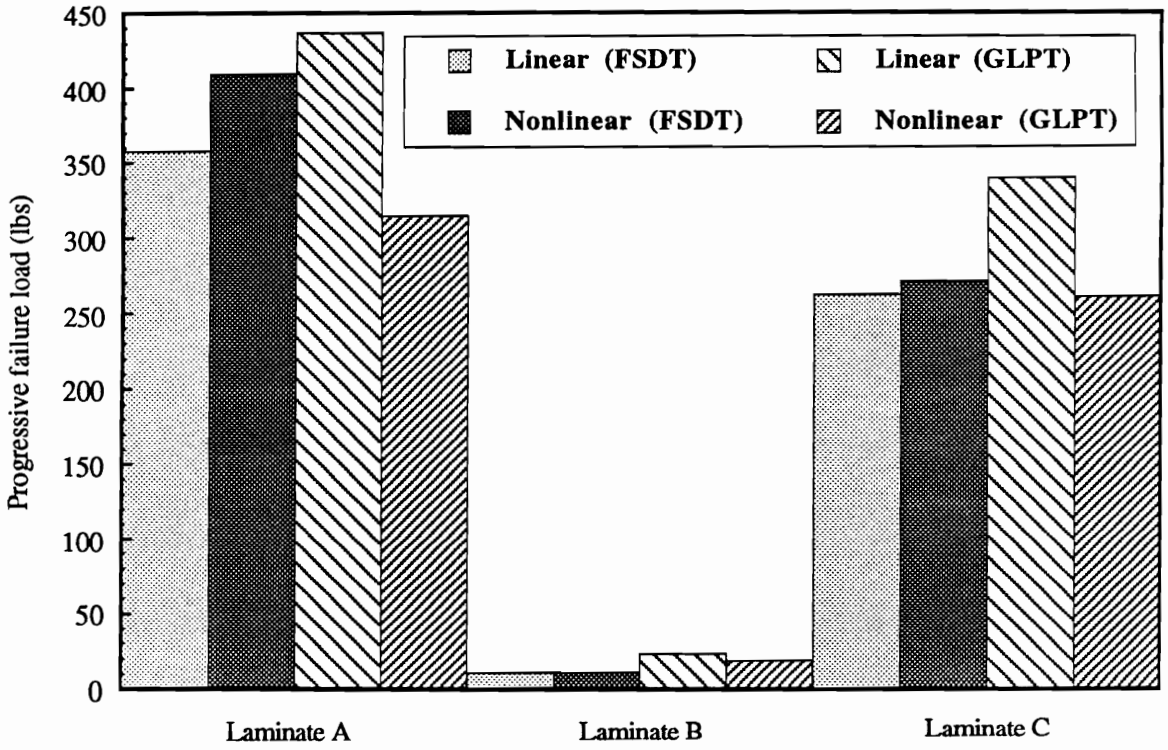

Figure 6.7 Comparison of linear and nonlinear progressive failure loads as predicted by FSDT and GLPT for different laminates (S/d =16, BC2)

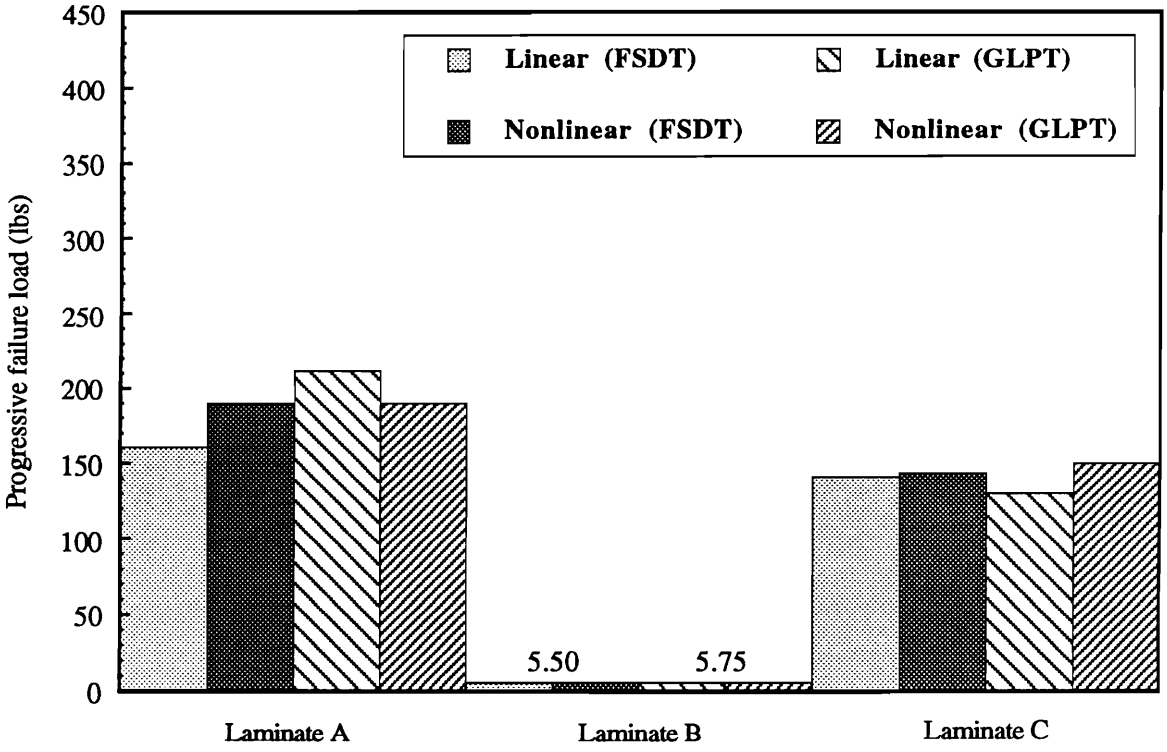

Figure 6.8 Comparison of linear and nonlinear progressive failure loads as predicted by FSDT and GLPT for different laminates (S/d =32, BC1)

Figure 6.9 shows the results of pregressive failure analysis for an S/d ratio of 32 and BC2. A sharp increase is observed in the nonlinear failure load for laminate A, while the linear failure load remains the same as the previous case. This is in agreement with the previous observation that laminate A is more sensitive to the stretching effect than laminate C. Also, both FSDT and GLPT predict the nonlinear failure loads more than the linear failure loads for laminates A and C. However, for laminate B the linear failure load is more than the nonlinear failure load. This was the case even for an S/d ratio of 16 and BC2 (see Figure 6.7). This implies that laminate B suffers more damage at the support in case of nonlinear anlysis when the specimen is not allowed to slide on the supports (BC2). It can also be concluded that the effect of geometric nonlinearity is not much in the case of laminate B because it fails at a small center displacement.

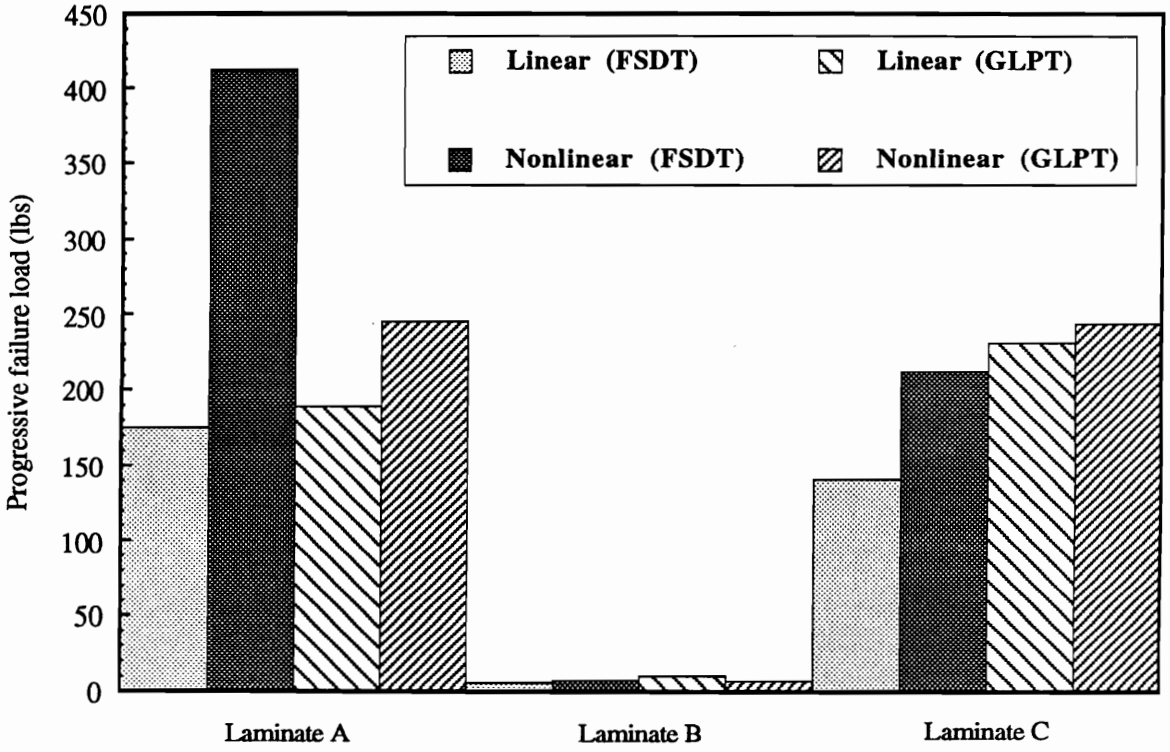

Figure 6.9 Comparison of linear and nonlinear progressive failure loads as predicted by FSDT and GLPT for different laminates (S/d =32, BC2)

CHAPTER 7

SUMMARY AND FUTURE WORK

7.1 Summary of Results

A progressive failure algorithm is developed and implemented in the finite element model. The progressive failure algorithm is based on the assumption that the material behaves like a stable progressively fracturing solid, and the damaged material can be replaced with an equivalent material of degraded properties. The finite element model is based on the Generalized Layerwise Plate Theory of Reddy.

A three dimensional stiffness reduction method is developed and implemented in the progressive failure algorithm. The stiffness reduction method assumes that the degraded properties of the equivalent material can be defined with a single Stiffness Reduction Coefficient (SRC). The Stiffness Reduction Coefficient is assumed to be a characteristic quantity of the composite lamina, and independent of the lamination sequence. The progressive failure algorithm is used to study damage and failures in tension, compression and bending.

It is demonstrated that the progressive failure algorithm is capable of predicting the failure loads and strains of composite laminates subjected to axial extension quite accurately. The results of the parametric study indicate that the out-plane stiffness properties (v_{23}, G_{23}) do not have much influence on the inplane tensile strength of composite laminates. The failure loads and strains are found to be quite sensitive to the out-of-plane shear strength property (X_{23}), boundary conditions and the stiffness

reduction method used.

The predictions of various phenomenological failure criteria indicates that, in general, polynomial failure criteria predict the lower bounds and independent failure criteria predict the upper bounds. The predictions of the Generalized Layerwise Plate Theory (GLPT) and the First Order Shear Deformation Theory (FSDT) demonstrate that it is necessary to take into account the interlaminar stress fields in order to predict the failure loads and strains of composite laminates accurately.

In the case of compressisve loading, the predictions are found to be in agreement with the experimental trends in a qualitative sense. The extreme sensitivity of the failure stresses and strains for the displacement boundary conditions (especially for the angle-ply laminates) suggests that an accurate simulation of the boundary conditions at the grips is essential for accurate prediction of the failure behavior of composite laminates. However, the existing gripping methods are too complex to simulate numerically. This in turn suggests the need for the development of simple gripping methods which can be simulated by a computational tool such as the finite element method with minimum cost and complexity.

The effect of geometric nonlinearity, span to depth ratio, boundary conditions at the support, and lamination sequence on the failure behavior of composite laminates subjected to bending load is studied. A three point bending test is chosen as an example problem. It is demonstrated that the effect of geometric nonlinearity is more pronounced at higher span to depth ratios, and when the laminate is not allowed to slide on the support. With regard to the lamination sequence, it is shown that the

effect of geometric nonlinearity is more severe for those laminates which undergo large displacements before failure. The predictions of GLPT are shown to be qualitatively different from those of FSDT, especially for those cases where the damage takes place near the support.

7.2 Recommendations for Future Work

Based on the experience of the present work, the following recommendations are made for the future work.

(1) The major draw back of the present model is the enormous computational cost associated with the Layerwise Plate Theory. Therefore, it is recommended to incorporate the global-local stress analysis techniques [45] in the first-ply and progressive failure model, in order to reduce the computational cost without sacrificing accuracy.

(2) Another limitation of the present model is the assumption that the material behaves like a stable progressively fracturing solid. Although the model could predict the failure behavior of polymer based composites satisfactorily, it cannot be used for metal matrix composites. Hence, the inclusion of plasticity in the numerical model is recommended.

(3) Further experimentation and study is recommended to verify the assumption that the Stiffness Reduction Coefficient (SRC) is a lamina property, independent of the lamination sequence.

APPENDIX A

ELEMENTS OF THE DIRECT STIFFNESS MATRIX

The direct stiffness matrix [K] can be written in terms of its submatrices as below:

$$[K] = \begin{bmatrix} [K^{11}] & [K^{12}] & [K^{13}] \\ [K^{21}] & [K^{22}] & [K^{23}] \\ [K^{31}] & [K^{32}] & [K^{33}] \end{bmatrix}$$

The submatrices can be further divided into linear and nonlinear parts as below:

$$[K^{\alpha\beta}] = \left[[K^{\alpha\beta}_{LN}] + [K^{\alpha\beta}_{NL}] \right] \quad (\alpha,\ \beta = 1, 3)$$

The expressions for the elements of linear and nonlinear parts of the submatrices are given below:

$$\begin{aligned} [K^{11}_{LN}] = \int_{\Omega_e} \Bigg(& A_{11km} \frac{\partial \psi_s}{\partial x} \frac{\partial \psi_r}{\partial x} + A_{16km} \frac{\partial \psi_s}{\partial x} \frac{\partial \psi_r}{\partial y} \\ & + A_{16km} \frac{\partial \psi_s}{\partial y} \frac{\partial \psi_r}{\partial x} + A_{66km} \frac{\partial \psi_s}{\partial y} \frac{\partial \psi_r}{\partial y} \\ & + D_{55km} \psi_s \psi_r \Bigg) \, dx dy \end{aligned}$$

$$[K^{11}_{NL}] = [0]$$

$$\begin{aligned} [K^{12}_{LN}] = \int_{\Omega^e} \Bigg(& A_{12km} \frac{\partial \psi_s}{\partial x} \frac{\partial \psi_r}{\partial y} + A_{16km} \frac{\partial \psi_s}{\partial x} \frac{\partial \psi_r}{\partial x} \\ & + A_{26km} \frac{\partial \psi_s}{\partial y} \frac{\partial \psi_r}{\partial y} + A_{66km} \frac{\partial \psi_s}{\partial y} \frac{\partial \psi_r}{\partial x} \\ & + D_{45km} \psi_s \psi_r \Bigg) \, dx dy \end{aligned}$$

$$[K^{12}_{NL}] = [0]$$

$$[K_{LN}^{13}] = \int_{\Omega^e} \left(B_{13km} \frac{\partial \psi_s}{\partial x} \psi_r + B_{36km} \frac{\partial \psi_s}{\partial y} \psi_r + C_{45km} \frac{\partial \psi_r}{\partial y} \psi_s + C_{55km} \frac{\partial \psi_r}{\partial x} \psi_s \right) dx dy$$

$$\begin{aligned}[K_{NL}^{13}] = & \frac{1}{2} \int_{\Omega^e} \left(E_{11km\ell} \frac{\partial W_\ell}{\partial x} \frac{\partial \psi_s}{\partial x} \frac{\partial \psi_r}{\partial x} \right. \\ & + E_{12km\ell} \frac{\partial W_\ell}{\partial y} \frac{\partial \psi_s}{\partial x} \frac{\partial \psi_r}{\partial y} + E_{16km\ell} \frac{\partial W_\ell}{\partial x} \frac{\partial \psi_s}{\partial x} \frac{\partial \psi_r}{\partial y} \\ & + E_{16km\ell} \frac{\partial W_\ell}{\partial x} \frac{\partial \psi_s}{\partial y} \frac{\partial \psi_r}{\partial x} + E_{16km\ell} \frac{\partial W_\ell}{\partial y} \frac{\partial \psi_s}{\partial x} \frac{\partial \psi_r}{\partial x} \\ & + E_{26km\ell} \frac{\partial W_\ell}{\partial y} \frac{\partial \psi_s}{\partial y} \frac{\partial \psi_r}{\partial y} + E_{66km\ell} \frac{\partial W_\ell}{\partial x} \frac{\partial \psi_s}{\partial y} \frac{\partial \psi_r}{\partial y} \\ & \left. + E_{66km\ell} \frac{\partial W_\ell}{\partial y} \frac{\partial \psi_s}{\partial y} \frac{\partial \psi_r}{\partial x} \right) dx dy\end{aligned}$$

$$[K_{LN}^{21}] = [K_{LN}^{12}]^T$$

$$[K_{NL}^{21}] = [0]$$

$$\begin{aligned}[K_{LN}^{22}] = & \int_{\Omega^e} \left(A_{22km} \frac{\partial \psi_s}{\partial y} \frac{\partial \psi_r}{\partial y} + A_{26km} \frac{\partial \psi_s}{\partial x} \frac{\partial \psi_r}{\partial y} \right. \\ & + A_{26km} \frac{\partial \psi_s}{\partial y} \frac{\partial \psi_r}{\partial x} + A_{66km} \frac{\partial \psi_s}{\partial x} \frac{\partial \psi_r}{\partial x} \\ & \left. + D_{44km} \psi_s \psi_r \right) dx dy\end{aligned}$$

$$[K_{NL}^{22}] = [0]$$

$$[K_{LN}^{23}] = \int_{\Omega^e} \left(B_{23km} \frac{\partial \psi_s}{\partial y} \psi_r + B_{36km} \frac{\partial \psi_s}{\partial x} \psi_r + C_{44km} \frac{\partial \psi_r}{\partial y} \psi_s + C_{45km} \frac{\partial \psi_r}{\partial x} \psi_s \right) dxdy$$

$$\begin{aligned}[K_{NL}^{23}] = & \frac{1}{2} \int_{\Omega^e} \left(E_{12km\ell} \frac{\partial W_\ell}{\partial x} \frac{\partial \psi_s}{\partial y} \frac{\partial \psi_r}{\partial x} \right. \\ & + E_{16km\ell} \frac{\partial W_\ell}{\partial x} \frac{\partial \psi_s}{\partial x} \frac{\partial \psi_r}{\partial x} + E_{22km\ell} \frac{\partial W_\ell}{\partial y} \frac{\partial \psi_s}{\partial y} \frac{\partial \psi_r}{\partial y} \\ & + E_{26km\ell} \frac{\partial W_\ell}{\partial x} \frac{\partial \psi_s}{\partial y} \frac{\partial \psi_r}{\partial y} + E_{26km\ell} \frac{\partial W_\ell}{\partial y} \frac{\partial \psi_s}{\partial y} \frac{\partial \psi_r}{\partial x} \\ & + E_{26km\ell} \frac{\partial W_\ell}{\partial y} \frac{\partial \psi_s}{\partial x} \frac{\partial \psi_r}{\partial y} + E_{66km\ell} \frac{\partial W_\ell}{\partial x} \frac{\partial \psi_s}{\partial x} \frac{\partial \psi_r}{\partial y} \\ & \left. + E_{66km\ell} \frac{\partial W_\ell}{\partial y} \frac{\partial \psi_s}{\partial x} \frac{\partial \psi_r}{\partial x} \right) dxdy\end{aligned}$$

$$[K_{LN}^{31}] = [K_{LN}^{13}]^T$$

$$[K_{NL}^{31}] = 2[K_{NL}^{13}]^T$$

$$[K_{LN}^{32}] = [K_{LN}^{23}]^T$$

$$[K_{NL}^{32}] = 2[K_{NL}^{23}]^T$$

$$\begin{aligned}[K_{LN}^{33}] = & \int_{\Omega^e} \left(A_{44km} \frac{\partial \psi_s}{\partial y} \frac{\partial \psi_r}{\partial y} + A_{45km} \frac{\partial \psi_s}{\partial y} \frac{\partial \psi_r}{\partial x} \right. \\ & + A_{45km} \frac{\partial \psi_s}{\partial x} \frac{\partial \psi_r}{\partial y} + A_{55km} \frac{\partial \psi_s}{\partial x} \frac{\partial \psi_r}{\partial x} \\ & \left. + D_{33km} \psi_s \psi_r \right) dxdy\end{aligned}$$

$$
\begin{aligned}
[K_{NL}^{33}] = \frac{1}{2}\int_{\Omega^e} \Bigg(& F_{13k\ell m}\frac{\partial W_\ell}{\partial x}\psi_s \frac{\partial \psi_r}{\partial x} \\
& + F_{23k\ell m}\frac{\partial W_\ell}{\partial y}\psi_s\frac{\partial \psi_r}{\partial y} + F_{36k\ell m}\frac{\partial W_\ell}{\partial x}\psi_s\frac{\partial \psi_r}{\partial y} \\
& + F_{36k\ell m}\frac{\partial W_\ell}{\partial y}\psi_s\frac{\partial \psi_r}{\partial x} + G_{13km\ell}\frac{\partial W_\ell}{\partial x}\frac{\partial \psi_s}{\partial x}\psi_r \\
& + G_{13\ell mk}W_\ell\frac{\partial \psi_s}{\partial x}\frac{\partial \psi_r}{\partial x} + G_{23km\ell}\frac{\partial W_\ell}{\partial y}\frac{\partial \psi_s}{\partial y}\psi_r \\
& + G_{23\ell mkl}W_\ell\frac{\partial \psi_s}{\partial y}\frac{\partial \psi_r}{\partial y} + G_{36km\ell}\frac{\partial W_\ell}{\partial y}\frac{\partial \psi_s}{\partial x}\psi_r \\
& + G_{36\ell mk}W_\ell\frac{\partial \psi_s}{\partial x}\frac{\partial \psi_r}{\partial y} + G_{36km\ell}\frac{\partial W_\ell}{\partial x}\frac{\partial \psi_s}{\partial y}\psi_r \\
& + G_{36\ell mk}W_\ell\frac{\partial \psi_s}{\partial y}\frac{\partial \psi_r}{\partial x} + H_{11k\ell mn}\frac{\partial W_n}{\partial x}\frac{\partial W_\ell}{\partial x}\frac{\partial \psi_s}{\partial x}\frac{\partial \psi_r}{\partial x} \\
& + H_{12k\ell mn}\frac{\partial W_n}{\partial x}\frac{\partial W_\ell}{\partial y}\frac{\partial \psi_s}{\partial x}\frac{\partial \psi_r}{\partial y} + H_{12k\ell mn}\frac{\partial W_n}{\partial y}\frac{\partial W_\ell}{\partial x}\frac{\partial \psi_s}{\partial y}\frac{\partial \psi_r}{\partial x} \\
& + H_{16\ell\ell mn}\frac{\partial W_n}{\partial x}\frac{\partial W_\ell}{\partial y}\frac{\partial \psi_s}{\partial x}\frac{\partial \psi_r}{\partial x} + H_{16k\ell mn}\frac{\partial W_n}{\partial x}\frac{\partial W_\ell}{\partial x}\frac{\partial \psi_s}{\partial x}\frac{\partial \psi_r}{\partial y} \\
& + H_{16k\ell mn}\frac{\partial W_n}{\partial y}\frac{\partial W_\ell}{\partial x}\frac{\partial \psi_s}{\partial x}\frac{\partial \psi_r}{\partial x} + H_{16k\ell mn}\frac{\partial W_n}{\partial x}\frac{\partial W_\ell}{\partial x}\frac{\partial \psi_s}{\partial y}\frac{\partial \psi_r}{\partial x} \\
& + H_{22k\ell mn}\frac{\partial W_n}{\partial y}\frac{\partial W_\ell}{\partial y}\frac{\partial \psi_s}{\partial y}\frac{\partial \psi_r}{\partial y} + H_{26k\ell mn}\frac{\partial W_n}{\partial y}\frac{\partial W_\ell}{\partial y}\frac{\partial \psi_s}{\partial x}\frac{\partial \psi_r}{\partial y} \\
& + H_{26k\ell mn}\frac{\partial W_n}{\partial y}\frac{\partial W_\ell}{\partial y}\frac{\partial \psi_s}{\partial y}\frac{\partial \psi_r}{\partial x} + H_{26k\ell mn}\frac{\partial W_n}{\partial y}\frac{\partial W_\ell}{\partial x}\frac{\partial \psi_s}{\partial y}\frac{\partial \psi_r}{\partial y} \\
& + H_{26k\ell mn}\frac{\partial W_n}{\partial x}\frac{\partial W_\ell}{\partial y}\frac{\partial \psi_s}{\partial y}\frac{\partial \psi_r}{\partial y} + H_{66k\ell mn}\frac{\partial W_n}{\partial x}\frac{\partial W_\ell}{\partial y}\frac{\partial \psi_s}{\partial y}\frac{\partial \psi_r}{\partial x} \\
& + H_{66k\ell mn}\frac{\partial W_n}{\partial x}\frac{\partial W_\ell}{\partial x}\frac{\partial \psi_s}{\partial y}\frac{\partial \psi_r}{\partial y} + H_{66k\ell mn}\frac{\partial W_n}{\partial y}\frac{\partial W_\ell}{\partial y}\frac{\partial \psi_s}{\partial x}\frac{\partial \psi_r}{\partial x} \\
& + H_{66k\ell mn}\frac{\partial W_n}{\partial y}\frac{\partial W_\ell}{\partial x}\frac{\partial \psi_s}{\partial x}\frac{\partial \psi_r}{\partial y}\Bigg)\, dxdy
\end{aligned}
$$

It should be noted that the linear part of the direct stiffness matrix is symmetric, whereas the nonlinear part is unsymmetric. As a result the total direct stiffness matrix becomes unsymmetric.

APPENDIX B

ELEMENTS OF THE FORCE VECTOR

The global force vector can be written in terms of its submatrices as below:

$$\{F\} = \begin{Bmatrix} \{F^1\} \\ \{F^2\} \\ \{F^3\} \end{Bmatrix}$$

The expressions for the elements of submatrices of the force vector are given below:

$$\{F^1\} = \int_{\Omega^e} q_{1m}\psi_s dx dy + \int_{\Gamma^e} (N_{1m}n_1 + N_{6m}n_2)\psi_s d\Gamma$$

$$\{F^2\} = \int_{\Omega^e} q_{2m}\psi_s dx dy + \int_{\Gamma^e} (N_{6m}n_1 + N_{2m}n_2)\psi_s d\Gamma$$

$$\{F^3\} = \int_{\Omega^e} q_{3m}\psi_s dx dy + \int_{\Gamma^e} (N_{5m}n_1 + N_{4m}n_2)\psi_s d\Gamma$$

The following definitions apply to the previous three equations:

q_{1m}, q_{2m}, q_{3m} Surface tractions applied on the xy-plane located at the m-th interface, along x, y and z directions respectively.

Γ^e The line boundary of the 2-D finite element.

n_1, n_2 Components of the outward unit normal to Γ^e, along x and y directions respectively.

N_{im} Force resultants as defined in (3.6a).

APPENDIX C

ELEMENTS OF THE TANGENT STIFFNESS MATRIX

The tangent stiffness matrix $[T]$ consists of two parts as below:

$$[T] = [K] + [R]$$

where $[K]$ is the direct stiffness matrix as defined in Appendix A, and $[R]$ is the additional matrix to be added to $[K]$ to obtain the total tangent stiffness matrix $[T]$. The expressions for the elements of $[R]$ are given below:

$$[R^{13}] = [K_{NL}^{13}]$$

$$[R^{23}] = [K_{NL}^{23}]$$

$$\begin{aligned}
[R^{33}] = \int_{\Omega^e} \Bigg(& E_{11\ell km} \frac{\partial U_\ell}{\partial x} \frac{\partial \psi_s}{\partial x} \frac{\partial \psi_r}{\partial x} + E_{12\ell km} \frac{\partial U_\ell}{\partial x} \frac{\partial \psi_s}{\partial y} \frac{\partial \psi_r}{\partial y} \\
& + E_{16\ell km} \frac{\partial U_\ell}{\partial x} \frac{\partial \psi_s}{\partial x} \frac{\partial \psi_r}{\partial y} + E_{16\ell km} \frac{\partial U_\ell}{\partial y} \frac{\partial \psi_s}{\partial x} \frac{\partial \psi_r}{\partial x} \\
& + E_{16\ell km} \frac{\partial U_\ell}{\partial x} \frac{\partial \psi_s}{\partial y} \frac{\partial \psi_r}{\partial x} + E_{26\ell km} \frac{\partial U_\ell}{\partial y} \frac{\partial \psi_s}{\partial y} \frac{\partial \psi_r}{\partial y} \\
& + E_{66\ell km} \frac{\partial U_\ell}{\partial y} \frac{\partial \psi_s}{\partial x} \frac{\partial \psi_r}{\partial y} + E_{66\ell km} \frac{\partial U_\ell}{\partial y} \frac{\partial \psi_s}{\partial y} \frac{\partial \psi_r}{\partial x} \\
& + E_{12\ell km} \frac{\partial V_\ell}{\partial y} \frac{\partial \psi_s}{\partial x} \frac{\partial \psi_r}{\partial x} + E_{16\ell km} \frac{\partial V_\ell}{\partial x} \frac{\partial \psi_s}{\partial x} \frac{\partial \psi_r}{\partial x} \\
& + E_{22\ell km} \frac{\partial V_\ell}{\partial y} \frac{\partial \psi_s}{\partial y} \frac{\partial \psi_r}{\partial y} + E_{26\ell km} \frac{\partial V_\ell}{\partial y} \frac{\partial \psi_s}{\partial x} \frac{\partial \psi_r}{\partial y} \\
& + E_{26\ell km} \frac{\partial V_\ell}{\partial x} \frac{\partial \psi_s}{\partial y} \frac{\partial \psi_r}{\partial y} + E_{26\ell km} \frac{\partial V_\ell}{\partial y} \frac{\partial \psi_s}{\partial y} \frac{\partial \psi_r}{\partial x} \\
& + E_{66\ell km} \frac{\partial V_\ell}{\partial x} \frac{\partial \psi_s}{\partial x} \frac{\partial \psi_r}{\partial y} + E_{66\ell km} \frac{\partial V_\ell}{\partial x} \frac{\partial \psi_s}{\partial y} \frac{\partial \psi_r}{\partial x} \\
& + \frac{1}{2} F_{13\ell km} \frac{\partial W_\ell}{\partial x} \psi_s \frac{\partial \psi_r}{\partial x} + \frac{1}{2} F_{23\ell km} \frac{\partial W_\ell}{\partial y} \psi_s \frac{\partial \psi_r}{\partial y}
\end{aligned}$$

$$
\begin{aligned}
&+\frac{1}{2}F_{36\ell km}\frac{\partial W_\ell}{\partial x}\psi_s\frac{\partial \psi_r}{\partial y}+\frac{1}{2}F_{36\ell km}\frac{\partial W_\ell}{\partial y}\psi_s\frac{\partial \psi_r}{\partial x}\\
&+\frac{1}{2}G_{13\ell mk}W_\ell\frac{\partial \psi_s}{\partial x}\frac{\partial \psi_r}{\partial x}+\frac{1}{2}G_{13km\ell}\frac{\partial W_\ell}{\partial x}\frac{\partial \psi_s}{\partial x}\psi_r\\
&+\frac{1}{2}G_{23\ell mk}W_\ell\frac{\partial \psi_s}{\partial y}\frac{\partial \psi_r}{\partial y}+\frac{1}{2}G_{23kmm\ell}\frac{\partial W_\ell}{\partial y}\frac{\partial \psi_s}{\partial y}\psi_r\\
&+\frac{1}{2}G_{36\ell mk}W_\ell\frac{\partial \psi_s}{\partial x}\frac{\partial \psi_r}{\partial y}+\frac{1}{2}G_{36km\ell}\frac{\partial W_\ell}{\partial y}\frac{\partial \psi_s}{\partial x}\psi_r\\
&+\frac{1}{2}G_{36\ell mk}W_\ell\frac{\partial \psi_s}{\partial y}\frac{\partial \psi_r}{\partial x}+\frac{1}{2}G_{36km\ell}\frac{\partial W_\ell}{\partial x}\frac{\partial \psi_s}{\partial y}\psi_r\\
&+H_{11k\ell mn}\frac{\partial W_\ell}{\partial x}\frac{\partial W_n}{\partial x}\frac{\partial \psi_s}{\partial x}\frac{\partial \psi_r}{\partial x}+\frac{1}{2}H_{12k\ell mn}\frac{\partial W_\ell}{\partial y}\frac{\partial W_n}{\partial y}\frac{\partial \psi_s}{\partial x}\frac{\partial \psi_r}{\partial x}\\
&+\frac{1}{2}H_{12k\ell mn}\frac{\partial W_\ell}{\partial y}\frac{\partial W_n}{\partial x}\frac{\partial \psi_s}{\partial x}\frac{\partial \psi_r}{\partial y}+\frac{1}{2}H_{12k\ell mn}\frac{\partial W_\ell}{\partial x}\frac{\partial W_n}{\partial x}\frac{\partial \psi_s}{\partial y}\frac{\partial \psi_r}{\partial y}\\
&+\frac{1}{2}H_{12k\ell mn}\frac{\partial W_\ell}{\partial x}\frac{\partial W_n}{\partial y}\frac{\partial \psi_s}{\partial y}\frac{\partial \psi_r}{\partial x}+H_{16k\ell mn}\frac{\partial W_\ell}{\partial x}\frac{\partial W_n}{\partial y}\frac{\partial \psi_s}{\partial x}\frac{\partial \psi_r}{\partial x}\\
&+H_{16k\ell mn}\frac{\partial W_\ell}{\partial x}\frac{\partial W_n}{\partial x}\frac{\partial \psi_s}{\partial x}\frac{\partial \psi_r}{\partial y}+H_{16k\ell mn}\frac{\partial W_\ell}{\partial y}\frac{\partial W_n}{\partial x}\frac{\partial \psi_s}{\partial x}\frac{\partial \psi_r}{\partial x}\\
&+H_{16k\ell mn}\frac{\partial W_\ell}{\partial x}\frac{\partial W_n}{\partial x}\frac{\partial \psi_s}{\partial y}\frac{\partial \psi_r}{\partial x}+H_{22k\ell mn}\frac{\partial W_\ell}{\partial y}\frac{\partial W_n}{\partial y}\frac{\partial \psi_s}{\partial y}\frac{\partial \psi_r}{\partial y}\\
&+H_{26k\ell mn}\frac{\partial W_\ell}{\partial y}\frac{\partial W_n}{\partial y}\frac{\partial \psi_s}{\partial x}\frac{\partial \psi_r}{\partial y}+H_{26k\ell mn}\frac{\partial W_\ell}{\partial x}\frac{\partial W_n}{\partial y}\frac{\partial \psi_s}{\partial y}\frac{\partial \psi_r}{\partial y}\\
&+H_{26k\ell mn}\frac{\partial W_\ell}{\partial y}\frac{\partial W_n}{\partial y}\frac{\partial \psi_s}{\partial y}\frac{\partial \psi_r}{\partial x}+H_{26k\ell mn}\frac{\partial W_\ell}{\partial y}\frac{\partial W_n}{\partial x}\frac{\partial \psi_s}{\partial y}\frac{\partial \psi_r}{\partial y}\\
&+H_{66k\ell mn}\frac{\partial W_\ell}{\partial x}\frac{\partial W_n}{\partial y}\frac{\partial \psi_s}{\partial x}\frac{\partial \psi_r}{\partial y}+\frac{1}{2}H_{66k\ell mn}\frac{\partial W_\ell}{\partial y}\frac{\partial W_n}{\partial x}\frac{\partial \psi_s}{\partial x}\frac{\partial \psi_r}{\partial y}\\
&+\frac{1}{2}H_{66k\ell mn}\frac{\partial W_\ell}{\partial y}\frac{\partial W_n}{\partial y}\frac{\partial \psi_s}{\partial x}\frac{\partial \psi_r}{\partial x}+\frac{1}{2}H_{66k\ell mn}\frac{\partial W_\ell}{\partial x}\frac{\partial W_n}{\partial y}\frac{\partial \psi_s}{\partial y}\frac{\partial \psi_r}{\partial x}\\
&+\frac{1}{2}H_{66k\ell mn}\frac{\partial W_\ell}{\partial x}\frac{\partial W_n}{\partial x}\frac{\partial \psi_s}{\partial y}\frac{\partial \psi_r}{\partial y}\\
&+H_{66k\ell mn}\frac{\partial W_\ell}{\partial y}\frac{\partial W_n}{\partial y}\frac{\partial \psi_s}{\partial y}\frac{\partial \psi_r}{\partial x}\Bigg)\,dxdy
\end{aligned}
$$

All other submatrices of $[R]$ are null matrices. The tangent stiffness matrix $[T]$, which is obtained by adding $[R]$ to $[K]$, is symmetric.

BIBLIOGRAPHY

(1) Reddy, J.N. and Pandey, A.K. "A First Ply Failure Analysis of Composite Laminates," Computers and Structures, Vol. 25, March 1987, pp. 371-393.

(2) Reddy, Y.S.N. and Reddy, J.N. "Linear and Non-linear Failure Analysis of Composite Laminate with Transverse Shear," Composites Science and Technology, Vol. 44, 1992, pp. 227-255.

(3) Reddy, J.N., "On Refined Computational Models of Composite Laminates," International Journal of Numerical Methods in Engineering, Vol. 27, 1989, pp. 361-382.

(4) Dougill, J. W., "On Stable Progressively Fracturing Solids," Journal of Applied Mathematics and Physics (ZAMP), Vol. 27, 1976, pp. 423-437.

(5) Robbins, D.H. and Reddy, J.N., "Modeling of Thick Composites Using a Layerwise Laminate Theory," (To be published).

(6) Masters J.E., and Reifsnider, K. L.,"An Investigation of Cumulative Damage Development in Quasi-Isotropic Graphite/Epoxy Laminates," Damage in Composite Materials, STP 775, K.L.Reifsnider.Ed, American Society for Testing Materials, Philadelphia, 1982, pp. 40-62.

(7) Highsmith, A. L., and Reifsnider, K. L., "Stiffness-Reduction Mechanisms in Composite Laminates" Damage in Composite Materials, STP 775, K.L.Reifsnider.Ed, American Society for Testing Materials, Phila-delphia,1982, pp. 103-117.

(8) Talreja, R., "Residual Stiffness Properties of Cracked Composite Laminates," Proceedings of Sixth International Conference on Fracture, ICF6, New Delhi, December 4 - 10, 1984.

(9) Talreja, R., "Transverse Cracking and Stiffness Reduction in Composite Laminates," Journal of Composite Materials, 1985, Vol 19, pp. 355-375.

(10) Hashin, Z., "Analysis of Cracked Laminates: A Variational Approach," Mechanics of Materials, Vol 4, 1985, pp. 121-136.

(11) Lee, J. W. and Daniel I.M., "Progressive Transverse cracking of Cross ply Composite Laminates," Journal of Composite Materials, Aug 1990, pp. 1225-1243.

(12) Daniel I.M., and Lee, J. W , "Damage Development in Composite Laminates Under Monotonic Loading," Journal of Composites Technology & Research, JCTRER,Vol 12,No. 2, Summer 1990, pp. 98-102.

(13) O'Brien, T.K., "Characterization of Delamination Onset and Growth in a Composite Laminate," Damage in Composite Materials, STP 775, K.L.Reifsnider.Ed., American Society for Testing Materials, Philadelphia, 1982, pp. 140-167.

(14) O'Brien, T.K., "Analysis of Local Delaminations and Their Influence on Composite Laminate Behavior," Delamination and Debonding of Materials, STP 876, W.S. Johnson,.Ed., American Society for Testing Materials, Phila-delphia, 1985, pp. 282-297.

(15) O'Brien, T.K., "The effect of Delamination on the Tensile Strength of Unnotched, Quasi-Isotropic, Graphite/Epoxy Laminates," Proceedings of the SESA/JSME Joint Conference on Experimental Mechanics, Part I, Honolulu, Hawaii, May 1982 (SESA, Brookfield Center, CT) pp. 236-243.

(16) Reifsnider K. L., Henneke, E. G., II, and Stinchcomb, W. W., "Delamination in Quasi-Isotropic Graphite-Epoxy Laminates," Composite Materials Testing and Design (Fourth Conference), ASTM STP 617, American Society for Testing and Materials, 1977, pp. 93-105.

(17) Petit, P. H. and Waddoups, M.E., "A Method of Predicting the Nonlinear Behavior of Laminated Composites," Journal of Composite Materials, Vol 3, Feb 1969, pp. 2-19.

(18) Sandhu, R.S., Sendeckyj, G. P., and Gallo, R.L., "Modelling of the Failure Process in Notched Laminates," Proceedings of the IUTAM Symposium on Mechanics of Composite Materials, VPI&SU, August 16-19, 1982.

(19) Tsai, S.W. and Azzi, V.D., "Strength of Laminated Composite Materials," AIAA Journal, Vol. 4, N0. 2, Feb. 1966, pp. 296-301.

(20) Chang, F.K., Scott, R.A. and Springer, G.S., "Failure Strength of Nonlinearly Elastic Composite Laminates Containing a Pin Loaded Hole ," Journal of Composite Materials, Vol. 18, Sep. 1984, pp. 464-477.

(21) Chang, F.K. and Chang, K.Y., "A Progressive Damage Model for Laminated Composites Containing Stress Concentrations," Journal of Composite Materials, Vol. 21, Sep. 1987, pp. 834-855.

(22) Chang, Fu-Kuo, Lessard, Larry and Tang, Jian-Mao , "Compression Response of Laminated Composites Containing an Open Hole," SAMPE Quarterly, Vol. 19, July 1988, pp. 46-51.

(23) Hahn, H. T., and Tsai S. W., "Nonlinear Elastic Behavior of Unidirectional Composite Laminates," Journal of Composite Materials, Vol. 7, July 1973, pp. 102-110.

(24) Yamada, S. E., and Sun, C. T., "Analysis of Laminate Strength and Its Distribution ," Journal of Composite Materials, Vol. 12, July 1978, pp. 275-284.

(25) Tan, S. C., "A Progressive Failure Model of Composite Laminates Containing Openings," Journal of Composite Materials, Vol. 25, 1991, pp 556-577.

(26) Ochoa, O. O., and Engblom J. J., "Analysis of Progressive Failure in Composites," Composites Science and Technology, Vol. 28, 1987, pp 87-102.

(27) Hashin, Z., "Failure Criteria for Unidirectional Fiber Composites," Journal of Applied Mechanics, Vol. 47, 1980, pp 329-334.

(28) Lee, J. D. "Three Dimensional Finite Element Analysis of Damage Accumulation in Composite Laminate," Computers & Structures, Vol 15, N0.3, 1982, pp. 335-350.

(29) Sun, C. T., "Failure Analysis of Laminated Composites by Using Iterative Three Dimensional Finite Element Method," Computers & Structures, Vol 33, No.1, 1989, pp. 41-47.

(30) Averill, R. C., "Nonlinear Analysis of Laminated Composite Shells Using a Micromechanics-Based Progressive Damage Model," Ph.D. Disseration, Virginia Polytechnic Institute and State University, 1992.

(31) Reddy, J. N., "A generalization of Two Dimensional Theories of Laminated Composite Plates," Communications in Applied Numerical Methods, Vol. 3, 1987, pp. 173-180.

(32) Reddy J. N., "On the Generalization of Displacement Based Laminate Theories," Applied Mechanics Reviews, Vol. 42, No. 11, part 2, 1989, S213-S222.

(33) Reddy, J. N., Barbero, E. J., and Teply, J. L., "A Plate Bending Element Based on a Generalized Laminate Theory," International Journal of Numerical Methods in Engineering, Vol. 28, 1989, pp. 2275-2292.

(34) Barbero, E. J., "On a Generalized Laminate Plate Theory with Application to Bending, Vibration, and Delamination Buckling in Composite Laminates," Ph. D. Dissertation, Virginia Polytechnic Institute and State University, 1989.

(35) Reddy, J. N., "A Review of Refined Theories of Laminated Composites Plates," Shock and Vibration Digest, Vol. 22, 1990, pp. 3-17.

(36) Barbero, E. J., Reddy, J. N. and Teply, J. L., "An Accurate Determination of Stresses in Thick Laminates Using a Generalized Plate Theory," International Journal of Numerical Methods in Engineering, Vol. 29, 1990, pp. 1-14.

(37) Barbero, E. J., and Reddy, J. N., "Nonlinear Analysis of Composite Laminates Using a Generalized Laminated Plate Theory," AIAA Journal, Vol. 28, No. 11, November, 1990, pp. 1987-1994.

(38) Tsai, S.W., and Wu, E.M., "A General Theory of Strength for Anisotropic Materials," Journal of Composite Materials, Vol. 5, Jan. 1971, pp. 58-80.

(39) Sun, C.T. and Zhou, S.G. "Failure of Quasi-Isotropic Laminates with Free Edges," Journal of Reinforced Plastics and Composites, Vol.7, Nov.1988, pp. 515-557.

(40) Jones, R. M., "Mechanics of Composite Materials", Scripta Book Company, Washington, D.C., 1975, pp. 41-44.

(41) Zweben, C., Hahn, H. T., and Chou, T. W., "Mechanical Behavior and Properties of Composite Materials," Delaware Composites Design Encyclopedia, Vol. 1, Eds. Carlsson, L. A., and Gillespie, J. W., Technomic Publishing Co., Inc, Lancaster, 1989, pp. 49 -54.

(42) Private communication with Prof. C. T. Sun.

(43) Clark, R. K. and Lisagor, W.B., "Compression Testing of Graphite/Epoxy Composite Materials," Test Methods and Design Allowables for Fibrous Composites, ASTM STP 734, C. C. Chamis, Ed., American Society for Testing and Materials, 1981, pp. 34-53.

(44) Turvey, G. J. and Osman, M. Y., "Exact and Approximate Linear and Nonlinear Initial Failure Analysis of Laminate Mindlin Plates in Flexure," Composite Structures 5, Ed., I. H. Marshal, Elsevier Applied Science, London, 1989, pp. 133-171.

(45) Robbins, D. H. and Reddy, J. N., "Global-local Stress Analysis of Laminated Composite Plates Using Variable Kinematic Finite Elements," presented at the 33rd SDM Conference, April 13-15, 1992, Dallas, Texas.

VITA

Yeruva S. Reddy was born on September 4, 1957 in Gobbur, Andhra Pradesh, India. He was raised and attended high school in Markapur, Andhra Pradesh, India. He obtained his Bachelor of Technology degree in Mechanical Engineering in April of 1981 from Regional Engineering College, Warangal, India. He worked at Naval Science and Technological Laboratory, Visakhapatnam, India, as a Scientist, for two and half years and then came back to Regional Engineering College, Warangal, to pursue his Master of Technology degree in Design and Production Engineering, in July 1984. He was appointed as a Lecturer in the Mechanical Engineering Department, in July 1986. He obtained his Master's degree in August 1987 and continued to work as a Lecturer in the same department.

The author started his Ph.D program in Mechanical Engineering at Clemson University, South Carolina, USA, in January 1989. He joined Virginia Polytechnic Institute and State University in August 1989, and continued his Ph.D program in Engineering Science and Mechanics Department. He completed all the requirements for his Ph.D. degree in August, 1992.

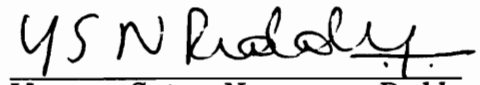

Yeruva Satya Narayana Reddy